

U.S. DEPARTMENT OF COMMERCE
National Technical Information Service

NACA-TR-408

GENERAL FORMULAS AND CHARTS FOR THE
CALCULATION OF AIRPLANE PERFORMANCE

W. B. Oswald

1932

NOTICE

THIS DOCUMENT HAS BEEN REPRODUCED FROM THE BEST COPY FURNISHED US BY THE SPONSORING AGENCY. ALTHOUGH IT IS RECOGNIZED THAT CERTAIN PORTIONS ARE ILLEGIBLE, IT IS BEING RELEASED IN THE INTEREST OF MAKING AVAILABLE AS MUCH INFORMATION AS POSSIBLE.

NACA TR

REPORT No. 408

**GENERAL FORMULAS AND CHARTS
FOR THE CALCULATION OF AIRPLANE PERFORMANCE**

**By W. BAILEY OSWALD
California Institute of Technology**

88258—32—1

1

JOSEPH S. AMES COLLECTION.

NATIONAL ADVISORY COMMITTEE FOR AERONAUTICS

NAVY BUILDING, WASHINGTON, D. C.

(An independent Government establishment, created by act of Congress approved March 3, 1915, for the supervision and direction of the scientific study of the problems of flight. Its membership was increased to 15 by act approved March 2, 1929 (Public, No. 908, 70th Congress). It consists of members who are appointed by the President, all of whom serve as such without compensation.)

JOSEPH S. AMES, Ph. D., *Chairman*,
President, Johns Hopkins University, Baltimore, Md.
DAVID W. TAYLOR, D. Eng., *Vice Chairman*,
Washington, D. C.
CHARLES G. ABBOT, Sc. D.,
Secretary, Smithsonian Institution, Washington, D. C.
GEORGE K. BURGESS, Sc. D.,
Director, Bureau of Standards, Washington, D. C.
ARTHUR B. COOK, Captain, United States Navy,
Assistant Chief, Bureau of Aeronautics, Navy Department, Washington, D. C.
WILLIAM F. DURAND, Ph. D.,
Professor Emeritus of Mechanical Engineering, Stanford University, California.
BENJAMIN D. FOULLOIS, Major General, United States Army,
Chief of Air Corps, War Department, Washington, D. C.
HARRY F. GUGGENHEIM, M. A.,
The American Ambassador, Habana, Cuba.
CHARLES A. LINDBERGH, LL. D.,
New York City.
WILLIAM P. MACCRACKEN, Jr., Ph. B.,
Washington, D. C.
CHARLES F. MARVIN, M. E.,
Chief, United States Weather Bureau, Washington, D. C.
WILLIAM A. MOFFETT, Rear Admiral, United States Navy,
Chief, Bureau of Aeronautics, Navy Department, Washington, D. C.
HENRY C. PRATT, Brigadier General, United States Army,
Chief, Matériel Division, Air Corps, Wright Field, Dayton, Ohio.
EDWARD P. WARNER, M. S.,
Editor "Aviation," New York City.
ORVILLE WRIGHT, Sc. D.,
Dayton, Ohio.

GEORGE W. LEWIS, *Director of Aeronautical Research*.

JOHN F. VICTORY, *Secretary*.

HENRY J. E. REID, *Engineer in Charge, Langley Memorial Aeronautical Laboratory, Langley Field, Va.*

JOHN J. IDE, *Technical Assistant in Europe, Paris, France.*

EXECUTIVE COMMITTEE

JOSEPH S. AMES, *Chairman*.

DAVID W. TAYLOR, *Vice Chairman*.

CHARLES G. ABBOT.

GEORGE K. BURGESS.

ARTHUR B. COOK.

BENJAMIN D. FOULLOIS.

CHARLES A. LINDBERGH.

WILLIAM P. MACCRACKEN, Jr.

CHARLES F. MARVIN.

WILLIAM A. MOFFETT.

HENRY C. PRATT.

EDWARD P. WARNER.

ORVILLE WRIGHT.

JOHN F. VICTORY, *Secretary*.

REPORT No. 408

GENERAL FORMULAS AND CHARTS FOR THE CALCULATION OF AIRPLANE PERFORMANCE

By W. BAILEY OSWALD

SUMMARY

In the present report submitted to the National Advisory Committee for Aeronautics for publication the general formulas for the determination of all major airplane performance characteristics are developed. A rigorous analysis is used, making no assumption regarding the attitude of the airplane at which maximum rate of climb occurs, but finding the attitude at which the excess thrust horsepower is maximum.

The characteristics of performance are given in terms of the three fundamental parameters λ_p , λ_s , and λ_t , or their engineering alternatives l_p , l_s , and l_t , where

$$\begin{aligned}\lambda_p &\propto l_p = \text{parasite loading} \\ \lambda_s &\propto l_s = \text{effective span loading} \\ \lambda_t &\propto l_t = \text{thrust horsepower loading}\end{aligned}$$

These combine into a new parameter of fundamental importance which has the alternative forms:

$$\Delta' \propto \Delta = \frac{l_s l_t^{1/2}}{l_p^{1/4}}$$

A correction is made for the variation of parasite resistance with angle of attack and for the nonelliptical wing loading by including in the induced drag term a factor e , called the "airplane efficiency factor." The correction is thus assumed proportional to C_L^2 .

A comprehensive study of full-scale data for use in the formulas is made. Using the results of this investigation, a series of performance charts is drawn for airplanes equipped with modern unsupercharged engines and fixed-pitch metal propellers.

Equations and charts are developed which show the variation of performance due to a change in any of the customary design parameters.

Performance determination by use of the formulas and charts is rapid and explicit. The results obtained by this performance method have been found to give agreement with flight test that is, in general, equal or superior to results obtained by present commonly used methods.

I. INTRODUCTION

The present report was started upon the suggestion of Mr. Arthur E. Raymond, assistant chief engineer of the Douglas Aircraft Corporation and professor of airplane design at the California Institute of Technology,

that a rapid algebraic or chart method of performance estimation would be of value to the industry. The analysis starts with the basic equations given by Dr. Clark B. Millikan in reference 1, and uses parameters of the airplane similar to those there introduced.

The general equations for maximum rate of climb are obtained by differentiating and equating expressions for thrust horsepower available and required, and using the excess horsepower at the optimum speed so determined. The accuracy of the charts therefore depends almost entirely upon the accuracy with which any general propeller and thrust-horsepower data represent the case at hand.

General supercharged engine data may be substituted in the general equations to give a series of charts. Variable-pitch propeller data may be used to give a series of charts. In short, the formulas developed are general formulas. The calculation and construction of charts for any general type of engine or propeller requires considerable labor; however, once the series of charts has been constructed, the calculation of the performance characteristics of any airplane similarly equipped may be carried out in a few minutes.

Besides giving to the designer the advantage of rapidity in performance calculation, the charts readily show the change in performance of the airplane with a change in any of its characteristics: Weight, span, equivalent parasite area, design brake horsepower, maximum propeller efficiency. The designer may, by the use of the charts, weigh the relative merits of a change in airplane characteristics in obtaining any desired performance.

Another advantage in the use of the charts is the fact that the absolute ceiling, maximum rate of climb, and the maximum velocity, having been specified, the charts may be solved in reverse order to determine the airplane characteristics necessary to give the specified performance. The designer's requirements and limits are definitely set, and his problem immediately becomes one of structure. Likewise, flight test data having been given, the charts may be solved in reverse order to determine the actual values of the airplane parameters.

It hardly need be pointed out that the selection of a propeller is made easy by the use of the charts. Maximum velocity depends upon propulsive efficiency,

which in turn depends upon maximum velocity. This cyclic process is rapidly solved by means of the charts.

The physical discussion of Λ' , presented in Section II B, is due to Dr. Clark B. Millikan's timely discovery of the fundamental physical nature of this major parameter of airplane performance.

The general performance formulas have been developed in Sections II and III in terms of the physical parameters λ_p , λ_s , λ_c , and Λ' in order that the results may be readily extended to any system of units. The results are extended to the American engineering system of units in Section V preliminary to the construction of the performance charts, which make use of the engineering parameters l_p , l_s , l_c , and Λ .

The method of performance determination is outlined in Sections VI and VII. Charts for the complete calculation of the performance of any airplane equipped with modern unsupercharged engines and fixed-pitch metal propellers have been collected at the end of the report. Hence, for the purpose of solving actual performance problems, Sections VI and VII may be read and used independently of the previous sections, and without the necessity for any reference to the contents of the earlier ones.

The author wishes to take this opportunity to express his appreciation of the many helpful suggestions and comments furnished by the members of the staff of the Guggenheim Graduate School of Aeronautics, at the California Institute of Technology. In addition, he expresses his gratitude to the Army Air Corps for data furnished, and to others who have given valuable aid in the preparation of this report. The author wishes particularly to express his appreciation of the contribution to the report in Section II B furnished by Dr. Clark B. Millikan.

II. GENERAL ALGEBRAIC PERFORMANCE FORMULAS

A. DEVELOPMENT OF THE FUNDAMENTAL PERFORMANCE EQUATION

The fundamental equation of airplane performance may be written in any consistent set of units in the form:

$$\frac{dh}{dt} = \frac{(t.hp_a - t.hp_r)}{W} A \quad (2.1)$$

where,

h = altitude

t = time

$t.hp_a$ = thrust horsepower available

$t.hp_r$ = thrust horsepower required

W = weight

A = horsepower conversion factor; 550 in American units and 75 in metric units.

If we define,

$$w_h = A \frac{t.hp_a}{W} = \text{"rising speed"} \quad (2.2)$$

$$w_s = A \frac{t.hp_r}{W} = \text{"sinking speed"} \quad (2.3)$$

then equation (2.1) takes the form,

$$\frac{dh}{dt} = w_h - w_s \quad (2.4)$$

The maximum horizontal velocity occurs at $\frac{dh}{dt} = 0$; maximum rate of climb at maximum $\frac{dh}{dt}$; absolute ceiling at maximum $\frac{dh}{dt} = 0$, etc.

Splitting up the drag into two terms in accordance with the Prandtl wing theory,

$$w_s = \frac{DV}{W} = \left(\frac{D_p}{W} + \frac{D_i}{W} \right) V \quad (2.5)$$

where,

D = total drag

D_p = parasite drag (that portion of drag whose coefficient is constant)

D_i = effective induced drag (that portion of drag whose coefficient is proportional to C_L^2)

V = velocity

C_L = lift coefficient.

From the Prandtl wing theory,

$$D_i = \frac{L^2}{\pi q b_e^2} \quad (2.6)$$

where,

L = lift

ρ = mass density of air

$$q = \frac{1}{2} \rho V^2$$

b_e = effective span.

For horizontal rectilinear flight, and angles of climb for which the cosine of the angle is nearly unity, the weight may be substituted for the lift. Hence,

$$\frac{D_i}{W} = \frac{2W}{\pi \rho V^2 b_e^2} \quad (2.7)$$

Defining f as the equivalent parasite area:

$$D_p = qf = \frac{1}{2} \rho V^2 f \quad (2.8)$$

$$\frac{D_p}{W} = \frac{\rho}{2} \frac{f}{W} V^2 \quad (2.9)$$

This definition of f is consistent with that used abroad, and is desirable because of its essential physical significance and freedom from constants. It differs from the present American definition of f by the factor 1.28. In the American definition f is called the "equivalent flat plate area" and is defined by the equation $D_p = 1.28 qf$.

The sinking speed becomes then,

$$w_s = \frac{\rho}{2} \frac{f}{W} V^3 + \frac{2W}{\pi \rho b_e^2} \frac{1}{V} \quad (2.10)$$

It has generally been customary to define b_s as the equivalent monoplane span kb , where k is Munk's span factor and b is the largest individual span of a wing cellule. This case corresponds to the ideal case in which the lift distribution is elliptical over each wing and the parasite drag coefficient is independent of C_L . There is actually an increase in drag over this ideal condition caused by interference, variation of parasite, and nonelliptical lift distribution. It has been found that the additional drag may well be represented by a correction proportional to C_L^2 . The correction may, therefore, be included in the induced drag term by introducing therein a factor e , which is called the "airplane efficiency factor." Hence, we define,

$$b_s^2 = e(kb)^2$$

where, e = airplane efficiency factor

k = Munk's span factor

b = largest individual span of the wing cellule.

The airplane efficiency factor is quite fully discussed in Section IV. In view of this definition, equation (2.10) becomes,

$$w_s = \frac{\rho}{2W} V^3 + \frac{2W}{\pi \rho e(kb)^2} \frac{1}{V} \quad (2.10a)$$

Writing $\sigma = \frac{\rho}{\rho_0}$ = relative air density, where ρ_0 = standard air density at sea level, and defining,

$$\lambda_p = \frac{2W}{\rho_0 f} \propto \text{parasite loading} \quad (2.11)$$

$$\lambda_s = \frac{2W}{\pi \rho_0 e(kb)^2} = \frac{2W}{\pi \rho_0 b_s^2} \propto \text{effective span loading} \quad (2.11a)$$

so that both λ_s and λ_p have the dimensions of (velocity)², we have from (2.10a),

$$w_s = \sigma \frac{V^3}{\lambda_p} + \frac{1}{\sigma} \frac{\lambda_s}{V} \quad (2.12)$$

If we similarly define,

$$\lambda_t = \frac{1}{A} \frac{W}{b \cdot \text{hp}_m \eta_m} = \frac{1}{A} \frac{W}{t \cdot \text{hp}_m} \propto \text{thrust horsepower loading}, \quad (2.13)$$

where,

V_m = design maximum velocity at sea level

$b \cdot \text{hp}_m$ = brake horsepower at V_m ($\sigma = 1$)

η_m = propulsive efficiency at V_m

$t \cdot \text{hp}_m$ = thrust horsepower at V_m

Then,

$$w_h = A \frac{t \cdot \text{hp}_a}{W} = \frac{1}{\lambda_t} \frac{t \cdot \text{hp}_a (\text{at } V, \sigma)}{t \cdot \text{hp}_m} \quad (2.14)$$

or,

$$w_h = \frac{1}{\lambda_t} T_a T_v \quad (2.15)$$

where,

$$T_v = \frac{t \cdot \text{hp}_a \text{ at velocity } V}{t \cdot \text{hp}_a \text{ at } V_m} \text{ (at sea level)}$$

$$= \text{function of } \frac{V}{V_m}$$

$$T_a = \frac{t \cdot \text{hp}_a \text{ at altitude}}{t \cdot \text{hp} \text{ at sea level}} \text{ (at constant velocity } V)$$

$$= \text{function of } \sigma \text{ and } \frac{V}{V_m}$$

Substituting equations (2.12) and (2.15) in (2.4) we get,

$$\frac{dh}{dt} = \frac{1}{\lambda_t} T_a T_v - \sigma \frac{V^3}{\lambda_p} - \frac{1}{\sigma} \frac{\lambda_s}{V} \quad (2.16)$$

Since the propulsive unit characteristics T_a and T_v are expressed in terms of $\frac{V}{V_m}$, V_m will be introduced explicitly in equation (2.16). Defining,

$$R_v = \frac{V}{V_m} = \text{dimensionless speed ratio}, \quad (2.17)$$

we have,

$$\frac{dh}{dt} = \frac{1}{\lambda_t} T_a T_v - \sigma R_v^3 \frac{V_m^3}{\lambda_p} - \frac{1}{\sigma R_v} \frac{\lambda_s}{V_m} \quad (2.18)$$

In order to bring out the physical basis of this equation we note that $\frac{1}{\lambda_t} = A \frac{t \cdot \text{hp}_a}{W}$ = the speed at which the airplane would rise if the thrust horsepower required for horizontal flight were zero. The entire $t \cdot \text{hp}_a$ would then be used in lifting the airplane vertically at a speed we might well call the "design rising speed" = $\left(\frac{dh}{dt}\right)_d$.

The symbols $\frac{1}{\lambda_t}$ and $\left(\frac{dh}{dt}\right)_d$ will be used interchangeably throughout this section. It is obvious that the actual rate of climb will depend very markedly on $\left(\frac{dh}{dt}\right)_d$, so it is natural to write the latter as a multiplicative factor. In this way we obtain,

$$\frac{dh}{dt} = \left(\frac{dh}{dt}\right)_d \left[T_a T_v - \sigma R_v^3 \frac{\lambda_s}{\lambda_p} \frac{V_m^3}{V^3} - \frac{1}{\sigma R_v} \frac{\lambda_s \lambda_t}{V_m} \right] \quad (2.19)$$

$$\left(\frac{dh}{dt}\right)_d = \frac{1}{\lambda_t} \quad (2.20)$$

In this form, the fundamental performance equation contains three design parameters,

$$\left(\frac{dh}{dt}\right)_d = \frac{1}{\lambda_t}, \frac{\lambda_s}{\lambda_p} V_m^3, \text{ and } \frac{\lambda_s \lambda_t}{V_m}$$

This is the same number with which we began ($\lambda_s, \lambda_p, \lambda_t$), so that no obvious simplification has as yet been attained. However, the explicit use of V_m and the dimensionless speed ratio R_v does actually lead to considerable simplification and produces a new fundamental form of the performance equation. For consider the conditions for V_m .

Then,

$$\sigma = R_v = T_a = T_v = 1 \text{ and } \frac{dh}{dt} = 0.$$

Equation (2.19) then gives,

$$\frac{\lambda_t}{\lambda_p} V_m^3 = 1 - \frac{\lambda_s \lambda_t}{V_m^3} \quad (2.21)$$

Substituting this into equation (2.19) we obtain,

$$\frac{dh}{dt} = \frac{1}{\lambda_t} \left[(T_a T_c - \sigma R_c^3) + \left(\sigma R_c^3 - \frac{1}{\sigma R_c} \right) \frac{\lambda_s \lambda_t}{V_m} \right] \quad (2.22)$$

Furthermore, from (2.21),

$$V_m = \frac{\lambda_p^{1/3}}{\lambda_t^{1/3}} \left(1 - \frac{\lambda_s \lambda_t}{V_m^3} \right)^{1/3} \quad (2.23)$$

or,

$$\frac{V_m}{\lambda_s \lambda_t} = \frac{\lambda_p^{1/3}}{\lambda_s \lambda_t^{4/3}} \left(1 - \frac{\lambda_s \lambda_t}{V_m^3} \right)^{1/3} \quad (2.24)$$

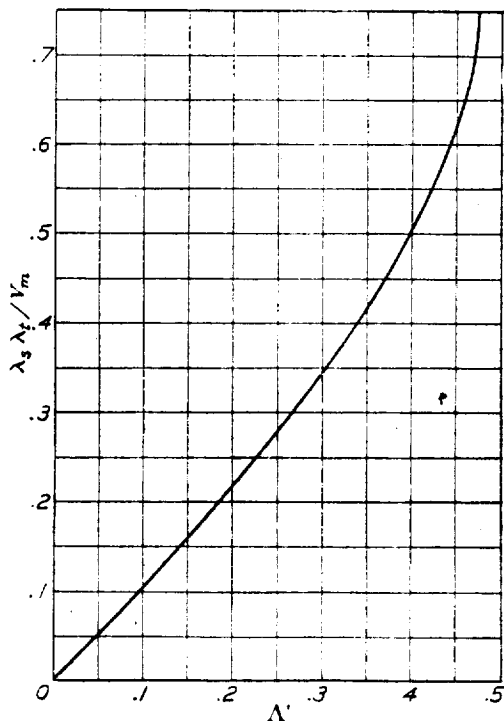


FIGURE 1. $\frac{\lambda_s \lambda_t}{V_m}$ as a function of $A' = \frac{\lambda_s \lambda_t^{4/3}}{\lambda_p^{1/3}}$

Now defining,

$$A' = \frac{\lambda_s \lambda_t^{4/3}}{\lambda_p^{1/3}} \quad (2.25)$$

Equation (2.24) gives,

$$A' = \frac{\lambda_s \lambda_t}{V_m} \left(1 - \frac{\lambda_s \lambda_t}{V_m^3} \right)^{1/3} \quad (2.26)$$

The relation between the dimensionless design parameters A' and $\frac{\lambda_s \lambda_t}{V_m}$ given by this equation has been plotted in Figure 1 and is used continually in the later calculations.

The fundamental performance equation (2.16) has thus been materially simplified since, in the form given in (2.22), it contains only the two parameters $\frac{1}{\lambda_t} = \left(\frac{dh}{dt} \right)_a$ and $\frac{\lambda_s \lambda_t}{V_m}$, and the latter is given by equation (2.26) as a definite function of the fundamental design

parameter A' . In schematic form, and employing equation (2.26), we may rewrite the fundamental performance equation (2.22) as,

$$\frac{dh}{dt} = \frac{1}{\lambda_t} \left[\text{(function (1) of } \sigma, R_c) + \text{(function (2) of } \sigma, R_c) \text{(function of } A') \right] \quad (2.27)$$

where the term in the brackets is dimensionless.

The essential advance in the present theory lies in the fact that it replaces the normally 3-parameter performance problem by two successive 2-parameter ones. For V_m is first determined from (2.26) as a function of A' and λ_s, λ_t , and all subsequent performance characteristics are then obtained from (2.27) in terms of the design parameters λ_s and A' . Indeed all characteristics for which $\frac{dh}{dt} = 0$, e. g., absolute ceiling and speed ratios at altitude, are given in terms of the single parameter A' .

Schrenk and Helmbold (references 2 and 3) have discovered the possibility of a reduction in the number of parameters for the power-required portion of the performance problem. However, they give no analytical discussion of the power-available problem. Indeed, it would be rather difficult to introduce this element into their analyses, since either the velocity for maximum L/D or that for minimum power required is taken as the fundamental velocity, instead of the design maximum velocity which is used in the present discussion. Driggs (reference 4) introduces analytical expressions for the variation of power available which are similar in nature to those here employed; however, Driggs's analysis rests on somewhat arbitrary assumptions concerning the attitude of the airplane at which the various performance characteristics occur. Furthermore, in Driggs's papers, general characteristics at altitude are not discussed. The reduction in the number of design parameters from three to two is not apparent and the fundamental parameter A' does not appear explicitly. Hence, the new form of the performance equations here presented is of some theoretical interest. It is also of practical importance, since it leads to the construction of the simple charts developed in this paper, and these in turn may be of considerable assistance in working out actual performance problems.

B. PHYSICAL SIGNIFICANCE OF THE PERFORMANCE PARAMETER A'

It is apparent that the parameter A' , which has been unearthed and shown to have such importance by the procedure outlined above, should have some simple physical significance. In the attempt to discover what this physical interpretation may be, it will be convenient to consider the sea-level characteristics of what we shall call an "ideal airplane." This

¹ This section (II B) was contributed by Dr. C. B. Millikan, of the California Institute of Technology, aeronautics staff.

will be defined as an airplane for which the thrust horsepower available is independent of speed so that $T_v = 1$, and in connection with which the phenomenon of burbling does not occur. The latter requirement implies that the equivalent parasite area, as defined above in Section II A, remains always constant and that the lift coefficient has an infinite maximum value. In other words, an ideal airplane is one that obeys the performance equation for all values of the velocity V , and for which (at least at sea level) $t.hp_a = t.hp_m$. The power-available and power-required curves for a normal airplane and for the corresponding ideal airplane are indicated in Figure 2.

Let us consider the conditions for the sea level horizontal flight of such an airplane, denoting the velocity for horizontal flight by V_h .¹ The conditions are,

$$\sigma = T_a = T_v = 1, \frac{dh}{dt} = 0, V = R_v V_m = V_h.$$

Introducing these into the fundamental performance equation (2.19) we obtain an equation exactly analogous to (2.26), i. e.,

$$\Lambda' = \frac{\lambda_s \lambda_t}{V_h} \left(1 - \frac{\lambda_s \lambda_t}{V_h} \right)^{1/3}. \quad (2.28)$$

For simplicity in writing we may express this in the form,

$$\Lambda' = \Gamma(1 - \Gamma)^{1/3}; \quad \Gamma = \frac{\lambda_s \lambda_t}{V_h}. \quad (2.29)$$

For a given Λ' this is a fourth degree expression for Γ which is plotted in Figure 3 for positive values of Γ and Λ' . There are two real and two complex roots of this expression for the range of values of Λ' which are of interest for the present problem. For a definite value of Λ' (for example Λ'_o in fig. 3) the smaller of these real roots (say Γ_{o1}) is obviously given by

$\Gamma_{o1} = \frac{\lambda_s \lambda_t}{V_m}$ since it corresponds to the largest value of V satisfying the sea level horizontal flight condition. Hence, the portion of the curve between $\Gamma = 0$ and $\Gamma = 0.75$ is identical with Figure 1. The larger of the two roots may be written as $\Gamma_{o2} = \frac{\lambda_s \lambda_t}{V_o}$ where V_o is the minimum value of V for the sea level horizontal flight of the ideal airplane defined by the design parameter Λ'_o . The velocity of V_o is indicated in Figure 2 and may be called the "ideal minimum speed." The ratio of the two roots is $\frac{\Gamma_{o1}}{\Gamma_{o2}} = \frac{V_o}{V_m}$ and will be called "ideal speed ratio." From Figure 3 it is obvious that to every permissible value of Λ' there is a definite value of the ideal speed ratio. The relation between

Λ' and $\frac{V_o}{V_m}$ may be calculated numerically from equation (2.29). This has been done and the result plotted in Figure 4. It should be noted that for practically all normal airplanes $\Lambda' < 0.15$ so that in practice,

$$\Lambda' = \frac{V_o}{V_m} \text{ approximately.} \quad (2.30)$$

The significance of the parameter Λ' is now apparent. It determines uniquely the "ideal speed ratio" of an airplane and for normal planes is very nearly equal to this speed ratio. In attempting to visualize the effect of the ideal speed ratio on performance it is

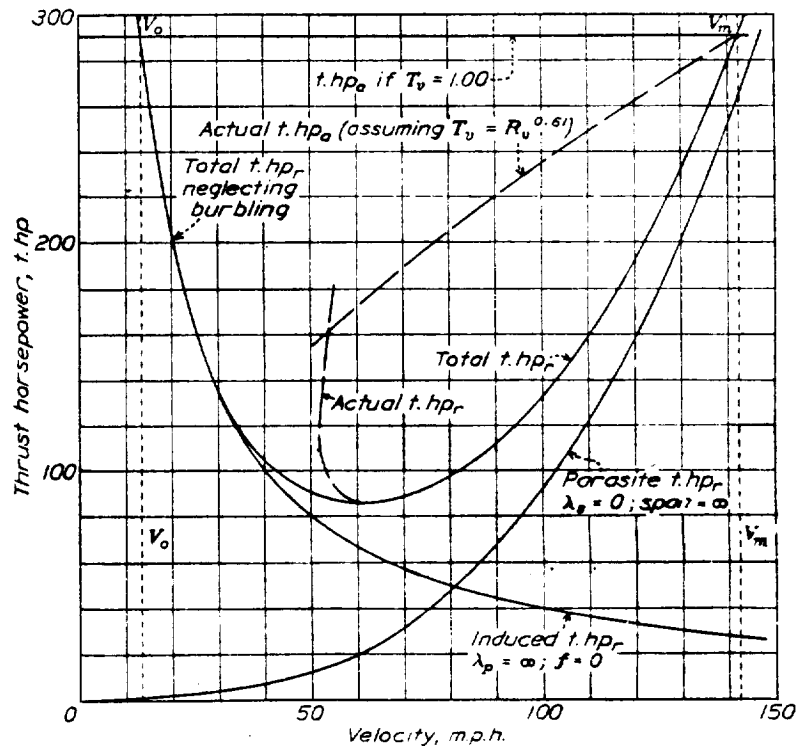


FIGURE 2.—Power curves for a normal airplane and its associated "ideal airplane." Assumed airplane characteristics: $\lambda_p = 250,000$; $\lambda_s = 800$; $\lambda_t = 0.025$; $\Lambda' = 0.0523$; $W = 4,000$ lb.; $S = 400$ sq. ft.; $C_{L_{max}} = 1.45$

very instructive to draw a series of actual and "ideal" power curves in which the span, parasite, and thrust horsepower loadings are varied individually. This procedure brings out very clearly the manner in which the various loadings affect the ideal speed ratio, and brings out the qualitative relation between the latter and the actual performance characteristics.

In addition to its intimate connection with the ideal speed ratio, Λ' also has the property of uniquely determining the speed ratios for maximum L/D and minimum power required. It is easy to show from the basic expression for sinking speed (see also Section VII) that,

$$\frac{\lambda_s \lambda_t}{V_{MP}} = (3\Lambda'^3)^{1/4} \text{ and } \frac{\lambda_s \lambda_t}{V_{LD}} = (\Lambda'^3)^{1/4} \quad (2.31)$$

where V_{MP} = velocity for minimum power required and V_{LD} = velocity for maximum L/D . But since

¹ In this section (II B) the subscript h represents horizontal flight and does not follow the convention given in the Summary of Notations.

$\frac{\lambda_s \lambda_t}{V_m}$ is a definite function of Λ' , it follows that $\frac{V_{MP}}{V_m}$ and $\frac{V_{LD}}{V_m}$ are also definite functions of Λ' . These relations have been calculated numerically and the results included in Figure 4. It is worthy of note that for $\Lambda' = 0.4725$ the velocity for minimum power required (V_{MP}), the ideal minimum velocity (V_o), and the design maximum velocity (V_m), all coincide. Hence, an airplane for which $\Lambda' = 0.4725$ could not leave the ground at sea level. This definite limit for the fundamental design parameter Λ' is one of the most interesting theoretical results brought out by the analysis of the present paper.

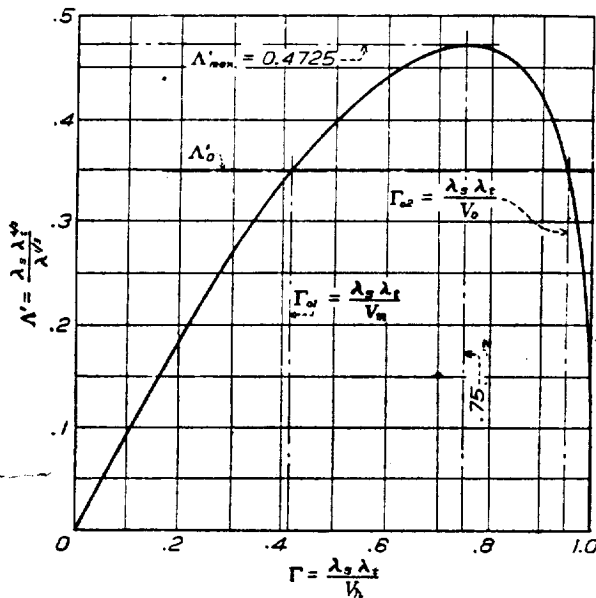


FIGURE 3.—Plot of the fourth degree relation connecting Λ' and Γ .

C. GENERAL FORMULAS FOR VARIOUS PERFORMANCE CHARACTERISTICS

Equations for the various performance characteristics of an airplane may be developed from the fundamental performance equation (2.22) and equation (2.26) for Λ' through the introduction of the appropriate special conditions governing each characteristic. The general formulas for the more important performance characteristics are given in this section.

These formulas are expressed in American engineering units in Section V. The effects of down load on the tail and inclination of the thrust axis are there numerically discussed.

Maximum velocity at sea level.—The two important forms of the maximum velocity equation have been developed earlier in the paper in equations (2.24) and (2.25) and are here rewritten for continuity,

$$V_m = \left(\frac{\lambda_p}{\lambda_t}\right)^{1/3} \left(1 - \frac{\lambda_s \lambda_t}{V_m}\right)^{1/3} \tag{2.32}$$

$$\frac{V_m}{\lambda_s \lambda_t} = \frac{1}{\Lambda'} \left(1 - \frac{\lambda_s \lambda_t}{V_m}\right)^{1/3} \tag{2.33}$$

Equation (2.33) is plotted in Figure 1. This figure is used in obtaining Λ' from $\frac{\lambda_s \lambda_t}{V_m}$ throughout the report, since the equations to be developed express performance in terms of $\frac{\lambda_s \lambda_t}{V_m}$ and it is more desirable that the final results be given in terms of Λ' .

Maximum velocity at altitude.—The condition for maximum velocity at altitude is $\frac{dh}{dt} = 0$. Introducing this condition equation (2.22) gives,

$$\frac{\lambda_s \lambda_t}{V_m} = \frac{T_a T_r \sigma R_{r_m} - \sigma^2 R_{r_m}^4}{1 - \sigma^2 R_{r_m}^4} \tag{2.34}$$

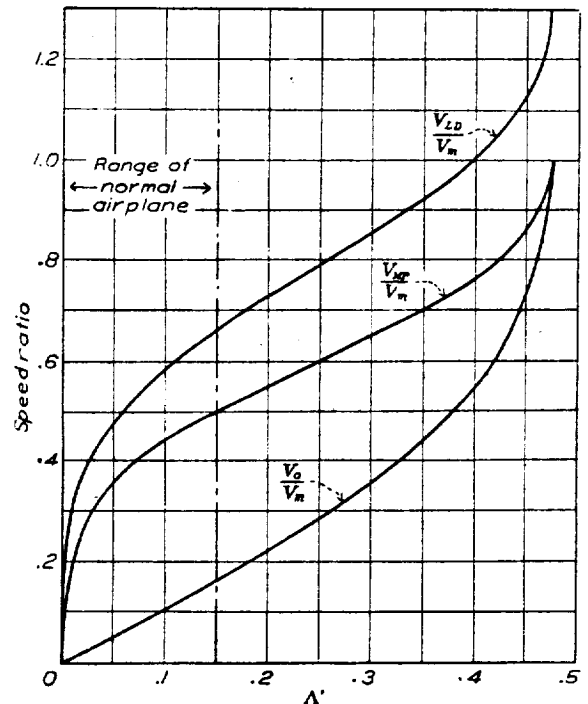


FIGURE 4.—Important speed ratios as functions of Λ' . V_m = design maximum velocity; V_o = ideal minimum velocity; V_{MP} = velocity for minimum power required; V_{LD} = velocity for maximum $\frac{L}{D}$; $\frac{V_o}{V_m}$ = ideal speed ratio

where,

$$R_{r_m} = \frac{V \text{ maximum at altitude}}{V \text{ maximum at sea level}} = \frac{V_m h}{V_m} \tag{2.35}$$

Substituting equation (2.34) in equation (2.26), we get,

$$\Lambda' = \frac{T_a T_r \sigma R_{r_m} - \sigma^2 R_{r_m}^4}{1 - \sigma^2 R_{r_m}^4} \tag{2.36}$$

$$\left(1 - \frac{T_a T_r \sigma R_{r_m} - \sigma^2 R_{r_m}^4}{1 - \sigma^2 R_{r_m}^4}\right)^{1/3}$$

Equation (2.36) is the general formula for Λ' in terms of σ and R_{r_m} . The substitution indicated for obtaining equation (2.36) from (2.34) is readily performed graphically from Figure 1, which gives Λ' as a function of $\frac{\lambda_s \lambda_t}{V_m}$.

It is seen then, that for any general type of airplane, i. e., for any specific functions T_a and T_v , R_{v_m} is given as a function of σ (corresponding to altitude) and Λ' . The maximum velocity at altitude V_{m_h} is then obtained from the maximum velocity at sea level and R_{v_m} according to equation (2.35).

Equation (2.36) has been plotted in Figure 5 for particular functions T_a and T_v corresponding to "normal present-day propulsive units" with unsupercharged engines to show the nature of the dependence of R_{v_m} on Λ' and altitude (σ).

Maximum rate of climb at any altitude; speed for maximum climb.—The speed at which maximum rate of climb occurs is obtained by differentiating $\frac{dh}{dt}$ with

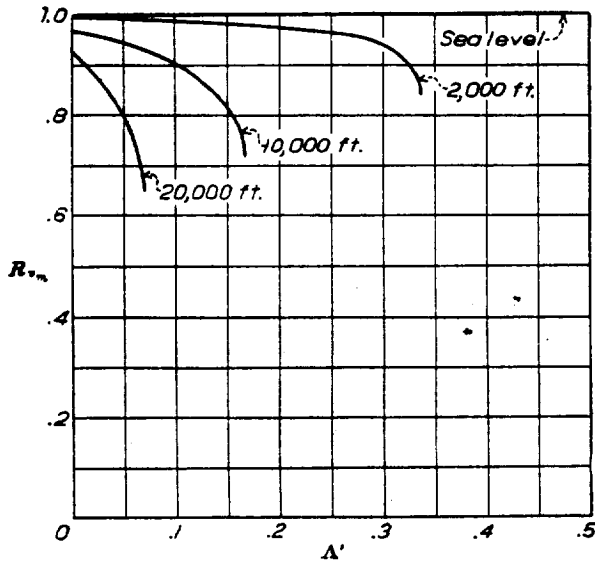


FIGURE 5.— R_{v_m} as a function of Λ' and altitude (σ)

respect to R_v and equating to zero. The rate of climb at this speed, hence the maximum rate of climb is obtained by incorporating the above result in the equation for rate of climb. Differentiating equation (2.22) with respect to R_v and equating to zero,

$$\frac{\partial}{\partial R_v} \frac{dh}{dt} = \frac{1}{\lambda_t} \left[\left(\frac{\partial T_a T_v}{\partial R_{v_c}} - 3\sigma R_{v_c}^2 \right) - \frac{\lambda_s \lambda_t}{V_m} \left(-\frac{1}{\sigma R_{v_c}^2} - 3\sigma R_{v_c}^2 \right) \right] = 0 \quad (2.37)$$

$$= \frac{1}{\sigma R_{v_c}^2 \lambda_t} \left[\left(\frac{\partial T_a T_v}{\partial R_{v_c}} \sigma R_{v_c}^2 - 3\sigma^2 R_{v_c}^4 \right) + \frac{\lambda_s \lambda_t}{V_m} (1 + 3\sigma^2 R_{v_c}^4) \right] = 0 \quad (2.38)$$

where,

$$R_{v_c} = \frac{\text{Speed for maximum climb at any altitude}}{\text{Maximum velocity at sea level}}$$

$$\frac{\partial T_a T_v}{\partial R_{v_c}} = \frac{\partial (T_a T_v)}{\partial R_v} \text{ at } R_{v_c} \text{ (}\sigma \text{ constant)} \quad (2.39)$$

whence,

$$\frac{\lambda_s \lambda_t}{V_m} = \frac{-\sigma R_{v_c}^2 \frac{\partial T_a T_v}{\partial R_{v_c}} + 3 \sigma^2 R_{v_c}^4}{1 + 3 \sigma^2 R_{v_c}^4} \quad (2.40)$$

Substituting equation (2.40) in equations (2.22) and (2.26),

$$\lambda_t C_h = \frac{1}{\sigma R_{v_c}} \left[(T_a T_v \sigma R_{v_c} - \sigma^2 R_{v_c}^4) - (1 - \sigma^2 R_{v_c}^4) \frac{-\sigma R_{v_c}^2 \frac{\partial T_a T_v}{\partial R_{v_c}} + 3 \sigma^2 R_{v_c}^4}{1 + 3 \sigma^2 R_{v_c}^4} \right] \quad (2.41)$$

where, C_h = maximum rate of climb.

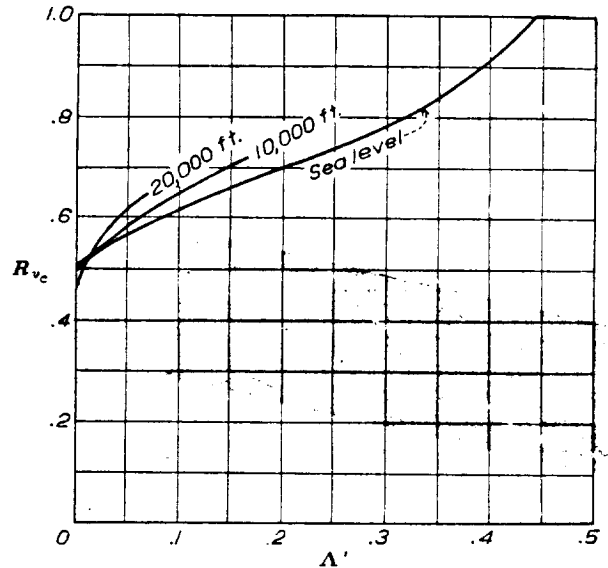


FIGURE 6.— R_{v_c} as a function of Λ' and altitude (σ)

$$\Lambda' = \frac{-\sigma R_{v_c}^2 \frac{\partial T_a T_v}{\partial R_{v_c}} + 3 \sigma^2 R_{v_c}^4}{1 + 3 \sigma^2 R_{v_c}^4} \quad (2.42)$$

$$\left(1 - \frac{-\sigma R_{v_c}^2 \frac{\partial T_a T_v}{\partial R_{v_c}} + 3 \sigma^2 R_{v_c}^4}{1 + 3 \sigma^2 R_{v_c}^4} \right)^{1/2}$$

The substitution of the equation (2.40) in equation (2.26) to obtain Λ' is most readily performed graphically by means of Figure 1, instead of analytically as has been done in obtaining equation (2.42).

Assuming the "normal propulsive unit" expressions for T_a and T_v which were used in obtaining Figure 5, equation (2.42) has been plotted in Figure 6. Equation (2.41), when combined with the results expressed in this figure, gives $\lambda_t C_h$ as a function of Λ' and σ , and this relation has been plotted in Figure 7. These two figures indicate clearly the nature of the dependence of R_{v_c} and $\lambda_t C_h$ on an airplane's design characteristics (Λ') and on altitude, and hence lead to a very rapid determination of the speed for best climb and the maximum rate of climb of the airplane at any altitude.

Maximum rate of climb at sea level is the special case of maximum rate of climb at altitude for which $\sigma = 1$ and $T_a = 1$. The general statements made in the preceding paragraphs concerning maximum rate of climb at any altitude apply to the maximum rate of climb at sea level.

Absolute ceiling; speed at absolute ceiling.—At absolute ceiling, the maximum rate of climb is zero. Therefore, putting $C_h = 0$ in equation (2.41), we get,

$$\frac{1 - \sigma_H^2 R_{vH}^4}{T_a T_v \sigma_H R_{vH} - \sigma_H^2 R_{vH}^4} = \frac{1 + 3\sigma_H^2 R_{vH}^4}{-\sigma_H R_{vH}^2 \frac{\partial T_v T_a}{\partial R_{vH}} + 3\sigma_H^2 R_{vH}^4} \tag{2.43}$$

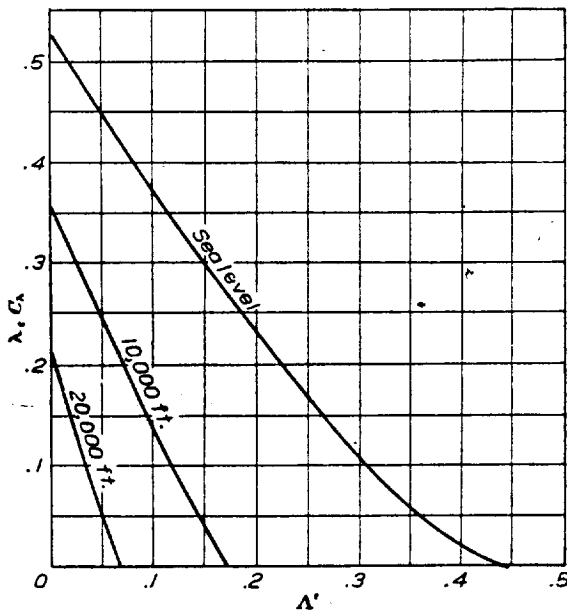


FIGURE 7.— $\lambda_c C_h$ as a function of A' and altitude (σ)

where,

$$R_{vH} = \frac{\text{Velocity at absolute ceiling}}{\text{Maximum velocity at sea level}} \tag{2.44}$$

$$\sigma_H = \text{relative density at absolute ceiling.} \tag{2.45}$$

Cross multiplying, collecting terms, and dividing throughout by $\sigma_H R_{vH}$,

$$T_a T_v (1 + 3\sigma_H^2 R_{vH}^4) + R_{vH} \frac{\partial T_v T_a}{\partial R_{vH}} (1 - \sigma_H^2 R_{vH}^4) - 4\sigma_H R_{vH}^3 = 0. \tag{2.46}$$

Equation (2.46) shows that for any general type of propulsive unit, R_{vH} (the speed ratio at absolute ceiling) is a function of σ_H (corresponding to altitude at absolute ceiling). Putting $\frac{dh}{dt} = 0$ and $\sigma = \sigma_H$ in equation (2.22), and replacing Rv by the value of R_{vH} given by equation (2.46), we get,

$$\frac{\lambda_s \lambda_t}{V_m} = \frac{T_a T_v \sigma_H R_{vH} - \sigma_H^2 R_{vH}^4}{1 - \sigma_H^2 R_{vH}^4} \tag{2.47}$$

and,

$$\Lambda' = \frac{T_a T_v \sigma_H R_{vH} - \sigma_H^2 R_{vH}^4}{1 - \sigma_H^2 R_{vH}^4} \tag{2.48}$$

$$\left(1 - \frac{T_a T_v \sigma_H R_{vH} - \sigma_H^2 R_{vH}^4}{1 - \sigma_H^2 R_{vH}^4}\right)^{1/3}$$

Equation (2.48) gives Λ' as a function of absolute ceiling, since R_{vH} is a function of absolute ceiling by equation (2.46). The value of R_{vH} corresponding to any σ_H must be found by a trial and error solution of equation (2.46). Λ' is then determined from these corresponding values of R_{vH} and σ_H . Therefore, by means of equations (2.46) and (2.48), absolute ceiling is obtained as a function of Λ' for any general type of propulsive unit.

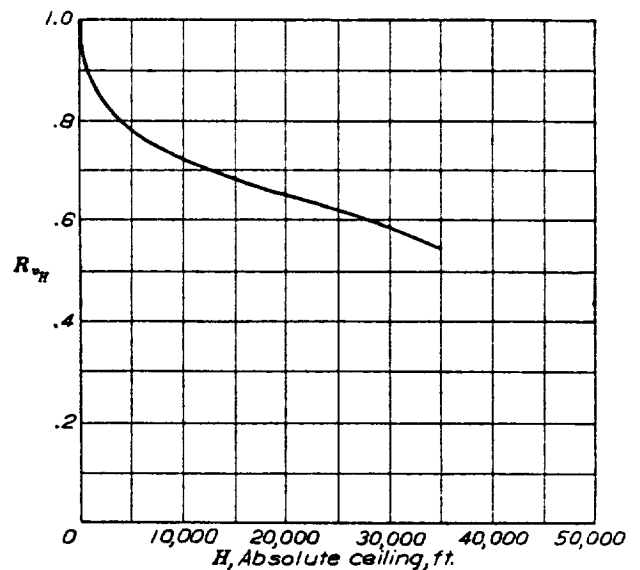


FIGURE 8.— R_{vH} as a function of absolute ceiling

Equation (2.48) is best solved graphically from equation (2.47) by means of Figure 1. The solution of equation (2.46) by trial and error is not particularly difficult when T_a and T_v are specified, i. e., the type of propulsive unit is specified. The solution then applies to all airplanes similarly equipped. Equation (2.46) has been plotted in Figure 8 assuming the "normal propulsive unit" mentioned above. The results given in this figure have been combined with equation (2.48) and the results plotted in Figure 9. These curves indicate the nature of the dependence of absolute ceiling on the airplane parameter Λ' and of the speed ratio at absolute ceiling on the ceiling altitude.

Absolute ceiling as a function of Λ' may be completely solved graphically from the maximum-rate-of-climb-at-altitude charts. At any altitude, the value of Λ' at which the maximum rate of climb becomes zero is the value of Λ' for absolute ceiling at that altitude. (See figs. 7 and 9.) It is suggested, therefore, that when curves for maximum rate of climb have been calculated, absolute ceiling as a function of Λ' may be obtained most easily in this manner.

Service ceiling.—By definition, service ceiling is the altitude at which the maximum rate of climb has a certain constant value C_{h_s} . The equations for service ceiling are, therefore, equations (2.41) and (2.42) for maximum rate of climb at altitude in which the substitution $C_h = C_{h_s}$ is made.

Service ceiling as a function of Λ' and λ_i may most readily be solved graphically from charts for maximum rate of climb at altitude. At any altitude, the value of Λ' at which the maximum rate of climb becomes $C_{h_s}\lambda_i$ is the value of Λ' for service ceiling at that altitude. For any value of λ_i , then, service ceiling may be plotted as a function of Λ' . A family of curves for a range of λ_i 's covering all normal values may be plotted in this manner, thereby giving service ceiling as a function of Λ' and λ_i . Figure 10 has been prepared in this way for the "normal propulsive unit" used above.

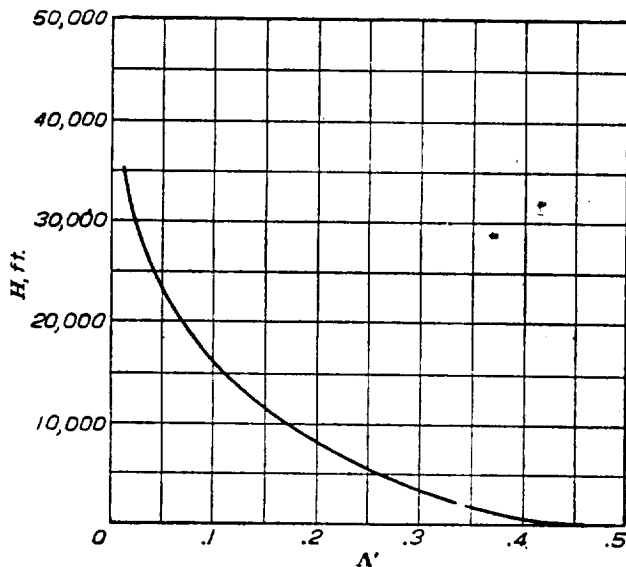


FIGURE 9.—Absolute ceiling as a function of Λ'

Minimum time to climb to any altitude.—The time required to climb through an infinitesimal change in altitude dh is $\frac{dt}{dh} dh$ where $\frac{dh}{dt}$ is the rate of climb. The minimum time required may be expressed by $\frac{1}{C_h} dh$, since C_h has been defined as the maximum rate of climb at the altitude considered. In order to find the minimum time required to climb from one altitude h_1 to a second altitude h_2 , the above expression must be integrated between the limits h_1 and h_2 . Then,

$$T = \int_{h_1}^{h_2} \frac{1}{C_h} dh \tag{2.49}$$

where T = the minimum time required to climb from altitude h_1 to altitude h_2 .

The equations and charts for maximum rate of climb have expressed the results in terms of $\lambda_i C_h$ and not simply C_h . Equation (2.49) must be divided

throughout by λ_i , in order that the integration may be performed in terms of $\lambda_i C_h$.

$$\frac{T}{\lambda_i} = \int_{h_1}^{h_2} \frac{1}{\lambda_i C_h} dh \tag{2.50}$$

Equation (2.50) shows the method by which time to climb must be determined. For any values of Λ' a curve giving $\frac{1}{\lambda_i C_h}$ against altitude is plotted. The integration of this curve between the desired altitudes leads to the corresponding values of $\frac{T}{\lambda_i}$ according to equation (2.50). This procedure is repeated for several values of Λ' . In this manner a chart is obtained giving $\frac{T}{\lambda_i}$ as a function of Λ' and altitude.

The integration indicated above must be performed graphically, by Simpson's Rule or some similar method.

General time-required-to-climb curves may be obtained in this manner for any general type of aircraft propulsive unit. Such curves are based on the

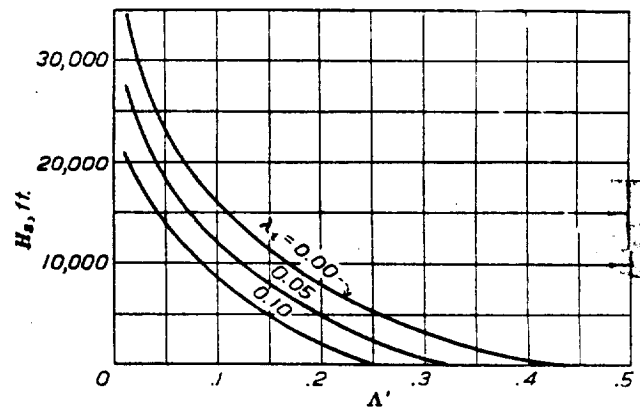


FIGURE 10.—Service ceiling as a function of Λ' and λ_i

actual rates of climb at altitude as determined by the fundamental equations for maximum rate of climb at altitude. The results obtained therefore have the same accuracy as the maximum rate of climb results. The complete integration need be performed only once for each general type of propulsive unit. Time to climb for airplanes having this type of propulsive unit may then be immediately obtained from the general chart. Figure 11, based on the "normal propulsive unit," shows the type of relation obtained between time to climb T , airplane design characteristics Λ' and λ_i , and altitude attained in time T .

III. VARIATION OF PERFORMANCE WITH A CHANGE OF PARAMETERS

One of the greatest advantages of the formulas and resulting charts is the explicit manner in which the dependence of each performance characteristic of the airplane upon its various parameters is shown. The variation of performance with each parameter of the airplane may easily be seen. Thus the particular

parameter that need be changed and the amount of change that will be necessary when a certain variation of performance is desired, consequently the particular detail of the airplane that need be changed, is readily determined. The parameter that is most effective in producing the desired change in performance is not necessarily the parameter that is most economically altered. Through the formulas and charts developed here, the relative merits and effectiveness of each parameter in producing the desired change in performance may be weighed. The designer is thus given a

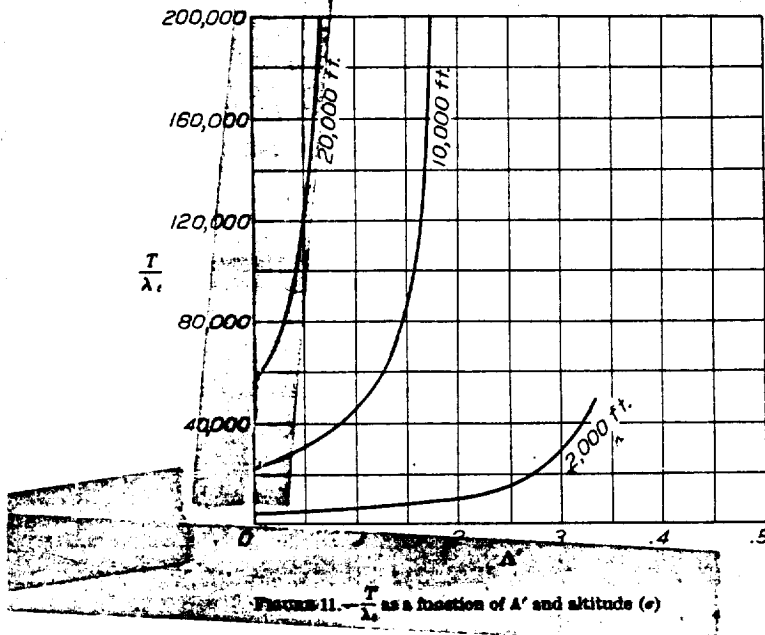


FIGURE 11.— $\frac{T}{\lambda_e}$ as a function of Λ' and altitude (e)

direct tool for making changes to fit his particular requirements.

The algebraic formulas of Section II and the accompanying curves are here used to develop simplified expressions which show explicitly the dependence of performance upon the parameters. These expressions may be used in combination with general performance curves for any type of propulsive unit to construct charts giving the change of the various performance characteristics resulting from a per cent change in the parameters: Weight, design thrust horsepower available, effective span, and equivalent parasite area.

Thus for reasonably small percentage changes in the parameters, the variation in performance is found by multiplying the change due to 1 per cent by the percentage change. Such curves have been drawn for airplanes equipped with unsupercharged engines and present-day metal propellers. The curves are shown in Figure 37 and their use described in Section VI.

Variation of maximum velocity at sea level.—From equation (2.23),

$$V_m = \left(\frac{\lambda_p}{\lambda_t}\right)^{\frac{1}{2}} \left(1 - \frac{\lambda_e \lambda_t}{V_m}\right)^{\frac{1}{2}} \quad (3.1)$$

All symbols are defined in Section II and in the Summary of Notation. The effect of the variation of the second parentheses upon maximum velocity is small, so to a first approximation we may take,

$$V_m = K \left(\frac{\lambda_p}{\lambda_t}\right)^{\frac{1}{2}} = 0.98 \left(\frac{\lambda_p}{\lambda_t}\right)^{\frac{1}{2}} = 75.8 \left(\frac{t.hp_m}{f}\right)^{\frac{1}{2}} \quad (3.2)$$

Equation (3.2) may be used to obtain maximum velocity within 1 or 2 per cent accuracy. The constant 0.98 has been obtained by using a mean $\frac{V_m}{\lambda_e \lambda_t} = 15$, which corresponds to a Λ' of about 0.06 (an average observation airplane).

We are well justified in substituting equation (3.2) for V_m in the term containing V_m on the right-hand side of equation (3.1). Thus for an explicit and accurate expression for maximum velocity at sea level,

$$V_m = \left(\frac{\lambda_p}{\lambda_t}\right)^{\frac{1}{2}} \left(1 - \frac{\lambda_e \lambda_t}{\lambda_p^{\frac{1}{2}} \frac{1}{0.98}}\right)^{\frac{1}{2}} \quad (3.3)$$

$$V_m = \left(\frac{\lambda_p}{\lambda_t}\right)^{\frac{1}{2}} (1 - 1.02 \Lambda')^{\frac{1}{2}} = 77.3 \left(\frac{t.hp_m}{f}\right)^{\frac{1}{2}} \quad (3.4)$$

$$\left(1 - 0.006419 \frac{W^2 f^{\frac{1}{2}}}{t.hp_m^{\frac{1}{2}} b_e^2}\right)^{\frac{1}{2}}$$

Where great accuracy is desired equation (3.4) should be used.

In order to find the variation of maximum velocity with the parameters of the airplane, V_m from equation (3.4) is differentiated with respect to each of the various parameters as a partial differentiation. Differentiating with respect to f , and dividing by V_m , we get,

$$\frac{1}{V_m} \frac{dV_m}{df} df = \frac{77.3 \left[-\frac{1}{3} \frac{t.hp_m}{f^{\frac{3}{2}}} \left(1 - 0.006419 \frac{W^2 f^{\frac{1}{2}}}{t.hp_m^{\frac{1}{2}} b_e^2}\right)^{\frac{1}{2}} + \frac{1}{3} \left(\frac{t.hp_m}{f}\right)^{\frac{1}{2}} \frac{\left(-\frac{1}{3} 0.006419 \frac{W^2 f^{-\frac{3}{2}}}{t.hp_m^{\frac{1}{2}} b_e^2}\right)}{\left(1 - 0.006419 \frac{W^2 f^{\frac{1}{2}}}{t.hp_m^{\frac{1}{2}} b_e^2}\right)^{\frac{1}{2}}}\right]}{77.3 \left(\frac{t.hp_m}{f}\right)^{\frac{1}{2}} \left(1 - 0.006419 \frac{W^2 f^{\frac{1}{2}}}{t.hp_m^{\frac{1}{2}} b_e^2}\right)^{\frac{1}{2}}} \quad (3.5)$$

$$\left(\frac{dV_m}{V_m}\right)_f = \left[-\frac{1}{3} \frac{1}{f} + \frac{1}{3} \left(\frac{-\frac{1}{3} 1.02 \Lambda' \frac{1}{f}}{1 - 1.02 \Lambda'}\right) \right] df \quad (3.6)$$

whence for the percentage variation of V_m with respect to a certain percentage variation of f ,

$$\left(\frac{dV_m}{V_m}\right)_f = \left(-\frac{1}{3} - \frac{1}{9} \frac{1.02\Lambda'}{1-1.02\Lambda'}\right) \frac{df}{f} = -\alpha \frac{df}{f} \quad (3.7)$$

Similarly for the variation with $t.hp_m$,

$$\left(\frac{dV_m}{V_m}\right)_{t.hp_m} = \left(\frac{1}{3} + \frac{4}{9} \frac{1.02\Lambda'}{1-1.02\Lambda'}\right) \frac{dt.hp_m}{t.hp_m} = \beta \frac{dt.hp_m}{t.hp_m} \quad (3.8)$$

For variation with W ,

$$\left(\frac{dV_m}{V_m}\right)_W = \left(-\frac{2}{3} \frac{1.02\Lambda'}{1-1.02\Lambda'}\right) \frac{dW}{W} = -\gamma \frac{dW}{W} \quad (3.9)$$

For variation with b_e ,

$$\left(\frac{dV_m}{V_m}\right)_{b_e} = \left(\frac{2}{3} \frac{1.02\Lambda'}{1-1.02\Lambda'}\right) \frac{db_e}{b_e} = \gamma \frac{db_e}{b_e} \quad (3.10)$$

It should be noted that the pseudoconstants α , β , $-\gamma$, and γ are functions of Λ' and Λ' is a function of each parameter. The percentage variations must be plotted against Λ' .

The variation of maximum velocity at sea level with a change in any parameter is readily determined from equations (3.7) to (3.10). These equations give a method of good precision for finding the effect of a change in any parameter on maximum velocity. If the change in the parameter causes considerable change in Λ' , the value of the pseudoconstant α , β , or γ corresponding to a mean Λ' should be used. This practice is seldom necessary. It is generally sufficiently accurate to multiply the variation due to a 1 per cent change in the parameter by the percentage change in the parameter. The curve for variation of V_m is plotted in Figure 12, and is indicative of the general nature of the variation curves developed in this section.

Variation of maximum rate of climb at sea level.—

The variation of $\lambda_i C_h$ with Λ' at sea level is very approximately a straight line, as may be seen in Figure 7. At any Λ' , assuming the straight line variation and denoting C_h at sea level by C_o , we have

$$\lambda_i C_o = B - D\Lambda' \quad (3.11)$$

where,

$$B = \lambda_i C_o \text{ at } \Lambda' = 0$$

$$-D = \text{slope.}$$

Then,

$$C_o = \frac{B}{\lambda_i} - D \frac{\Lambda'}{\lambda_i} = B' \frac{t.hp_m}{W} - D' \frac{Wf^{3/4}}{t.hp_m^{3/4} b_e^2} \quad (3.12)$$

Differentiating with respect to each parameter and dividing by C_o in order to find the percentage variation of C_o , we get, for variation of C_o with W ,

$$\frac{1}{C_o} \frac{dC_o}{dW} dW = \frac{-B' \frac{t.hp_m}{W^2} - D' \frac{f^{3/4}}{t.hp_m^{3/4} b_e^2}}{B' \frac{t.hp_m}{W} - D' \frac{Wf^{3/4}}{t.hp_m^{3/4} b_e^2}} dW \quad (3.13)$$

$$\left(\frac{dC_o}{C_o}\right)_W = \left(\frac{-B - D\Lambda'}{B - D\Lambda'}\right) \frac{dW}{W} = -s \frac{dW}{W} \quad (3.14)$$

Similarly for variation with $t.hp_m$,

$$\left(\frac{dC_o}{C_o}\right)_{t.hp_m} = \left(\frac{B + \frac{3}{4}D\Lambda'}{B - D\Lambda'}\right) \frac{dt.hp_m}{t.hp_m} = r \frac{dt.hp_m}{t.hp_m} \quad (3.15)$$

For variation with b_e ,

$$\left(\frac{dC_o}{C_o}\right)_{b_e} = \left(\frac{2D\Lambda'}{B - D\Lambda'}\right) \frac{db_e}{b_e} = 6t \frac{db_e}{b_e} \quad (3.16)$$

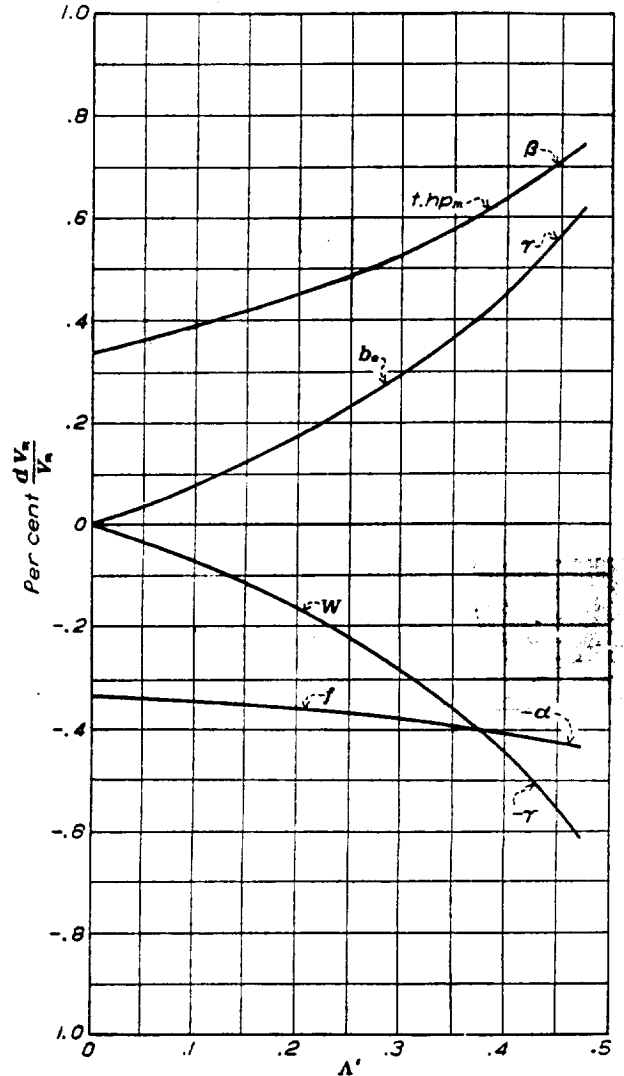


FIGURE 12.—Per cent change in maximum velocity due to 1 per cent (+ 1 per cent) change in parameter

For variation with f ,

$$\left(\frac{dC_o}{C_o}\right)_t = \left(\frac{-\frac{3}{4}D\Lambda'}{B - D\Lambda'}\right) \frac{df}{f} = -t \frac{df}{f} \quad (3.17)$$

Equations (3.14) to (3.17) furnish an excellent means of determining the variations of maximum rate of climb at sea level with a change in the various parameters. The pseudoconstants are functions of Λ' and also depend on the type of propulsive unit (T_a and T_s). Their numerical values have been determined for the specific type of propulsive unit considered in Sections V and VI, and the corresponding curves are plotted in Figure 37.

A similar analysis may be used to give the variation of maximum rate of climb at any altitude with a change in parameters.

Variation of absolute ceiling.—For small variations of Λ' , i. e., for airplanes of the same type, the variation H with Λ' may be assumed to be linear. Then,

$$H = F - G\Lambda' \quad (3.18)$$

where
and

$$-G = \text{slope}$$

$$\frac{dH}{H} = \left(\frac{-G\Lambda'}{F - G\Lambda'} \right) \frac{d\Lambda'}{\Lambda'} \quad (3.19)$$

Differentiating Λ' with respect to the various parameters, we get for the various equations of variation,

$$\left(\frac{dH}{H} \right)_w = \left(\frac{-2G\Lambda'}{F - G\Lambda'} \right) \frac{dW}{W} = -6v \frac{dW}{W} \quad (3.20)$$

$$\left(\frac{dH}{H} \right)_{t.\text{hp}_m} = \left(\frac{-\frac{1}{2}G\Lambda'}{F - G\Lambda'} \right) \frac{dt.\text{hp}_m}{t.\text{hp}_m} = 4v \frac{dt.\text{hp}_m}{t.\text{hp}_m} \quad (3.21)$$

$$\left(\frac{dH}{H} \right)_{b_s} = \left(\frac{2G\Lambda'}{F - G\Lambda'} \right) \frac{db_s}{b_s} = 6v \frac{db_s}{b_s} \quad (3.22)$$

$$\left(\frac{dH}{H} \right)_f = \left(\frac{-\frac{1}{2}G\Lambda'}{F - G\Lambda'} \right) \frac{df}{f} = -v \frac{df}{f} \quad (3.23)$$

Equations (3.20) to (3.23) may be used to find the variation of absolute ceiling due to a variation in the parameters, and show the relative effect of a variation in each. The numerical values of the pseudoconstants are given in Figure 37 in the same manner as has been done for the constants of the preceding paragraph.

Variation of time to climb to altitude.—Considering the variation of $\frac{T}{\lambda_s}$ with Λ' to be linear for a small range of variation of Λ' , we obtain, as in the previous analysis for maximum rate of climb, the equations of variation for time to climb.

$$\left(\frac{dT}{T} \right)_w = x \frac{dW}{W} \quad (3.24)$$

$$\left(\frac{dT}{T} \right)_{t.\text{hp}_m} = -y \frac{dt.\text{hp}_m}{t.\text{hp}_m} \quad (3.25)$$

$$\left(\frac{dT}{T} \right)_{b_s} = -6z \frac{db_s}{b_s} \quad (3.26)$$

$$\left(\frac{dT}{T} \right)_f = z \frac{df}{f} \quad (3.27)$$

The values of the pseudoconstants x , $-y$, $-6z$, and z have been determined for the time to climb to 5,000 and 10,000 feet for the type of propulsive unit considered in Sections V and VI, and the results indicated in Figure 37.

Variation of the major parameter of performance, Λ' .—The variation of Λ' with the various parameters

of the airplane is readily determined by the use of equation (2.25) for Λ' given in Section II,

$$\Lambda' = \frac{\lambda_s \lambda_f^{3/4}}{\lambda_p^{3/4}} = \frac{2W}{\pi \rho_o b_s^2} \frac{W^{3/4}}{A^{3/4} t.\text{hp}_m^{3/4}} \frac{\rho_o^{3/4} f^{3/4}}{2^{3/4} V^{3/4}} \quad (3.28)$$

$$= \frac{2^{3/4}}{\pi} \frac{1}{A^{3/4} \rho_o^{3/4} t.\text{hp}_m^{3/4} b_s^2} W^{2f^{3/4}} \quad (3.28)$$

$$\Lambda' = 0.5055 \frac{1}{A^{3/4} \rho_o^{3/4} t.\text{hp}_m^{3/4} b_s^2} W^{2f^{3/4}} \quad (3.29)$$

The variation equations are,

$$\left(\frac{d\Lambda'}{\Lambda'} \right)_w = 2 \frac{dW}{W} \quad (3.30)$$

$$\left(\frac{d\Lambda'}{\Lambda'} \right)_f = \frac{1}{3} \frac{df}{f} \quad (3.31)$$

$$\left(\frac{d\Lambda'}{\Lambda'} \right)_{b_s} = -2 \frac{db_s}{b_s} \quad (3.32)$$

$$\left(\frac{d\Lambda'}{\Lambda'} \right)_{t.\text{hp}_m} = -\frac{4}{3} \frac{dt.\text{hp}_m}{t.\text{hp}_m} \quad (3.33)$$

It is notable that all variations that tend to decrease performance cause an increase in Λ' . Hence an increase in Λ' is accompanied by a decrease in performance of the airplane.

IV. INVESTIGATION OF FULL-SCALE DATA

The general fundamental performance formulas have been developed in Sections II and III. For the application of these formulas to any general type of airplane, the functions T_s and T_a (see equation (2.15)), must be expressed analytically, or graphically as functions of R , and σ . The best value of the efficiency factor e (equation (2.11a)) for any type airplane must be determined. This section deals briefly with an investigation of full-scale data for determining these characteristics.

Brake horsepower variation with r. p. m.—Modern airplane engines quite generally have their rated brake horsepower occurring at an r. p. m. which is less than 80 per cent of the r. p. m. at which the peak brake horsepower occurs. From an investigation of a number of brake horsepower curves, it has been found that below the rated horsepower, the variation of brake horsepower with r. p. m. is well represented by the simple relation,

$$b.\text{hp} = K \times \text{r. p. m.} \quad (4.0)$$

where K is a constant depending upon the particular engine, or

$$\frac{b.\text{hp}}{b.\text{hp}_m} = \frac{\text{r. p. m.}}{\text{r. p. m.}_m} \quad (4.0a)$$

where subscript m denotes *rated*. This variation has been suggested by Diehl for use with modern engines. (Reference 5.)

In all calculations to follow requiring the variation of brake horsepower with r. p. m. a general linear variation corresponding to the equation (4.0a) is used. The general performance charts presented at the end of the report, which are developed for modern airplanes with fixed-pitch metal propellers, are based on the linear variation of brake horsepower with r. p. m. (below the rated maximum r. p. m.)

Fixed-pitch metal propeller data.—

The fixed-pitch metal propeller (adjustable on the ground) is the type that is most in use at the present; so the following discussion applies in particular to this type. National Advisory Committee for Aeronautics Technical Report No. 306 (reference 6) presents complete full-scale characteristics of Navy propeller No. 4412. In a subsequent report concerning an investigation of five metal propellers (reference 7), it may be seen that the change in characteristics for the various propellers is small. Owing to the fact that the characteristics of any propeller change with the type installation, it is felt that the characteristics of Navy propeller No. 4412 may well be taken as the general representative of all fixed-pitch metal propellers. Efficiencies given are propulsive efficiencies and are of great value in determining performance as a mean slip-stream and a mean cowling effect are thus included.

Figure 13 has been plotted directly from data of National Advisory Committee for Aeronautics Technical Report No. 306. The proper propeller diameter and setting for any airplane and engine combination is found by use of this chart. The airplane and engine combination determines a particular value of the coefficient C_s , from which is found the $\frac{V}{ND}$ ratio corresponding to the "Best performance propeller" or the "Peak efficiency propeller" as desired. The coefficient is defined by,

$$C_s = \frac{\rho^{1/2} V}{(550 \text{ b. hp})^{1/2} \times N^{3/4}} = \frac{0.638 \text{ m. p. h.}}{\text{b. hp}^{1/2} \text{ r. p. m.}^{3/4}} \quad (4.1)$$

(at sea level)

and $J = V/ND$ is defined by,

$$J = \frac{V}{ND} = \frac{88 \text{ m. p. h.}}{\text{r. p. m.} \times D} \quad (4.2)$$

where,

D = diameter in ft.

N = revolutions per second of propeller

V = velocity in ft./sec.

(A chart for the solution of C_s is given in Figure 26.)

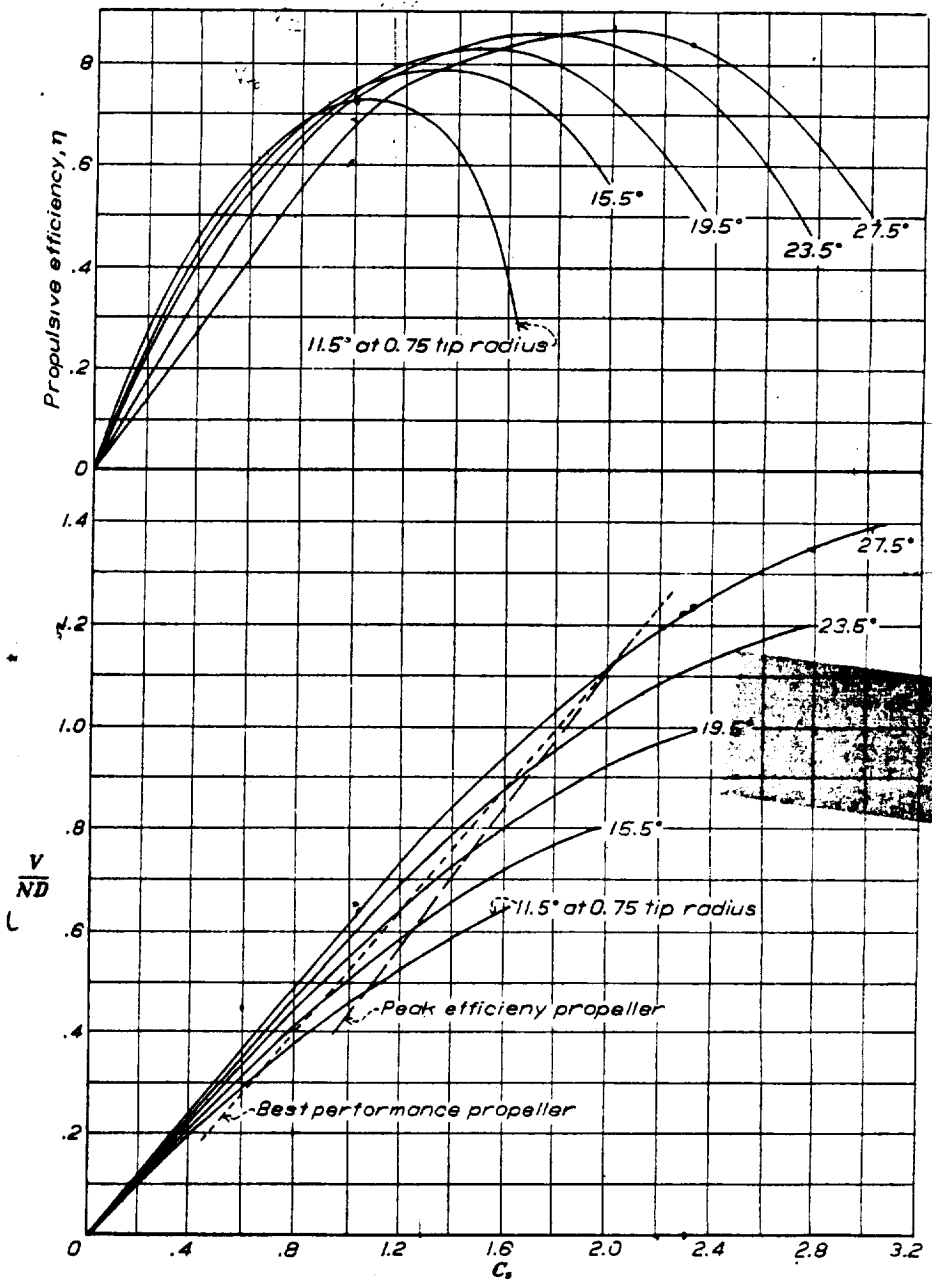


FIGURE 13.—Propeller characteristics of Navy metal propeller No. 4412. (National Advisory Committee for Aeronautics Technical Report No. 306.) Propellers set for best performance and peak efficiency are indicated

Assuming that the maximum rate of climb of an airplane occurs at $R_v = 0.625$, which has been found from Army flight test data to be a good mean value, an investigation has been made to determine at what position on the propeller-efficiency curve maximum velocity should occur in order that the airplane might have the maximum possible rate of climb. The results are clearly set forth in Figures 14a and 14b; the results are plotted in terms of C_s and $\frac{V}{ND}$. It is well known

that for maximum possible velocity the propeller should be set so that V_{\max} occurs on the envelope of the efficiency versus C_s curves. The ratio $\frac{C_s \text{ at } V_m}{C_s \text{ peak}}$ at which this occurs is represented by the curve labeled "FOR MAXIMUM VELOCITY." Obviously with V_{\max} set on the peak of the efficiency curve, $\frac{C_s \text{ at } V_m}{C_s \text{ peak}} = 1.00$; this line is designated "PEAK PROPELLER." The setting of the propeller at V_m in order that maximum possible rate of climb be attained is represented by the curve labeled "FOR MAXIMUM CLIMB." This curve discloses the very interesting and fortunate fact that the propeller should be set at approximately the same setting both for the attainment of maximum possible velocity and climb. Thus a propeller for which maximum velocity occurs at the peak produces both a lower maximum velocity

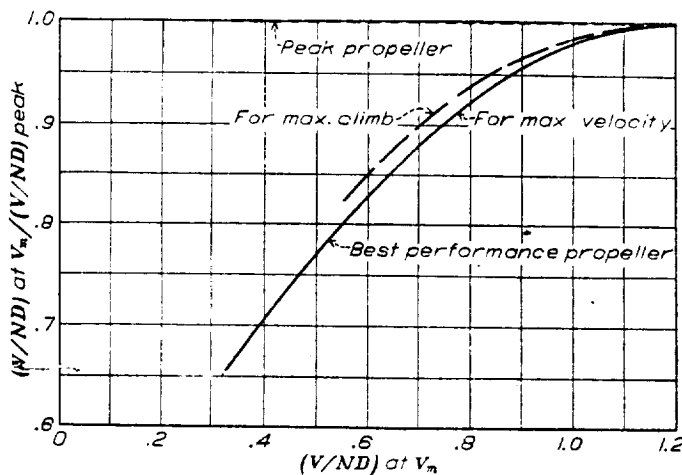


FIGURE 14a.—Comparison of propeller settings at V_{\max} for obtaining best maximum climb, best maximum velocity, and propeller set on peak efficiency

and a lower maximum rate of climb than a propeller set for maximum possible velocity. This result follows from the fact that for a maximum velocity propeller the decrease in the r. p. m. at full throttle with a decrease in velocity is not so great as in the case of the peak propeller. Consequently at any velocity the brake horsepower available is greater; and as the efficiency holds up well, the thrust horsepower available is greater for the maximum velocity propeller than for the peak propeller. The only redeeming feature of the peak propeller lies in its more favorable take-off characteristics.

It is therefore concluded that for maximum possible all-around performance in the air, a metal fixed-pitch propeller should have the setting corresponding to the envelope of the efficiency curve against C_s . A propeller having this setting is called "BEST PERFORMANCE PROPELLER" throughout this report; the propeller set on its peak efficiency is called "PEAK EFFICIENCY PROPELLER." The propeller setting is not critical however, since the difference in maximum rate of climb between the two cases

is generally less than 5 per cent. Charts are later developed for both propeller settings.

An investigation of the propeller settings on a number of airplanes by the method of the decrease in r. p. m. at speed for maximum rate of climb from r. p. m. at V_m has been made. The results are plotted in Figure 15. Curves have been drawn showing the decrease in r. p. m. to be expected for a propeller set for BEST PERFORMANCE and for a propeller set on the PEAK EFFICIENCY, for values of R_v from 0.55 to 0.70. The speeds for maximum rate of climb of all the airplanes investigated lie within these limits of R_v . The decrease in r. p. m. at speed for maximum rate of climb has been calculated from Army flight tests of more than 50 airplanes, and these points have been plotted on the same figure. This figure shows very strikingly that the propeller settings of all the airplanes correspond to no one case; however, the

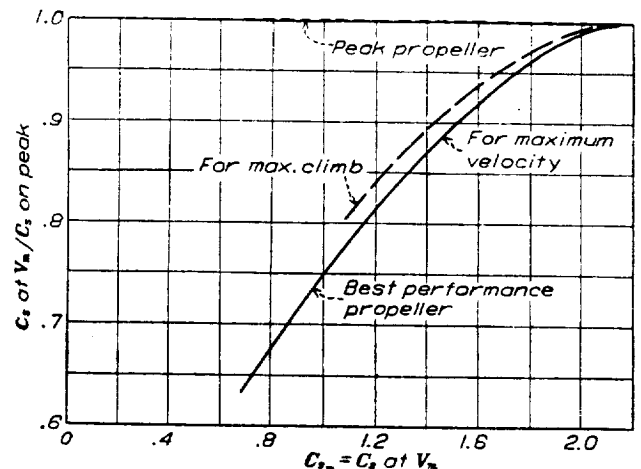


FIGURE 14b.—Comparison of propeller settings at V_{\max} for obtaining best maximum climb, best maximum velocity, and propeller set on peak efficiency

grouping taken *en masse* seems to center about and along the BEST PERFORMANCE PROPELLER.

Propeller efficiency at maximum velocity.—Curves have been drawn from which the propulsive efficiency at maximum velocity V_m corresponding to the BEST PERFORMANCE PROPELLER and PEAK EFFICIENCY PROPELLER may be found. (Reference 6.) These curves are given in Figures 16a and 16b, which give the efficiencies against $\frac{V}{ND_m}$ and C_{s_m} , respectively. The subscript m denotes *design maximum velocity*. The curves in Figure 16b are to be preferred in general, since for any one airplane and engine the value of the coefficient C_{s_m} is very approximately constant, hence the relative efficiencies of the two cases are readily seen. For the same airplane and engine combination, the $\frac{V}{ND_m}$ is different for the two cases since the diameter is different. Since C_{s_m} is essentially a parameter of the airplane, whereas $\frac{V}{ND}$ is a compound parameter of the airplane and the

propeller, it is recommended that the parameter C_s be used almost exclusively in considerations of airplane performance.

A few remarks follow on the choice of a propulsive efficiency to be used in computing performance.

- (2) For every 10 per cent increase in $\frac{d}{D}$ above 0.40 decrease propulsive efficiency 1 per cent.
- (3) For pointed narrow engine cowling, decrease propulsive efficiency from 0 to 2 per cent.

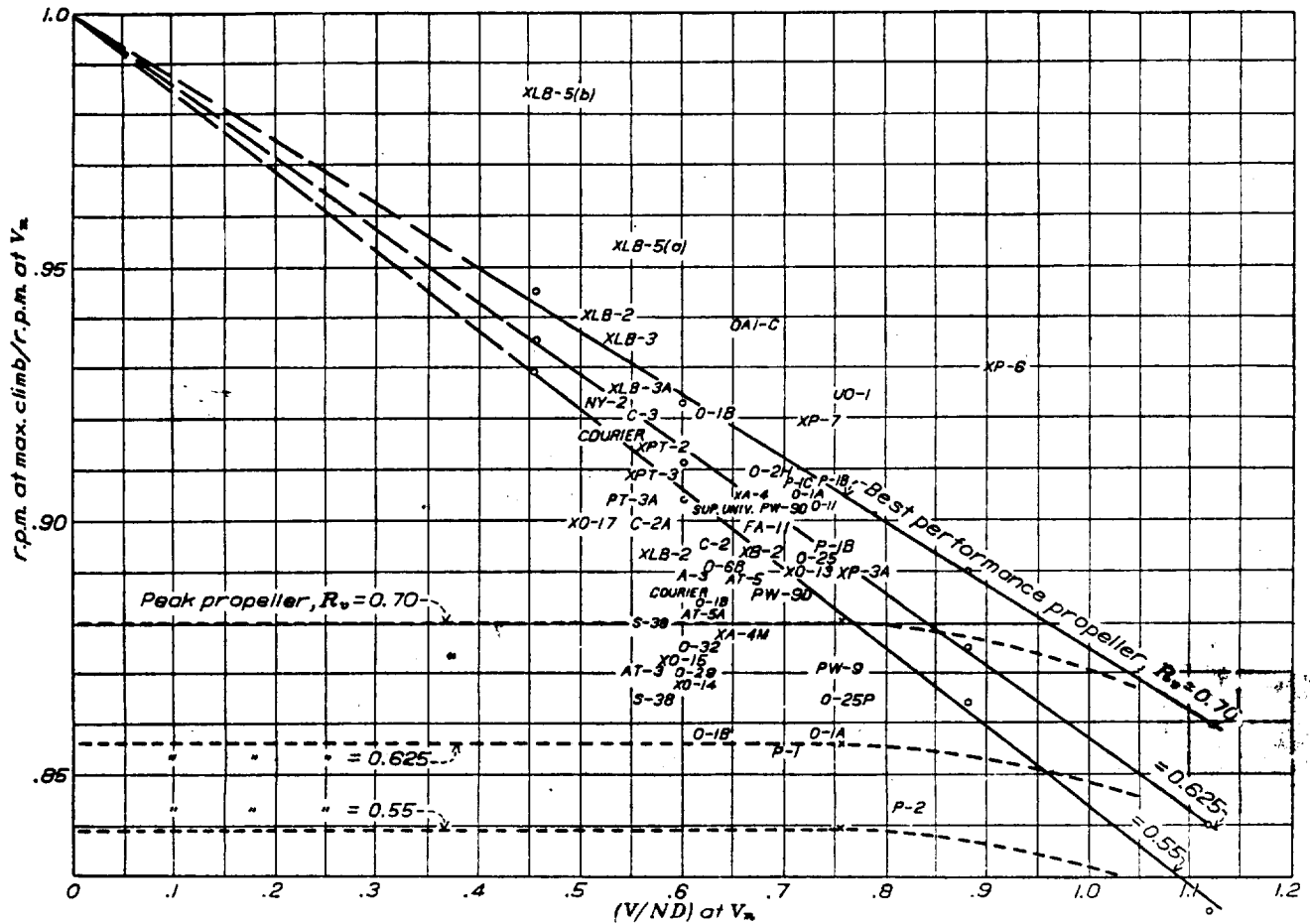


FIGURE 15.—Curve for investigation of type propeller setting of various airplanes from flight test

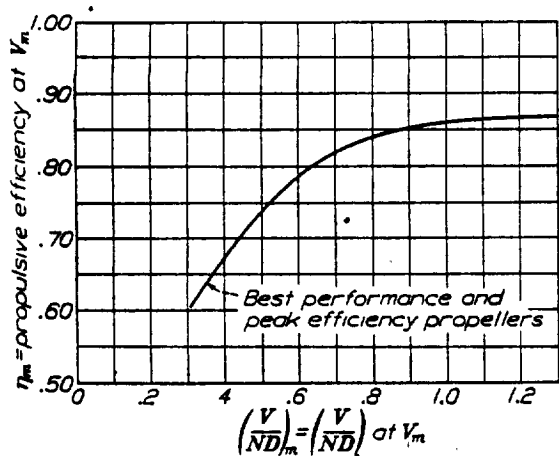


FIGURE 16a.—Propulsive efficiency at V_{max} as a function of $(\frac{V}{ND})_m$

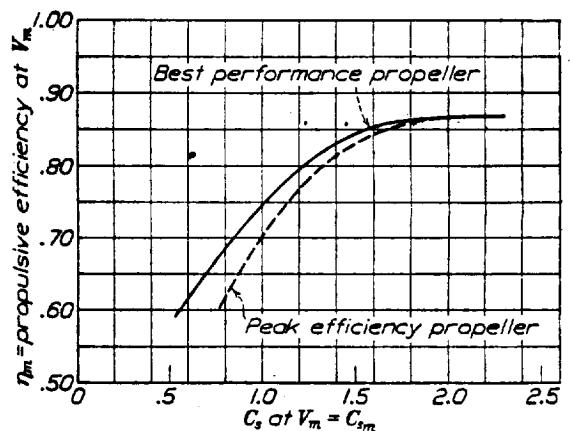


FIGURE 16b.—Propulsive efficiency at V_{max} as a function of C_{sm}

- (1) For modern 2-blade metal propellers with normal engine cowling, and where $\frac{d}{D}$ (the ratio of engine diameter to propeller diameter) is approximately 0.40, use propulsive efficiencies obtained from Figures 16a, 16b, or, better, Figure 27.

- (4) For National Advisory Committee for Aeronautics cowling increase from 1 to 2 per cent.
- (5) For unfavorable body shapes and cowlings, decrease from 0 to 5 per cent.
- (6) If tip speed is greater than 1,020 feet per second apply tip-speed correction. (Apply only at V_{max} , reference 8.)

(7) For 3-blade propellers decrease 3 per cent.

The above results are obtained from references 6, 7, 8, and 9.

Variation of r. p. m. with speed.—The variation of r. p. m. with velocity has been calculated both for the BEST PERFORMANCE PROPELLER at several settings and for the PEAK EFFICIENCY PROPELLER. The 19.5° setting has been taken as repre-

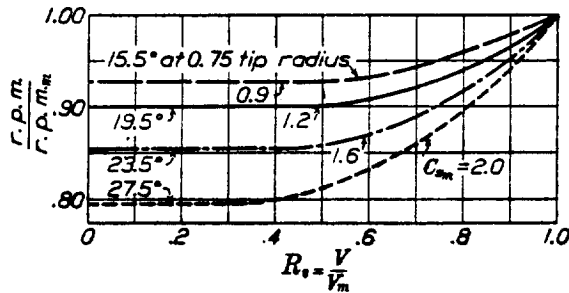


FIGURE 17.—Variation of full-throttle r. p. m. with velocity. Best performance propeller

sentative of the general peak efficiency curve. The curves are plotted in Figures 17 and 19, respectively. Each setting corresponds to a definite C_{sm} and η_m for the BEST PERFORMANCE PROPELLER, as indicated; the curve for PEAK EFFICIENCY PROPELLER is general for all values of C_{sm} .

Variation of r. p. m. with altitude (constant velocity).—The variation of r. p. m. with altitude has been

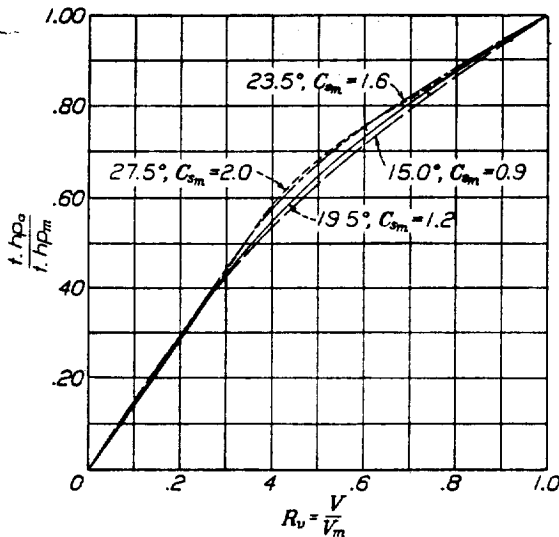


FIGURE 18.—Variation of full-throttle thrust horsepower available with velocity. Best performance propeller

calculated for the cases of BEST PERFORMANCE PROPELLER indicated on the curves in Figure 21. The calculations have been made on the basis of the expression for C_s at altitude. (Reference 6.)

$$C_{s_h} = \sigma^{1/2} C_{s_0} \quad (4.3)$$

where

$$C_{s_h} = C_s \text{ at altitude}$$

$$C_{s_0} = C_s \text{ at sea level.}$$

The effects of changes in R_v and propeller setting on t.hp. variation with altitude were found to be so

small that no further computation of other cases was necessary. The computed variation of r. p. m. with altitude, using the full-scale propeller data, gives good agreement with the variation found in flight test by the Army.

Variation of thrust horsepower available with speed.—Using the linear variation of brake horsepower

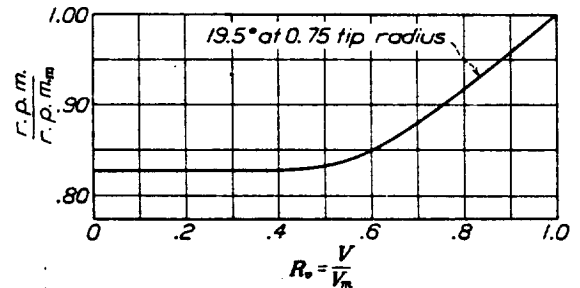


FIGURE 19.—Variation of full-throttle r. p. m. with velocity. Peak efficiency propeller

with r. p. m. as has been found most representative of modern engines, the variation of r. p. m. as given in Figures 17 and 19, and the propeller curves in Figure 13, the variation of thrust horsepower with speed has been calculated for all cases of the BEST PERFORMANCE PROPELLER and for the general case of the PEAK EFFICIENCY PROPELLER. The results are to be found in Figures 18 and 20, respectively.

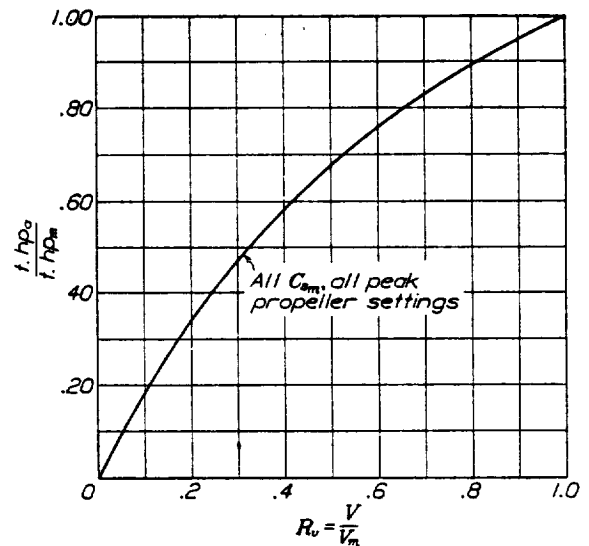


FIGURE 20.—Variation of full-throttle thrust horsepower available with velocity. Peak efficiency propeller

It has been found that for values of $R_v = \frac{V}{V_m}$ greater than 0.5, T_v (the ratio of thrust horsepower at velocity V to that at V_m) may, for the variations according to Figures 18 and 20, well be represented by a function of R_v of the type:

$$T_v = R_v^m \quad (4.4)$$

The quality of the representation may be seen by the accompanying table.

TABLE I

Setting	Best performance propeller				Peak efficiency propeller
	15.5°	19.5°	23.5°	27.5°	
C_{pm}	0.90	1.20	1.60	2.00	All.
J_m	0.45	0.65	0.85	1.10	All.
	T_a fig. 18	T_a fig. 18	T_a fig. 18	T_a fig. 18	T_a fig. 20
$R_m = 1.00$	1.00	1.00	1.00	1.00	1.00
.80	.868	.865	.873	.873	.884
.60	.716	.717	.732	.733	.757
.40	.534	.550	.546	.571	.577
.20	.302	.351	.306	.375	.297
0	0	0	0	0	0

In view of the excellent representation of T_a by the empirical formula R_m , the performance charts are

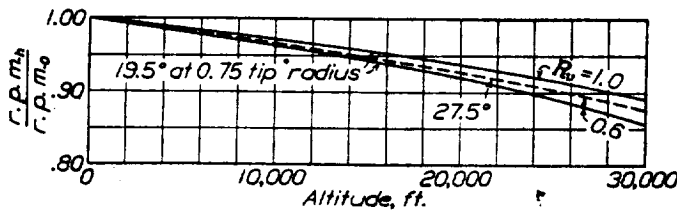


FIGURE 21.—Variation of full-throttle r. p. m. at constant velocity with altitude

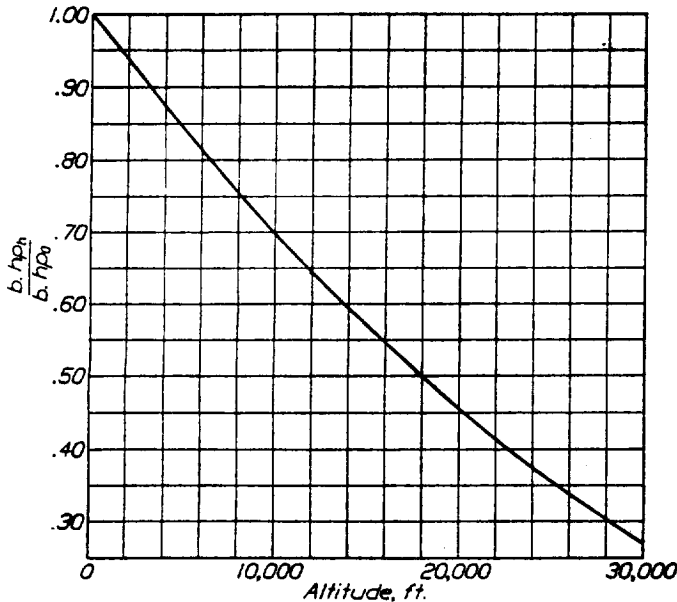


FIGURE 22.—Variation of full-throttle brake horsepower at constant r. p. m. with altitude

developed on this basis. The particular value of m corresponding to each C_{pm} (or each setting of the propeller) may be seen in the table.

Variation of thrust horsepower with altitude (constant velocity).—The variation of brake horsepower with altitude that is used in computing the t.hp_a variation desired has been plotted in Figure 22. These data have been obtained from National Advisory Committee for Aeronautics Technical Report No. 295 and British A. R. C. Reports and Memoranda No. 1141,

which are believed to give the best data available. By the incorporation of the brake horsepower variation with altitude at constant r. p. m., the variation of r. p. m. with altitude as represented in Figure 21, and the propeller curves of Figure 13, the variation of thrust horsepower with altitude at constant velocity has been computed. The cases were investigated for which the variation of r. p. m. with altitude were computed, and it was found that the variation of thrust horsepower with altitude may be represented by a single curve for all speeds of flight R , and all settings of BEST PERFORMANCE PROPELLER and PEAK EFFICIENCY PROPELLER. The curve obtained is plotted in Figure 23. This curve is to be the general representative for modern unsupercharged engines in the charts that are to be developed. The variation function T_a is therefore a function of σ only, being independent of R .

In seeking for an empirical formula to represent the curve in Figure 23, it has been found that the type of

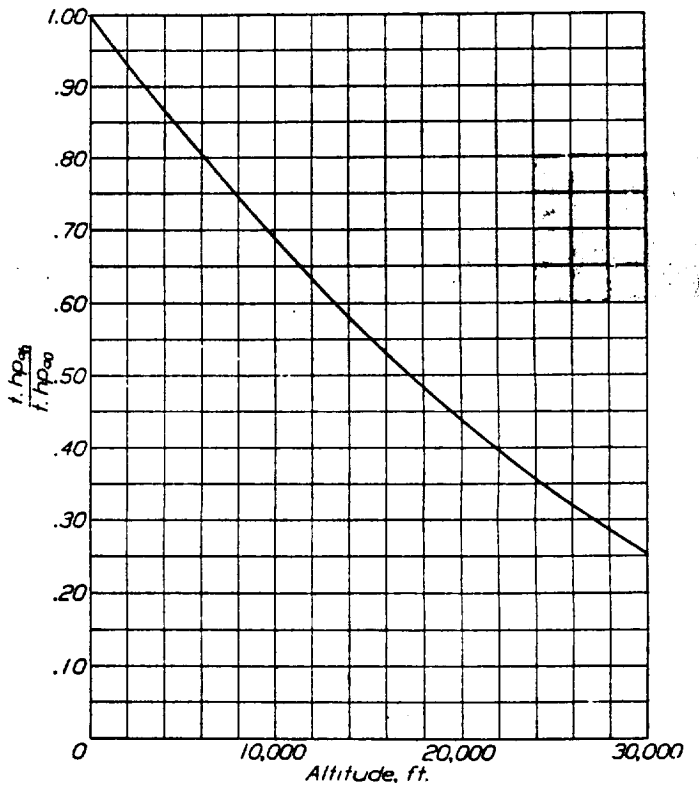


FIGURE 23.—Variation of full-throttle thrust horsepower available at constant velocity with altitude

formula proposed by Bairstow some years ago will, with proper values of the constants, give an excellent representation of the curve. The formula follows:

$$T_a = \frac{\sigma - 0.165}{0.835} \tag{4.5}$$

where,

$$T_a = \frac{\text{t.hp}_a \text{ at altitude (constant velocity)}}{\text{t.hp}_a \text{ at sea level velocity}}$$

The quality of representation may be seen by the accompanying table.

TABLE II

Altitude	T_e (fig. 23)	T_e (eq. (4.5))
Sea level.	1.000	1.000
7,500	.760	.758
15,000	.557	.556
22,500	.385	.388
30,000	.253	.250

for sinking speed w_s . The parasite drag coefficient was defined then as the total drag coefficient minus the effective induced drag coefficient which was calculated as the minimum induced drag produced by an effective span. The customary definition of the parasite drag coefficient has been that expressed in the past by the equation

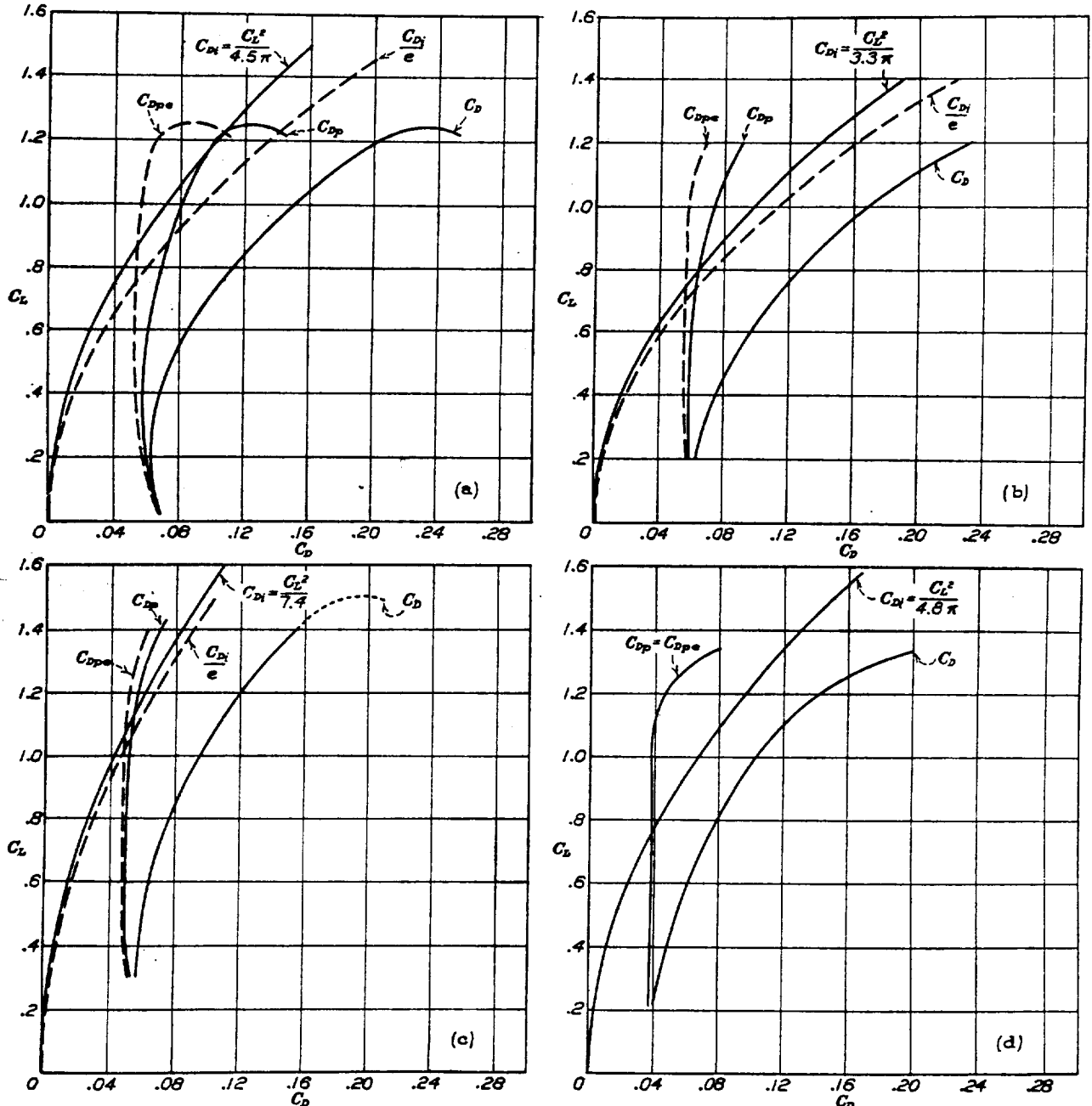


FIGURE 24a.—Flight test polar diagrams showing the effect of introducing the airplane efficiency factor, ϵ

$$C_{D_p} = C_D - C_{D_i}; C_{D_{p0}} = C_D - \frac{C_{D_i}}{\epsilon}; \text{ (a) Douglas XO-14, } \epsilon = 0.75$$

(Ref. A. D. M. 3112); (b) Sperry Messenger, $\epsilon = 0.85$ (Ref. National Advisory Committee for Aeronautics Technical Report No. 304); (c) Fairchild F. C.-2W2, $\epsilon = 0.90$; (Ref. National Advisory Committee for Aeronautics Technical Note No. 362); (d) Vought V. E. -7, $\epsilon = 1.00$; (Ref. National Advisory Committee for Aeronautics Technical Report No. 292)

AIRPLANE EFFICIENCY FACTOR

It was pointed out in Section II that the variation in parasite drag coefficient could well be expressed as a correction proportional to CL^2 , thus it could be included in the induced drag term of the expression

$$C_{D_p} = C_{D_{(total)}} - C_{D_{i_{(min)}}} \tag{4.6}$$

where C_{D_i} represents the induced drag coefficient based on the equivalent monoplane span (kb). The parasite drag coefficient as calculated according to

this definition for eight flight test polars is seen in Figures 24a and 24b. The curve C_{D_p} may be seen to have, in general, a parabolic shape over the normal flying range. This shape might have been expected since the total induced drag has not been accounted for

and assuming that the variation in the parasite resistance coefficient is proportion to C_L^2 , we get:

$$C_{D_{pe}} = C_D - \frac{C_{D_i \min.}}{e} = C_D - C_{D_{ie}} \quad (4.7)$$

where,

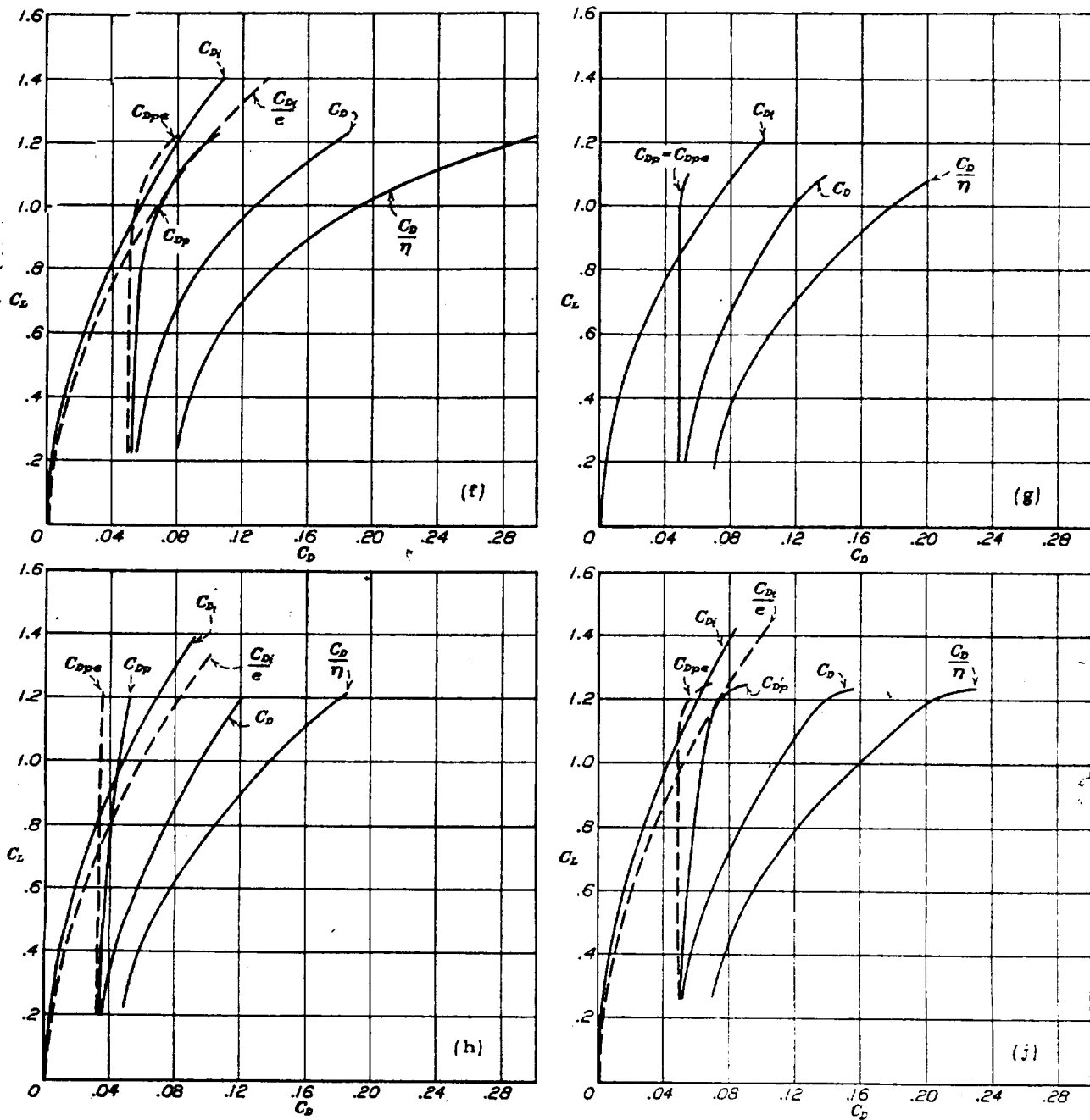


FIGURE 24b.—Flight test polar diagrams showing the effect of introducing the airplane efficiency factor, e . $C_{D_p} = C_D - C_{D_i}$; $C_{D_{pe}} = C_p - \frac{C_{D_i}}{e}$ Data from Luftfahrtforschung, Mar., 1930, B. 6. H. 5. $\frac{C_D}{\eta}$ from test. η assumed to get C_D . (f) Rumpler C IV, $\eta=70$ per cent—60 per cent, $e=0.80$; (g) Heinkel HD22, $\eta=75$ per cent—65 per cent, $e=1.00$; (h) Junkers W33, $\eta=75$ per cent—65 per cent, $e=0.80$; (j) Junkers A35, $\eta=75$ per cent—65 per cent, $e=0.50$

because we have in no case an elliptical lift distribution corresponding to the minimum C_{D_i} . There has therefore been included in the parasite drag coefficient a portion of the actual induced drag coefficient. Including in the induced drag term, where it obviously belongs, this excess over the minimum induced drag,

- $C_{D_{pe}}$ — Effective parasite drag coefficient at maximum velocity.
- C_D — Total drag coefficient.
- C_{D_i} — Minimum induced drag coefficient for equivalent monoplane span.

$C_{D_{ie}}$ —Effective induced drag coefficient.

e —Airplane efficiency factor defined by equation (4.7).

$C_{D_{pe}}$ according to this definition has also been plotted in Figures 24a and 24b, and it is seen that for all the airplanes there represented $C_{D_{pe}}$ is there very approximately constant throughout the flying range. The effective span loading has therefore been defined as

$$\lambda_e = \frac{2W}{\pi\rho_0(kb)^2 e} \quad (4.8)$$

All symbols have been defined in Section II and in the Summary of Notation.

The sinking speed then, due to the parasite loading, is that due only to the effective parasite drag coefficient at V_m , and the sinking speed due to the effective span loading is that due to the *actual* induced drag plus that due to the variation in parasite drag which is assumed proportional to C_L^2 . The correction for variation of parasite drag proportional to C_L^2 is believed to be of excellent quality, as the variation is small and, by reference to the polars in Figures 24a and 24b, it may be seen that a correction proportional to C_L^2 will leave a portion called effective parasite drag coefficient, which will not vary appreciably with angle of attack within the normal flying range.

The efficiency factor e may be determined from test data by the method described in Section VI. The value has been computed for a large number of airplanes; the range of values suggested for use in performance calculations are included in the accompanying table.

TABLE III

VALUES OF e FOR VARIOUS TYPES OF AIRPLANES

Type of airplane	Use value of e varying with "cleanness"	From—	To—
Flying wing.....		0.95	-1.00
Cantilever monoplane.....		.85	-1.00
Semicantilever monoplane.....		.80	-.95
Single bay biplane.....		.75	-.95
Multiple bay biplane.....		.70	-.90

Airplanes with normal fairing and cowling correspond to the mean values of e ; airplanes with square bodies, rectangular wings, little fairing, and with otherwise poor aerodynamic form correspond to the lower values of e ; airplanes with exceptionally smooth bodies, elliptical wings, and complete fairing correspond to the upper values.

EFFECTIVE PARASITE COEFFICIENT

The effective parasite coefficient has been defined as that portion of the total drag coefficient which remains constant with angle of attack. From the preceding paragraphs and Section II, equation (2.8), we have, for the relation between the effective parasite coefficient

$C_{L_{pe}}$ and the equivalent parasite area,

$$C_{D_{pe}} = \frac{D_p}{qS} = \frac{f}{S} \quad (4.9)$$

and from the definition of λ_p in equation (2.11) of Section II,

$$\frac{f}{S} = \frac{2W}{\rho_0 S} \frac{1}{\lambda_p} \quad (4.10)$$

The value of λ_p may be computed from the observed maximum velocity measured in flight test, hence the over-all parasite drag coefficient $\frac{f}{S}$ may be determined

by equation (4.10). The value of $\frac{f}{S}$ has thus been calculated for a large number of airplanes from Army flight test data and commercial test data that are believed reliable. The results are plotted in Figure 25. For performance estimation $\frac{f}{S}$, hence the equivalent parasite area f , may be estimated from Figure 25 by reference to the corresponding type of airplane.

The parameter $\frac{f}{S}$ is the most useful in determining the over-all cleanness of the airplane. It is interesting to note that the parasite drag coefficient $\frac{f}{S}$ of a wing alone has a value of approximately 0.01.

V. PERFORMANCE FORMULAS IN ENGINEERING UNITS FOR AIRPLANES EQUIPPED WITH MODERN UNSUPERCHARGED ENGINES AND FIXED-PITCH METAL PROPELLERS

The analysis of the general performance formulas in Section II was carried through using physical quantities and parameters, in order that application to any consistent set of units might easily be made and that the physical meaning of the parameters and equations might be emphasized. It is, however, much more convenient for the designer and engineer to use parameters which are simple "loadings" without extra constants. For practical purposes it is also a great advantage to have performance formulas and charts expressed in terms of engineering units. Hence in this section the performance formulas previously developed are rewritten using engineering parameters and the standard American engineering system of notation. The expressions for T_a and T_r developed in Section IV are introduced into these formulas and, from a numerical solution of the latter, engineering charts are plotted for the important performance characteristics. If sufficient data were at hand relative to the functions T_a and T_r , the general cases of supercharged engines and of variable-pitch propellers might be developed in the same manner.

A numerical discussion of the effects of down load on the tail and inclination of the thrust axis is de-

scribed and corrections for these effects are given where necessary.

THE ENGINEERING PARAMETERS

The engineering parameters are defined as:

$$l_p = \frac{W}{f} = \lambda_p \frac{\rho_o}{2} \quad (\text{engineering}) \text{ parasite loading (lb./sq. ft.)} \quad (5.1)$$

$$l_s = \frac{W}{e(kb)^2} = \frac{W}{b_s^2} = \lambda_s \frac{\pi \rho_o}{2} \quad (\text{engineering}) \text{ effective span loading (lb./sq.ft.)} \quad (5.2)$$

$$l_t = \frac{W}{b \cdot \text{hp}_m \eta_m} = \frac{W}{t \cdot \text{hp}_m} = A \lambda_t = (\text{engineering}) \text{ horsepower loading (lb./hp.)} \quad (5.3)$$

$$\Lambda = \frac{l_p l_s^{3/4}}{l_t^{3/4}} = \frac{W^2 f^{3/4}}{t \cdot \text{hp}_m^{3/4} b_s^2} = \frac{\pi A^{3/4} \rho_o^{3/4}}{2^{3/4}} \Lambda' = (\text{engineering}) \text{ major performance parameter.} \quad (5.4)$$

The performance characteristics are given in the following units:

- V_m — design maximum velocity at sea level in miles per hour.
- C_h — maximum rate of climb in feet per minute.
- H — absolute ceiling in feet.
- $A = 550 = \frac{\text{ft. lb./sec.}}{\text{b.hp}}$

THE FUNCTIONS T_a AND T_s FOR AIRPLANES OF TYPE 1

Airplanes classified here by type 1 are all airplanes equipped with modern unsupercharged engines and fixed-pitch metal propellers. Modern engines are those for which the brake horsepower may be assumed to vary linearly with r. p. m. for r. p. m.'s lower than the rated r. p. m.

It has been shown in Section IV, equations (4.4) and (4.5), that for airplanes of type 1 the functions T_a and T_s may be expressed in the form,

$$T_s = R_s^m \quad (5.5)$$

where,

- $m = 0.65$ for BEST PERFORMANCE PROP. $C_{l,m} = 0.9$
- $= 0.61$ for BEST PERFORMANCE PROP. $C_{l,m} = 1.2$
- $= 0.55$ for BEST PERFORMANCE PROP. $C_{l,m} \geq 1.6$
- $= 0.55$ for PEAK EFFICIENCY PROP. all $C_{l,m}$

and

$$T_a = \frac{\sigma - 0.165}{0.835} = 1.198 (\sigma - 0.165). \quad (5.6)$$

FUNDAMENTAL EQUATION OF PERFORMANCE

The fundamental equation of performance (2.22) becomes in engineering units,

$$C_h = \frac{dh}{dt} = \frac{33,000}{\sigma R_s} \frac{1}{l_t} \left[(T_a T_s \sigma R_s - \sigma^2 R_s^4) - \frac{l_p l_t}{3.014 V_m} (1 - \sigma^2 R_s^4) \right] \text{ feet per minute} \quad (5.7)$$

which gives for airplanes of type 1,

$$l_t C_h = \frac{33,000}{\sigma R_s} \left[1.198 (\sigma - 0.165) \sigma R_s^{m+1} - \sigma^2 R_s^4 - \frac{l_p l_t}{3.014 V_m} (1 - \sigma^2 R_s^4) \right]. \quad (5.7a)$$

The expression for Λ becomes from equation (2.26),

$$\Lambda = 52.8 \frac{l_p l_t}{V_m} \left(1 - 0.332 \frac{l_p l_t}{V_m} \right)^{3/4}. \quad (5.8)$$

Equation (5.8) is used to give the relation between Λ and $\frac{l_p l_t}{V_m}$ throughout the report and in developing the charts. Equation (5.8) is plotted in Figure 30 (in the curve marked STABLE WING SECTION).

Maximum velocity at sea level.—Equations (2.32) and (2.33) become respectively,

$$V_m = 52.8 \left(\frac{l_p}{l_t} \right)^{3/4} \left(1 - 0.332 \frac{l_p l_t}{V_m} \right)^{3/4} \text{ (m. p. h.)} \quad (5.9)$$

and

$$\frac{V_m}{l_t} = 52.8 \frac{1}{\Lambda} \left(1 - 0.332 \frac{l_p l_t}{V_m} \right)^{3/4}. \quad (5.10)$$

These expressions will be found plotted in Figures 29 and 30, respectively.

It should be noticed that the above equations are exact only for the case of an airplane flying at maximum velocity with no down load on the tail. An airplane with a stable wing section may be said to satisfy this condition. Unfortunately, as stable wing sections have not as yet come into general use, the case of an airplane flying with a normal, unstable wing section must be investigated. Assuming a mean center of gravity position of 0.33 chord, and a mean length from center of gravity position to center of pressure on the tail surface of 2.75 times the chord, the down load on the tail was calculated for airplanes with various speed ranges. Assuming a mean aspect ratio of the wing of 6, and an aspect ratio of the tail surface of 3, the effect of the calculated down load on the tail has been applied to equations (5.9) and (5.10), and the results plotted in Figure 30. The results are also plotted in the supplementary curve in Figure 29. The curve labeled "Normal Wing Section" represents the mean curve obtained in this manner from the investigation of 5 frequently used airfoils, namely: Clark Y, Göttingen 387 and 398, and U. S. A. 27 and 35 B. (Airfoil data from reference 10.) The down load on the tail causes an increase in induced drag, which is accounted for by a change in l_t at V_m .

An approximate solution of equation (5.9) is obtained by expanding and retaining only the first two terms. In the second term the substitution $V_m = 52.8 \left(\frac{l_p}{l_t} \right)^{3/4}$ is made.

$$V_m = 52.8 \left(\frac{l_p}{l_t} \right)^{3/4} - 0.11 l_t l_t \text{ (m.p.h.)} \quad (5.11)$$

This form has been given by Dr. Clark B. Millikan in reference 1.

For an airplane with no down load on the tail, equations (5.9) or (5.10) are to be used. For an airplane with normal down load on the tail, the correction indicated on the curves in Figures 29 and 30 is to be used.

Maximum velocity at altitude.—Expressing equation (2.34) in engineering units, we obtain

$$\frac{l_i l_t}{V_m} = 3.014 \frac{T_a T_s \sigma R_{v_m} - \sigma^2 R_{v_m}^4}{1 - \sigma^2 R_{v_m}^4} \quad (5.12)$$

where

$$R_{v_m} = \frac{\text{Max. velocity at altitude}}{\text{Max. velocity at sea level}} = \frac{V_m}{V_m}$$

For airplanes of type 1, equation (5.12) becomes

$$\frac{l_i l_t}{V_m} = 3.014 \frac{1.198(\sigma - 0.165)\sigma R_{v_m}^{m+1} - \sigma^2 R_{v_m}^4}{1 - \sigma^2 R_{v_m}^4} \quad (5.12a)$$

Equation (5.12a) is used in conjunction with equation (5.8) to develop the chart given in Figure 31. The three values of m from equation (5.5) are used.

Maximum rate of climb at altitude; speed for maximum rate of climb.—Equation (2.40) for speed ratio for maximum rate of climb becomes,

$$\frac{l_i l_t}{V_m} = 3.014 \frac{-\sigma R_{v_c}^2 \frac{\partial T_a T_s}{\partial R_{v_c}} + 3\sigma^2 R_{v_c}^4}{1 + 3\sigma^2 R_{v_c}^4} \quad (5.13)$$

where,

$$R_{v_c} = \frac{\text{Speed for max. rate of climb at alt.}}{\text{Max. velocity at sea level}} = \frac{V_c}{V_m}$$

The engineering equation for maximum rate of climb from (2.41),

$$C_h = \frac{33,000}{\sigma R_{v_c}} \frac{1}{l_t} \left[(T_a T_s \sigma R_{v_c} - \sigma^2 R_{v_c}^4) - (1 - \sigma^2 R_{v_c}^4) \frac{l_i l_t}{3.014 V_m} \right] \text{ft. per min.} \quad (5.14)$$

For airplanes of type 1, the last two equations become

$$\frac{l_i l_t}{V_m} = 3.014 \frac{-1.198(\sigma - 0.165)\sigma R_{v_c}^{m+1} + 3\sigma^2 R_{v_c}^4}{1 + 3\sigma^2 R_{v_c}^4} \quad (5.13a)$$

$$C_h = \frac{33,000}{\sigma R_{v_c}} \frac{1}{l_t} \left[1.198(\sigma - 0.165)\sigma R_{v_c}^{m+1} - \sigma^2 R_{v_c}^4 - (1 - \sigma^2 R_{v_c}^4) \frac{l_i l_t}{3.014 V_m} \right] \quad (5.14a)$$

Equations (5.13a) and (5.14a) are used in conjunction with equation (5.8) to develop the chart for speed for maximum rate of climb plotted in Figure 32, and the chart for maximum rate of climb plotted in Figure 33.

The effects of down load on the tail and inclination of the thrust axis have been investigated for various types of airplanes ranging from heavy bombardment to high-speed pursuit. It has been found that the two effects are of opposite sign and within 1 or 2 per cent of the same value. It is concluded, therefore, that at the attitude of the airplane for maximum rate of climb, the combined effects of down load on the tail surface and inclination of the thrust axis may well be neglected.

Maximum rate of climb at sea level is obviously the special case of maximum rate of climb at altitude, in which $\sigma = 1$ and $T_a = 1$.

Absolute ceiling; speed at absolute ceiling.—The relation between σ_H and R_{v_H} at absolute ceiling, equation (2.46), is unchanged,

$$T_a T_s \left(1 + 3\sigma_H^2 R_{v_H}^4 \right) + R_{v_H} \frac{\partial T_a T_s}{\partial R_{v_H}} \left(1 - \sigma_H^2 R_{v_H}^4 \right) - 4\sigma_H R_{v_H}^3 = 0 \quad (5.15)$$

where,

$$R_{v_H} = \frac{\text{Velocity at absolute ceiling}}{\text{Max. velocity at sea level}}$$

$$\sigma_H = \sigma \text{ at absolute ceiling.}$$

For airplanes of type 1, this gives,

$$1.198(\sigma_H - 0.165) R_{v_H}^m (1 + 3\sigma_H^2 R_{v_H}^4) + 1.198m$$

$$R_{v_H}^m (\sigma_H - 0.165) (1 - \sigma_H^2 R_{v_H}^4) - 4\sigma_H R_{v_H}^3 = 0. \quad (5.15a)$$

Equation (5.15a), when solved by the trial and error method, gives the relation between speed at absolute ceiling and altitude. This solution has been performed graphically in developing the charts by finding the speed at which the high speed at altitude and speed for maximum rate of climb at altitude intersect. This method is recommended. The results are given in Figures 31 and 39.

The equation for $\frac{l_i l_t}{V_m}$ at absolute ceiling becomes from equation (2.47),

$$\frac{l_i l_t}{V_m} = 3.014 \frac{T_a T_s \sigma_H R_{v_H} - \sigma_H^2 R_{v_H}^4}{1 - \sigma_H^2 R_{v_H}^4} \quad (5.16)$$

which gives for airplanes of type 1,

$$\frac{l_i l_t}{V_m} = 3.014 \frac{1.198(\sigma_H - 0.165)\sigma_H R_{v_H}^{m+1} - \sigma_H^2 R_{v_H}^4}{1 - \sigma_H^2 R_{v_H}^4} \quad (5.16a)$$

The solutions of equation (5.15a), R_{v_H} , and σ_H , when substituted in equation (5.16a), give an equation which, when used in conjunction with equation (5.8), gives the absolute ceiling as a function of Λ . This solution has been performed graphically, however, by finding the value of Λ at which the maximum rate of climb at any one altitude becomes zero. This method is recommended. The results are plotted in Figure 34.

Service ceiling.—Service ceiling is found by putting $C_h = 100$ in exactly the manner described in Section II. The corresponding engineering equations and curves are to be used, however, instead of the physical equations there referred to. For airplanes of type 1, the results are given in Figure 34.

Time to climb.—In engineering units we have for the time to climb, from equation (2.50),

$$T = l_t \int_{h_1}^{h_2} \frac{1}{h_1 l_t C_h} dh. \quad (5.17)$$

This integration is carried out in the manner indicated in Section II, except that the engineering equa-

tions, parameters, and charts are used. Results for airplanes of type 1 are plotted in Figure 35.

PERFORMANCE VARIATION EQUATIONS AND CHARTS

The variation equations of Section III are essentially unchanged, since they express percentage variations. They may all be immediately transformed to engineering notation by the substitution of Λ for Λ' according to the relation

$$\Lambda = 158.9\Lambda'. \quad (5.26)$$

This operation is quite obvious and the equations will not be rewritten. Making this indicated substitution and obtaining the necessary constants for the equations from the performance charts developed in Section V, a set of variation charts has been constructed in Figure 37. These give the variation in performance characteristics due to a 1 per cent change in the various parameters for airplanes with type 1 propulsive units. The charts are based on the design $C_{s,m} = 1.2$, and may be regarded as representative for all propeller settings since the propeller setting has a negligible effect upon the variation of performance.

GENERAL REMARKS

The performance charts have been developed for the following cases:

- (1) BEST PERFORMANCE PROPELLER for $C_{s,m} = 0.9$, or $J_m = 0.45$; $m = 0.65$.
- (2) BEST PERFORMANCE PROPELLER for $C_{s,m} = 1.2$, or $J_m = 0.65$; $m = 0.61$.
- (3) BEST PERFORMANCE PROPELLER for $C_{s,m} \geq 1.6$, or $J_m \geq 0.85$; $m = 0.55$.
- (4) PEAK EFFICIENCY PROPELLER for all $C_{s,m}$, all J_m ; $m = 0.55$.

The cases indicated here have all been plotted throughout the charts, forming families of three curves. A single curve is used throughout for the PEAK EFFICIENCY SETTING, while for the BEST PERFORMANCE PROPELLER interpolation must be made for the proper value of $C_{s,m}$.

A curve has been plotted for the graphical determination of Λ explicitly from the parameters l_p , l_s , and l_t . The curve is found in Figure 28.

For convenience in determining the major performance characteristic of an airplane (the maximum velocity at sea level, maximum rate of climb at sea level, and absolute ceiling) a combination chart giving V_m , l , C_o , and H as functions of Λ has been plotted in Figure 36.

VI. PERFORMANCE DETERMINATION

For the aid of the designer, the method of determining the performance of an airplane through the use of the charts developed above is given in this section. After a few applications, the designer may discover alternative procedures which are more suitable to his particular needs, but in general the methods

of using the charts will probably be similar to those indicated below, which the author has found most convenient. After the general outline, an illustrative example is included. The use of the charts in determining the airplane characteristics (parameters), when the performance is known or specified, is also shown. This reversed solution of the charts is of considerable interest. Examples of this process are given. Finally, a problem on the change in performance caused by changes in the parameters of the airplane is worked out.

GENERAL OUTLINE OF THE DETERMINATION OF THE PERFORMANCE OF ANY AIRPLANE EQUIPPED WITH A MODERN UNSUPERCHARGED ENGINE AND A FIXED-PITCH METAL PROPELLER

The following data must be specified:

- W —Weight (lb.).
- S —Total wing area (sq. ft.). (Wing areas include portion cut out by fuselage.)
- Airfoil section.
 - S_1 —Area of the longer wing (sq. ft.).
 - S_2 —Area of the shorter wing (sq. ft.).
 - b_1 —Span of longer wing (ft.).
 - b_2 —Span of shorter wing (ft.).
 - G —Gap (ft.).
- $b. hp_m$ —Brake horsepower at V_{max} . (Rated $b. hp$.)
- $r. p. m_m$ —Revolutions per minute at V_m of propeller.
- f —Equivalent parasite area (sq. ft.).

The equivalent parasite area f is found either by estimating the total parasite drag coefficient or by summing up the drag coefficients of the various parts of the airplane.

(1) Estimation.—For performance estimation f , hence f , may be estimated from Figure 25 by careful reference to the corresponding type of airplane, proper allowance being made for irregularities of each particular design. For a normal airplane the estimation can generally be made to within 20 per cent of the correct value, which leads to an accuracy of within 7, 2, and 4 per cent in the calculated V_m , C_o , and H , respectively.

(2) Summation.—The equivalent parasite area of the airplane is found by summing up the individual equivalent parasite areas of the various component parts including the wing profile drag. For conservative design, an allowance for interference drag should be made. This allowance is generally made by multiplying the result of the summation by a factor I varying from 1.00 to 1.30 depending upon the type of airplane. A table of suggested values is given here.

TABLE IV

Type airplane	Interference factor I	
	From—	To—
Flying wing.....	1.00	1.10
Cantilever monoplane.....	1.00	1.15
Semicantilever monoplane.....	1.05	1.20
Single bay biplane.....	1.05	1.25
Multiple bay biplane.....	1.10	1.30

Data are found in references 5 and 11.

The following constants and parameters of the airplane are then determined:

e —Airplane efficiency factor. (Table III, Sec. IV.)

k —Munk's span factor ($k=1$ for monoplane).

Charts for the rapid solution of k are given in reference 5, chapter 2.

$$l_p = \frac{W}{f}$$

$$l_s = \frac{W}{e(kb_1)^2}$$

C_{s_m} —Coefficient C_s at V_m . Figure 26.

η_m —Propulsive efficiency at V_m .

These values are found thus: Assume a V_{max} .

Find C_{s_m} from Figure 26.

Find η_m from Figure 27, and suggestions in Section IV.

Calculate $l_t = \frac{W}{b \cdot hp_m \cdot \eta_m}$.

From $\frac{l_p}{l_t}$ find V_{max} from Figure 29.

If this V_m does not check the V_m originally assumed, make a judicious choice of a new V_m , and repeat the process until a check is obtained. This is a rapidly converging process.

D —Propeller diameter ($\frac{V}{ND}$ is found from C_{s_m} in Figure 13, whence D from equation (4.2), Sec. IV).

$$l_t = \frac{W}{b \cdot hp_m \cdot \eta_m}$$

$$\Lambda = \frac{l_s l_t^{3/4}}{l_p^{1/4}} \text{ (fig. 28.)}$$

$$l_w = \frac{W}{S}$$

$C_{L_{max}}$. (Table VI, Sec. VII.)

MAJOR PERFORMANCE CHARACTERISTICS FROM CHARTS

All major performance characteristics are now obtained by the use of the charts, from the parameters l_p , l_s , l_t , Λ , l_w , and $C_{L_{max}}$. Interpolation for the proper value of C_{s_m} is made in the case of the BEST PERFORMANCE PROPELLER. No interpolation is necessary for the PEAK EFFICIENCY PROPELLER. Performance is obtained as indicated below:

Landing speed.—From l_w , $C_{L_{max}}$ in Figure 40.

Maximum velocity at sea level.—From $\frac{l_p}{l_t}$ in Figure 29, or find $\frac{V_m}{l_s l_t}$ from Λ in Figure 30. Whence V_m . (If tip speed is greater than 1,020 ft./sec. apply correction factor to l_t in $\frac{l_p}{l_t} \frac{V_m}{l_s l_t}$, and Λ here. (Reference 8.) Do not apply in obtaining other performance.)

Maximum velocity at altitude.—Find R_{r_m} at various altitudes from Λ in Figure 31. Then $V_{m_h} = R_{r_m} V_m$.

Speed for maximum rate of climb at any altitude.—Find R_{r_c} at various altitudes from Λ in Figure 32. Then $V_c = R_{r_c} V_m$.

Speed at absolute ceiling.—Find R_{r_H} from Λ in Figure 31. Then $V_H = R_{r_H} V_m$.

Maximum rate of climb at any altitude.—Find $l_t C_h$ at various altitudes from Λ in Figure 33. Whence C_h .

Absolute ceiling.—From Λ in Figure 34.

Service ceiling.—From Λ and proper interpolation for l_t in Figure 34.

Time to climb to any altitude.—Find $\frac{T}{l_t}$ at various altitudes from Λ in Figure 35. Whence T .

Special performance problems such as maximum $\frac{L}{D}$, speed for minimum power, and thrust horsepower required at any speed and altitude are found as described in Section VII.

EXAMPLE: The processes described for finding e , k , η_m , C_{s_m} , and D are either quite well known or direct; so these will be assumed given for brevity. Given:

$W = 5,000$ lb. $e = 0.85$
for a single bay biplane.

$S = 400$ sq. ft. $k = 1.13$
 $b \cdot hp_m = 500$ $C_{s_m} = 1.40$
 $f = 19.2$ sq. ft. $\eta_m = 0.83$
 $b_1 = 43$ ft.

Clark Y airfoil section.
Then

$$l_p = 260, l_s = 2.49, l_t = 12.05, \Lambda = 10.8, l_w = 12.5$$

$$C_{L_{max}} = 1.27$$

$$\frac{l_p}{l_t} = 21.6, l_s l_t = 30.0.$$

Propeller is set for Best Performance. Interpolating for the proper value of C_{s_m} on the charts, we get by the method described above:

Standard altitude	Level flight			Climb					
	V_m	R_{r_m}	V_{m_h}	R_{r_c}	V_c	$l_t C_h$	C_h	$\frac{T}{l_t}$	T
0	142.0			0.578	82.1	14,070	1,168	0	0
5,000		0.972	138.0	0.590	83.8	10,280	853	1.42	5.1
10,000		.933	132.5	.603	85.6	6,850	568	1.02	12.3
15,000		.872	124.0	.629	88.0	3,500	290	2.05	24.7
20,000		.696	99.0	.645	91.6	300	25		
Serv. ceil. 18,500									
Abs. ceil. 20,000				0.617	91.8				

Landing speed = 62.0 m. p. h.

DETERMINATION OF THE PARAMETERS OF THE AIRPLANE WHEN THE PERFORMANCE IS KNOWN

When the three major performance characteristics of the airplane, maximum velocity at sea level, maximum rate of climb at sea level, and absolute ceiling, are known, the three fundamental parameters of the airplane, l_p , l_s , and l_i may readily be determined. This determination gives a method of finding η_m , e , and f from flight test data. The method given below was used in finding the values of e from Army flight test data for approximately 50 airplanes. The summary of the results is to be found in Table, III, Section IV.

Having given the flight test data for—

- H —Absolute ceiling
- C_o —Maximum rate of climb at sea level
- V_m —Maximum velocity at sea level

and having given

$$W, kb_1, b, \text{hp}_m, \text{r. p. m}_m$$

the parameters of the airplane are found in the following manner:

From $b, \text{hp}_m, \text{r. p. m}_m$, and V_m determine C_{sm} from Figure 26.

Interpolation for the proper value of C_{sm} is then made throughout the following development.

From Figure 34 obtain Λ .

From Λ in Figure 33 obtain $l_i C_n$. Whence l_i .

From Λ in Figure 30 obtain $\frac{V_m}{l_i}$. Whence l_s .

From Λ, l_s , and l_i , obtain l_p from Figure 28, or better, from V_m and Figure 29 obtain $\frac{l_p}{l_i}$.

Whence l_p .

The values of the parameters l_p, l_s , and l_i actually developed in flight test are thus known. From the definitions of these parameters f, e , and η_m are immediately found. From equations (5.1), (5.2), and (5.3),

$$e = \frac{W}{l_i (kb_1)^2} \tag{6.1}$$

$$f = \frac{W}{l_p} \tag{6.2}$$

$$\eta_m = \frac{W}{b \cdot \text{hp}_m l_i} \tag{6.3}$$

This process is very rapid, and gives much valuable information.

EXAMPLE: Let us suppose that the airplane for which performance was calculated in the preceding example has been flight tested with the following results:

$V_m = 140.0$ m. p. h.	$W = 5,000$ lb.	
$C_o = 1,100$ ft./min.	$b \cdot \text{hp}_m = 500$	$(kb_1)^2 = 2,360$
$H = 21,000$ ft.	$\text{r. p. m}_m = 1,500$	$C_{sm} = 1.38$

From Figure 34 $\Lambda = 10.2$

From Figure 33, $l_i C_o = 14,250$; $l_i = 12.95$; from equation (6.3) $\eta_m = 0.77$.

From Figure 30, $\frac{V_m}{l_i} = 4.98$; $l_s = 2.18$; from equation (6.1) $e = 0.97$.

From Figure 29, $\frac{l_p}{l_i} = 20.7$; $l_p = 268$; from equation (6.2) $f = 18.7$.

EXAMPLE: Let us now suppose that a performance specification has been given, and we are designing to meet it.

Specifications:

$$\begin{aligned} V_m &= 140 \text{ m. p. h.} \\ C_o &= 1,100 \text{ ft./min.} \\ H &= 21,000 \text{ ft.} \end{aligned}$$

Assumed from type airplane:

$$\begin{aligned} e &= 0.85 \\ k &= 1.13 \\ C_{sm} &= 1.40 \\ \eta_m &= 0.83 \end{aligned}$$

Exactly as in the preceding problem, Λ, l_i, l_s , and l_p are found,

$$\Lambda = 10.2$$

$$l_i = 12.95; \text{ from equation (6.3) } b \cdot \text{hp}_m = 0.0930 W$$

$$l_s = 2.18; \text{ from equation (6.1) } b_1^2 = 0.423 W$$

$$l_p = 268; \text{ from equation (6.2) } f = 0.00374 W$$

The characteristics are now determined by an estimation of the weight. If the design characteristics can not be obtained with the estimated weight, the latter must be reestimated until the dimensions and weight are compatible. If the final weight is

$$W = 5,000 \text{ lb. then, } b \cdot \text{hp}_m = 465$$

$$b_1^2 = 2,110 \quad b_1 = 46.0 \text{ ft.}$$

$$f = 18.7 \text{ sq. ft.}$$

DETERMINATION OF THE VARIATION OF PERFORMANCE OF THE AIRPLANE DUE TO A CHANGE IN ITS PARAMETERS

For airplanes equipped with modern unsupercharged engines and fixed-pitch metal propellers the variations of performance characteristics are readily determined from Figure 37. The chart is based upon equations that have been developed in Sections III and V.

The chart shows the percentage variation in the major performance characteristics due to a 1 per cent increase in each of the fundamental parameters:

$$t \cdot \text{hp}_m = b \cdot \text{hp}_m \cdot \eta_m$$

$$b_s = e^{1/2} (kb_1)$$

$$f$$

$$W$$

The rates of variation are functions of the major parameter Λ , hence Λ must be known. For reasonably small changes in a parameter the change in performance is given by merely multiplying the variation due to 1 per cent by the percentage change in the parameter. In general, for changes larger than 10 per cent the average rate of variation should be used, since Λ ,

and hence the rate, varies considerably. The average percentage change in parameter should also be used.

EXAMPLE: Consider the preceding problem of design to meet specification:

Specification:

$$V_m = 140.0$$

$$C_o = 1100$$

$$H = 21,000$$

Required characteristics:

$$W = 5,000$$

$$b.\text{hp}_m = 465$$

$$f = 18.6$$

$$b_1 = 46.0$$

As before, $\Lambda = 10.2$.

From Figure 37:

Parameter varied	Percentage variation of performance due to 1 per cent increase in parameter				
	V_m	C_o	H	T_{1000}	T_{10000}
t.hp _m	0.365	1.30	0.65	-1.40	-1.55
b_o	.045	.50	.95	-.55	-.85
f	-.340	-.10	-.15	.10	.15
W	-.045	-1.50	-.95	1.55	1.85

Suppose that after the airplane were in the assembly line it became evident that it would be 250 pounds overweight, but a change in engine were possible at 2 horsepower. What brake horsepower is required to meet minimum over-all specification? From the table it is seen that the relative effect of a change in weight to a change in horsepower is the greater in the case of absolute ceiling; so this will be the criterion.

$$100 \left(0.65 \frac{\Delta b.\text{hp}_m}{465} + (-0.95) \frac{\Delta b.\text{hp}_m \times 2}{5000} \right) + 100(-0.95) \frac{250}{5000} = 0$$

$$(0.140 - 0.038) \Delta b.\text{hp}_m = 4.75$$

$$\Delta b.\text{hp}_m = +46.5 \text{ (10.0 per cent change)}$$

$$W = 250 + 2(46.5) = +343 \text{ (6.86 per cent change)}$$

Resulting characteristics:

$$W = 5343$$

$$b.\text{hp}_m = 512$$

$$b_1 = 46.0$$

$$f = 18.6$$

Resulting performance:

$$H = 21,000$$

$$C_o = 1100 + 1100(1.30 \times 0.10 - 1.50 \times 0.0686) = 1100 + 30 = 1130$$

$$V_m = 140.0 + 140.0(0.365 \times 0.10 - 0.045 \times 0.0686) = 140.0 + 4.7 = 144.7$$

It is notable and fortunate that the equivalent parasite area f has the least over-all effect on airplane performance. For the airplane just considered a 10

per cent error in the estimated parasite area would result in errors of 3.40, 1.0, and 1.5 per cent in V_m , C_o , and H , respectively. A 10 per cent change in any of the parameters, b_o , t.hp_m, and W , would cause at least a 10 per cent change in one characteristic of performance.

THE ENGINEERING SIGNIFICANCE OF PARAMETER Λ

The parameter Λ may well be called the major (or characteristic) parameter of airplane performance, for Λ appears as the abscissa of all performance charts developed in this report, and occurs insistently in the algebraic formulas. For the modern unsupercharged engine for which the charts are developed, it may be seen by reference to Figures 33 and 34 that for a value of Λ of about 70, the absolute ceiling of the airplane considered is at sea level. For values of Λ greater than 70, the machine under consideration can hardly be called an airplane, for it would have an absolute ceiling below sea level. Parameter Λ is thus seen to be a critical parameter, peculiarly characteristic of an airplane, setting the critical limit at which a machine may be classed as an airplane. The absolute ceiling of an airplane is a function of Λ alone. The speed ratios for maximum speed at altitude, for the best climb, for absolute ceiling, and l_c , times maximum rate of climb, time to climb divided by l_c , and maximum velocity divided by l_c , are each functions of Λ . It is on the basis furnished by Λ that the formulas and charts have been developed.

The parameter Λ is a function of the primary parameters of the airplane, for

$$\Lambda = \frac{l_c l_i^{3/4}}{V_m^{1/4}} = \frac{W^{2/3} f^{1/4}}{t.\text{hp}_m^{1/2} b_o^{1/2}} = \frac{W^{2/3} f^{1/4}}{b.\text{hp}_m^{1/2} \eta_m^{1/4} e (kb)^2} \quad (6.4)$$

All symbols have been defined in Section V and in the Summary of Notation.

Parameter Λ may be shown to be a combination of several familiar parameters by the proper grouping of the terms in equation (6.4). As a physical conception of Λ is more easily attained by such a grouping, the following forms are given:

$$\Lambda = \left(\frac{W}{t.\text{hp}_m} \right) \left(\frac{W}{e(kb)^2} \right) \left(\frac{f}{t.\text{hp}_m} \right)^{1/4} \propto \frac{l_c l_i^{3/4}}{V_m} \text{ (approx.)} \quad (6.5)$$

It will be noted that the first term in the group is the thrust horsepower loading, the second is the effective span loading, and the third term is approximately inversely proportional to the maximum velocity at sea level by equation (5.8). In still another form,

$$\Lambda = \left(\frac{W}{t.\text{hp}_m} \right)^{2/3} \left(\frac{W}{e(kb)^2} \right)^{1/3} \left(\frac{f}{e(kb)^2} \right)^{1/4} \propto \left(\frac{L}{D} \right)_{\text{max}}^{3/4} \quad (6.6)$$

The terms here are the thrust horsepower loading to the four-thirds power, the effective span loading to the two-thirds power, and the equivalent parasite area per

unit of effective span squared to the one-third power. The last term is inversely proportional to the two-thirds power of the maximum lift/drag ratio by equation (7.7).

All airplanes of similar type have values of Δ in the same range, the ranges for modern airplanes being approximately:

TABLE V

Type airplane	Δ from—	To—
Pursuit.....	4	11
Observation.....	7	14
Training.....	10	19
Bombardment.....	10	20
Heavy flying boats.....	15	30

Commercial types lie in their respective places.

VII. SPECIAL PERFORMANCE PROBLEMS

The cases considered in this section are mainly problems dealing with the thrust horsepower required equation, i. e., the equation for sinking speed w_s . The general results are quite well known, but are here discussed in the light of the preceding analysis, and employing the parameters of this report. The results are presented in convenient chart form. Where data are needed only full-scale data are presented. The parameters l , l_p , and l_s are defined here as in Section V, equations (5.1), (5.2), and (5.3).

LANDING SPEED

The problem of landing speed of airplanes is one concerning a great number of variables, most of which can not be included in a theoretical analysis. Some factors which might be mentioned are: Piloting, control of airplane at low speeds, wing form, rigging, ground effect, interference between wings, body, struts, and so on *ad infinitum*. It is believed that the best method of taking these effects into general consideration is to calculate the maximum lift coefficient from reliable full-scale flight tests, and to classify these results for any one airfoil as regards type of airplane: Biplane, high wing monoplane, low wing monoplane, etc. The results of the investigation of a number of airplanes are given in the Table VI. (References 12 and 13.)

The landing speed is determined by use of the equation,

$$V_s = \sqrt{\frac{2W}{\rho S C_{L_{max}}}} = 29.0 \sqrt{\frac{l_w}{\sigma C_{L_{max}}}} \text{ (ft./sec.)} \quad (7.1)$$

$$V_s = 19.78 \sqrt{\frac{l_w}{\sigma C_{L_{max}}}} \text{ (m. p. h.)} \quad (7.2)$$

where,

- V_s —landing speed
- $C_{L_{max}}$ —maximum lift coefficient
- S —wing area (sq. ft.) including portion cut out by fuselage
- l_w —wing loading = W/S .

A chart giving V_s at sea level as a function of l_w and $C_{L_{max}}$ is plotted in Figure 40. The use of maximum lift coefficient values from the Table VI for the solution of V_s should produce satisfactory results. Only airfoil sections for which flight test data are available are included in the Table. The chart may obviously be used with any data, but only flight test data reduced by the chart or equation (7.2) or full-scale Reynolds Number wind tunnel data may be expected to give satisfactory results.

TABLE VI.—MAXIMUM LIFT COEFFICIENTS FOR SEVERAL AIRPLANES

Airfoil section	Flight test maximum lift coefficient							
	Monoplane				Biplane			
	N	High wing	N	Low wing	N	Single bay	N	Multiple bay
Aeromarine 2 A.....					1	1.17		
Albatross.....							3	1.15
Boeing 103.....					3	1.34		
Clark Y.....	2	1.37	1	1.4	25	1.27		
Curtiss C-42.....					1	1.11		
Curtiss C-72.....							2	1.4
Eiffel 36.....					1	1.18		
Fokker.....	7	1.36						
Ford-Stout.....	4	1.39						
Göttingen 387.....	2	1.39						
Göttingen 398.....					7	1.34		
Göttingen 436.....					7	1.27	3	1.3
G. S. No. 1 (Sikorsky).....							1	1.47
Loening 2 A.....					1	1.2	2	1.08
Loening 10 A.....	1	1.03					1	1.09
R. A. F. 15.....					9	1.07	1	1.11
T. M.—22.....							1	1.11
U. S. A. 5.....					2	1.26		
U. S. A. 27.....					2	1.3		
U. S. A. 35 B.....					1	1.37		
U. S. A. 45.....							6	1.10

N=number of airplanes averaged.

MAXIMUM LIFT/DRAG RATIO; SPEED FOR MAXIMUM LIFT/DRAG RATIO

From equation (2.5) we get,

$$\frac{D}{W} = \frac{w_s}{V} \quad (7.3)$$

Substituting for w_s in equation (7.3) from equation (2.12), using engineering units, and noting that in horizontal flight $W=L$,

$$\frac{D}{L} = 0.002558 \frac{\sigma}{l_p} V^2 + 124.4 \frac{l_s}{\sigma} \frac{1}{V^2} \text{ (V in m. p. h.)} \quad (7.4)$$

The speed at which maximum lift/drag ratio occurs is obtained by differentiating $\frac{D}{L}$ with respect to velocity and equating to zero.

$$\frac{d}{dV} \left(\frac{D}{L} \right) = 0.005116 \frac{\sigma}{l_p} V - 248.8 \frac{l_s}{\sigma} \frac{1}{V^3} = 0 \quad (7.5)$$

Whence,

$$V_{LD} = 14.85 \frac{(l_s l_p)^{1/4}}{\sigma^{1/2}} \text{ (m.p.h.)} \quad (7.6)$$

Equation (7.6) is the expression for the velocity at which maximum $\frac{L}{D}$ occurs. Substituting equation (7.6) into equation (7.4), inverting, and solving for $\frac{L}{D}$ which is now the maximum value for the ratio, we get

$$\left(\frac{L}{D}\right)_{\max} = 0.886 \left(\frac{l_p}{l_s}\right)^{1/2} \quad (7.7)$$

Charts have been plotted for equations (7.7) and (7.6) which give $\left(\frac{L}{D}\right)_{\max}$ and velocity at $\left(\frac{L}{D}\right)_{\max}$ explicitly in terms of l_p and l_s . These charts are found in Figures 41 and 42, respectively.

The value of $\left(\frac{L}{D}\right)_{\max}$ is of particular interest in determining the general "cleanness of design" of an airplane, the minimum gliding angle, and the maximum range. The airplane will necessarily fly at approximately the speed for maximum $\frac{L}{D}$ where maximum range is desired. Knowing $\left(\frac{L}{D}\right)_{\max}$ and the speed for maximum $\frac{L}{D}$, the thrust horsepower required is readily determined.

Dividing $l_p l_s$ by V_{LD} from equation (7.6) we obtain,

$$\frac{l_p l_s}{V_{LD}} = 0.0673 (\Lambda)^{1/2} \quad (7.8)$$

$\frac{l_p l_s}{V_{LD}}$ may thus be expressed as a function of Λ . This

is analogous to that for $\frac{l_p l_s}{V_m}$, hence the ratio between V_{MP} and V_m is a function of Λ . This speed ratio for maximum $\frac{L}{D}$ has been plotted against Λ' (the physical parameter, $\Lambda = 158.9 \Lambda'$) in Section II, Figure 4.

SPEED FOR MINIMUM POWER

The condition for minimum power is $\frac{dw_s}{dV} = 0$. Differentiating equation (2.12) with respect to V , equating to zero, and using engineering units we have,

$$\frac{dw_s}{dV} = 0.011253 \frac{\sigma}{l_p} V^3 - 182.5 \frac{l_s}{\sigma} \frac{1}{V^2} = 0. \quad (7.9)$$

Whence,

$$V_{MP} = 11.28 \frac{(l_s l_p)^{1/2}}{\sigma^{1/2}} \quad (\text{m. p. h.}) \quad (7.10)$$

Equation (7.10) is the expression for speed for minimum thrust horsepower required, assuming equation (2.12) for w_s to be valid at this speed. This assumption is seldom justified, since it has been found from an investigation of more than 50 airplanes that in most cases the speed determined from equation (7.10) is lower than the stalling speed by several per cent. In these cases the speed for minimum power is primarily a function of the stalling speed, since the rapid increase of drag at stalling speed has here caused the slope of the w_s curve to become zero.

From an investigation of Army flight test data and flight test polars (Figs. 24 a and 24 b) it has been found that the speed for minimum power generally occurs within 5 per cent of a value of 1.08 times the stalling speed. It is concluded therefore that the following method is to be used in determining V_{MP} (speed for minimum power):

Find

$$V_{MP} \text{ by equation (7.10), if } V_{MP} \geq 1.08 V_s \quad (7.11)$$

or

$$V_{MP} = 1.08 V_s, \text{ if } V_{MP} \text{ (equation (7.10)) } \leq 1.08 V_s.$$

A chart is included for finding V_{MP} by equation (7.10). By comparison of equations (7.10) and (7.6) it is readily seen that

$$V_{MP} = 0.760 V_{LD} \quad (7.12)$$

Speed for minimum power according to equation (7.10) is found from an additional scale on Figure 42.

Dividing $l_p l_s$ by V_{MP} equation (7.10) gives,

$$\frac{l_p l_s}{V_{MP}} = 0.0886 (\Lambda)^{1/2} \quad (7.13)$$

We have then $\frac{l_p l_s}{V_{MP}}$ as a function of Λ and hence the ratio $\frac{V_{MP}}{V_m}$ is a function of Λ . This speed ratio for minimum power has been plotted against the physical parameter Λ' in Figure 4, Section II.

THRUST HORSEPOWER REQUIRED AT ANY SPEED AND ANY ALTITUDE

The two terms of equation (2.12) have been separated and the sinking speed due to each term plotted as indicated below.

Writing:

$$w_s = w_{s_p} + w_{s_e} \text{ ft./sec.} \quad (7.14)$$

where,

w_{s_p} - sinking speed due to parasite loading

w_{s_e} - sinking speed due to effective span loading

equation (2.12) gives, upon transformation to engineering units,

$$w_{s_p} = 0.003751 \frac{\sigma}{l_p} V^3 \text{ ft./sec.} \quad (V \text{ in m. p. h.}) \quad (7.15)$$

and,

$$w_{s_e} = 182.5 \frac{l_s}{\sigma} \frac{1}{V} \text{ ft./sec.} \quad (V \text{ in m. p. h.}) \quad (7.16)$$

Equations (7.15) and (7.16) have been plotted in Figures 43 and 44, respectively, from which w_{s_p} and w_{s_e} may be found explicitly in terms of l_s , l_p , and V for any altitude.

Thrust horsepower required at any velocity, and the thrust horsepower required curve for any airplane at any altitude are now readily determined by the use of these charts, and the relation,

$$\text{t. hp}_r = (w_{s_p} + w_{s_e}) \frac{W}{550} \quad (7.17)$$

The thrust horsepower required at cruising speed at any altitude is easily determined. To a first and good approximation the propulsive efficiency in throttled level flight at speeds near the maximum velocity may be taken equal to the propulsive efficiency at maximum velocity. The brake horsepower required is thus determined.

VIII. CONCLUSION

General algebraic performance formulas have been developed which are based on the induced drag viewpoint of performance. By the incorporation of data applying to any general type of propulsive unit, formulas and charts may be obtained which apply to all airplanes equipped with the same type of propulsive unit. Consequently supercharged engine data and variable-pitch propeller data may be incorporated when satisfactory data are available.

Formulas and charts have been developed which may be used to determine the performance characteristics of all airplanes equipped with modern unsupercharged engines and fixed-pitch metal propellers. The use of these charts is very rapid, and they produce results of good accuracy, generally within 5 per cent of flight test data.

These same charts may be used to reduce flight test data and obtain the actual airplane parameters.

The equations, and hence the charts developed, are expressed in terms of the three engineering parameters of the airplane: l_p , the parasite loading; l_s , the effective span loading; and l_t , the thrust horsepower loading.

A new parameter of fundamental importance $\Lambda = \frac{l_s l_t^{3/4}}{l_p^{1/2}}$ is revealed by the formulas, and is used as the abscissa of the performance charts. Λ may be called the major (or characteristic) parameter of airplane performance.

The dependence of performance upon each parameter is readily seen from the charts developed. The effect of varying any characteristic of the airplane is immediately determined.

The propeller set to give best maximum velocity at sea level produces also the best maximum rate of climb. This is called the "BEST PERFORMANCE PROPELLER."

The variation of parasite drag with angle of attack, and the increase in induced drag over the minimum case of a wing with elliptical lift distribution may well be included in a correction proportional to C_L^2 , which introduces e , the "airplane efficiency factor."

DANIEL GUGGENHEIM GRADUATE SCHOOL OF AERONAUTICS,
CALIFORNIA INSTITUTE OF TECHNOLOGY,
PASADENA, CALIF., April 27, 1931.

SUMMARY OF NOTATION

ENGINEERING

Subscript m denotes at design maximum velocity (sea level).

Subscript h denotes at altitude.

Subscript o denotes at sea level.

V - velocity $\left\{ \begin{array}{l} \text{miles per hour in performance} \\ \text{charts.} \\ \text{feet per second in propeller charts.} \end{array} \right.$

V_L - landing speed.

V_{MP} - velocity for minimum power required (m. p. h.).

V_{LD} - velocity for maximum lift/drag ratio (m. p. h.).

V_m - design maximum velocity at sea level (m. p. h.).

R_{s_m} - maximum velocity at altitude

maximum velocity at sea level

R_{s_o} - velocity for maximum rate of climb

maximum velocity at sea level

R_{v_H} - velocity at absolute ceiling

maximum velocity at sea level

C - maximum rate of climb (ft. per second).

H - absolute ceiling (feet).

H_s - service ceiling (feet).

T - minimum time required to climb to altitude (minutes).

$\left(\frac{L}{D}\right)_{max}$ - maximum lift/drag ratio.

w_{s_p} - sinking speed due to effective parasite drag (ft. per second).

w_{s_i} - sinking speed due to effective induced drag (ft. per second).

b. hp - brake horsepower.

t. hp_a - thrust horsepower available.

t. hp_r - thrust horsepower required.

r. p. m. - revolutions per minute.

N - revolutions per second.

η - propulsive efficiency.

$C_{s_o} = \frac{0.638 V(m.p.h.)}{b.hp^{1/2} r.p.m.^{3/4}}$

C_L - lift coefficient.

C_{L_m} - maximum lift coefficient (at landing speed).

C_D - drag coefficient.

C_{Dpe} — effective parasite drag coefficient.
 C_{Di} — effective induced drag coefficient.
 W — weight (pounds).
 f — equivalent parasite area (sq. ft.); by defining equation, $f = C_{Dpe} S$
 e — airplane efficiency factor (Sec. IV).
 k — Munk's span factor.
 b_1 — largest individual span of wing cellule.
 b_e — $e^{1/2} (kb_1)$ = effective span.
 S — wing area including portion cut out by fuselage (sq. ft.).

$$l_w = \frac{W}{S} \text{ — wing loading (lb./sq. ft.)}$$

$$l_p = \frac{W}{f} \text{ — parasite loading (lb./sq. ft.)}$$

$$l_s = \frac{W}{b_e^2} \text{ — effective span loading (lb./sq. ft.)}$$

$$l_t = \frac{W}{t \cdot \text{hp}_m} \text{ — thrust horsepower loading (lb./hp.)}$$

$$\Lambda = \frac{l_s l_t^{1/2}}{l_p^{1/2}} \text{ — major performance parameter}$$

PHYSICAL

V_o — ideal minimum velocity

A — horsepower conversion factor (550 in American system, 75 in metric system)

$\rho_o = 0.002378$ (lb./ft.³, sec. system) = mass density of standard air at sea level.

$$\lambda_p = \frac{2}{\rho_o} l_p = 841.0 l_p \text{ (ft., lb., sec. system)}$$

$$\lambda_s = \frac{2}{\pi \rho_o} l_s = 267.7 l_s \text{ (ft., lb., sec. system)}$$

$$\lambda_t = \frac{1}{A} l_t = 0.001818 l_t \text{ (ft., lb., sec. system)}$$

$$\Lambda' = \frac{\lambda_s \lambda_t^{1/2}}{\lambda_p^{1/2}} = 0.006293 \Lambda \text{ (ft., lb., sec. system)}$$

REFERENCES

1. Millikan, Clark B.: The Induced Drag Viewpoint of Performance. *Aviation*, Aug. 17, 1929.
2. Schrenk, M.: Calculation of Airplane Performances without the Aid of Polar Diagrams. N. A. C. A. Technical Memorandum No. 456, Mar., 1928. From the 1927 Yearbook of the Deutsche Versuchsanstalt für Luftfahrt, pp. 145-51.
- 2a. Schrenk, M.: A Few More Mechanical-Flight Formulas without the Aid of Polar Diagrams. N. A. C. A. Technical Memorandum No. 457, 1928. From the 1927 Yearbook of the Deutsche Versuchsanstalt für Luftfahrt, pp. 104-112.
3. Helmbold, H. B.: Die generalisierten Koordinaten der Flugmechanik. *Zeitschrift für Flugtechnik und Motorluftschiffahrt*, No. 22, Vol. 18, Nov. 28, 1927.
4. Driggs, Ivan H.: A Simple Theoretical Method of Analyzing and Predicting Airplane Performance. *Air Service Information Circular*, No. 553, Vol. 6, Feb. 1, 1926.
5. Diehl, Walter S.: *Engineering Aerodynamics*. The Ronald Press, 1928.
6. Weick, Fred E.: Full-Scale Wind-Tunnel Tests of a Series of Metal Propellers on a VE-7 Airplane. N. A. C. A. Technical Report No. 306, 1929.
7. Weick, Fred E.: Full-Scale Wind-Tunnel Tests on Several Metal Propellers Having Different Blade Forms. N. A. C. A. Technical Report No. 340, 1930.
8. Weick, Fred E.: *Aircraft Propeller Design*. McGraw-Hill Book Co. (Inc.), 1930.
9. Weick, Fred E.: Working Charts for the Selection of Aluminum Alloy Propellers of a Standard Form to Operate With Various Aircraft Engines and Bodies. N. A. C. A. Technical Report No. 350, 1930.
10. Loudon, F. A.: Collection of Wind-Tunnel Data on Commonly Used Wing Sections. N. A. C. A. Technical Report No. 331, 1929.
11. Engineering Division, Army Air Corps: *Handbook of Instructions for Airplane Designers*. Sixth edition, 2 volumes, March, 1931.
12. Lee, John G.: The Landing Speed of Airplanes. *Aeronautical Engineering*, Trans. A. S. M. E., Vol. 1, No. 2, April-June, 1929.
13. Ridley, Kenneth F.: An Investigation of Airplane Landing Speeds. N. A. C. A. Technical Note No. 349, Sept., 1930.

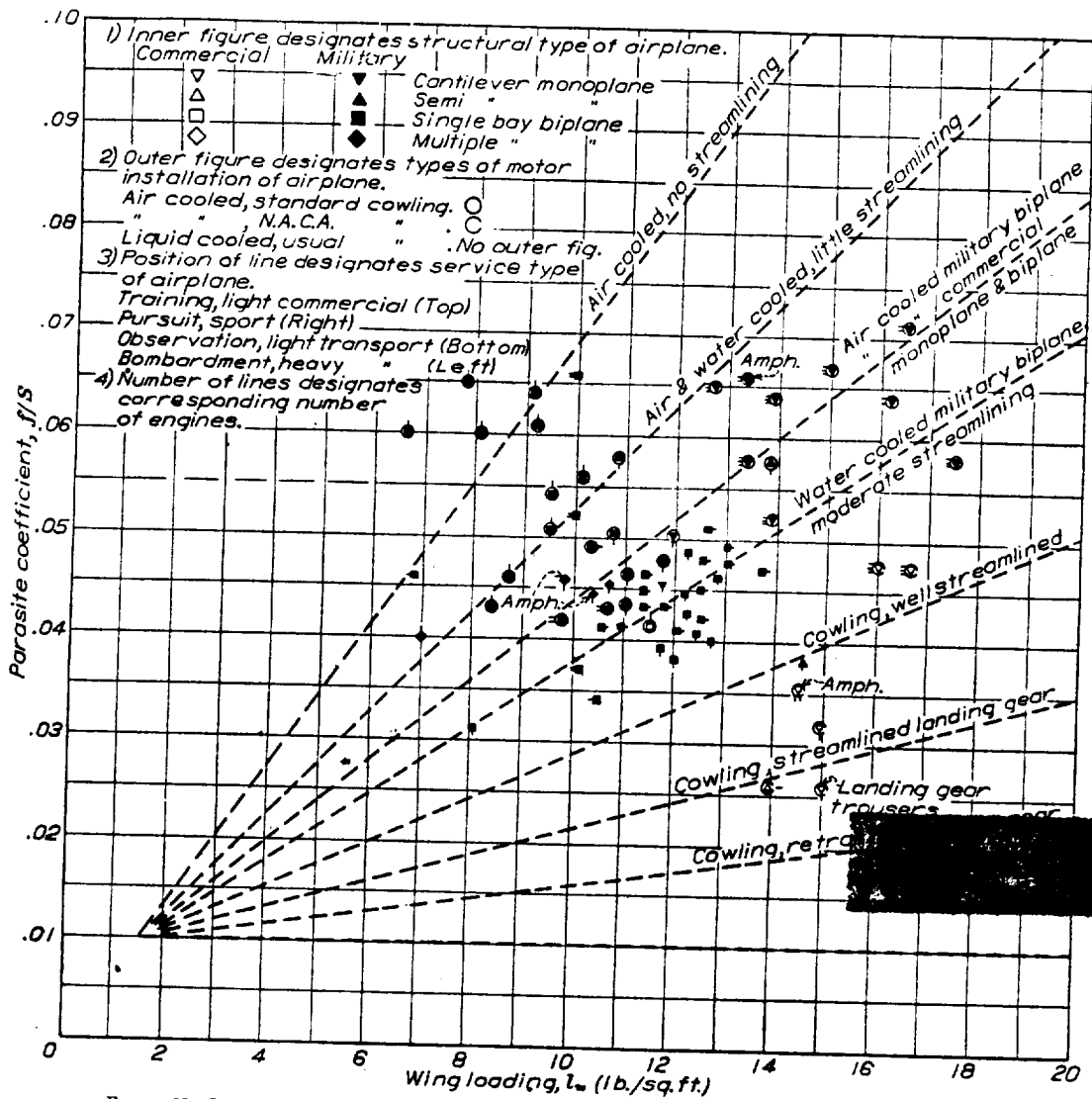
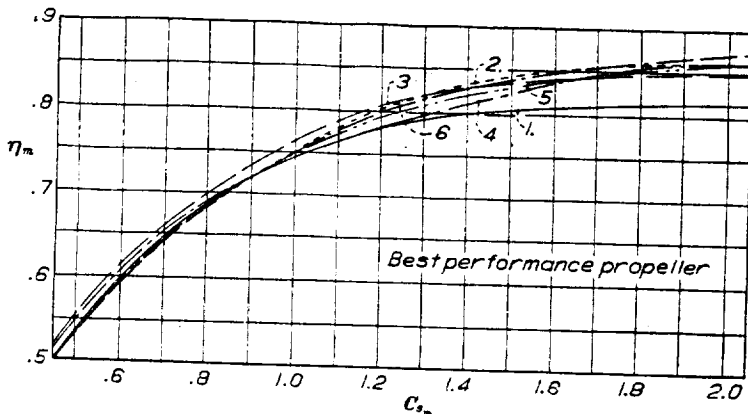


FIGURE 25.—Parasite coefficient as a function of wing loading for contemporary airplanes. Data from flight test.



1. Open cockpit fuselage, 400 hp D-12 W.C. engine. Smoothly faired nose, no radiator.
 2. Complete V.E.-7 airplane with wings. Open cockpit fuselage, 180 hp W.C. engine. Nose radiator.
 3. Open cockpit fuselage, 200 hp A.C. engine. Medium cowling.
 4. Cabin fuselage, monoplane wing, 200 hp J-5 A.C. engine. No cowling.
 5. Cabin fuselage, no wing, 200 hp J-5 A.C. engine. Good cowling.
 6. Cabin fuselage, no wing, 200 hp J-5 A.C. engine. N.A.C.A. cowling.
- (See remarks in Section III on the choice of a propulsive efficiency for computing performance.)

FIGURE 27.—Propulsive efficiency at V_{max} as a function of C_d for various aircraft engines and bodies. Nine-foot metal propeller. Navy No. 4412. Data from National Advisory Committee for Aeronautics. Technical Report 350

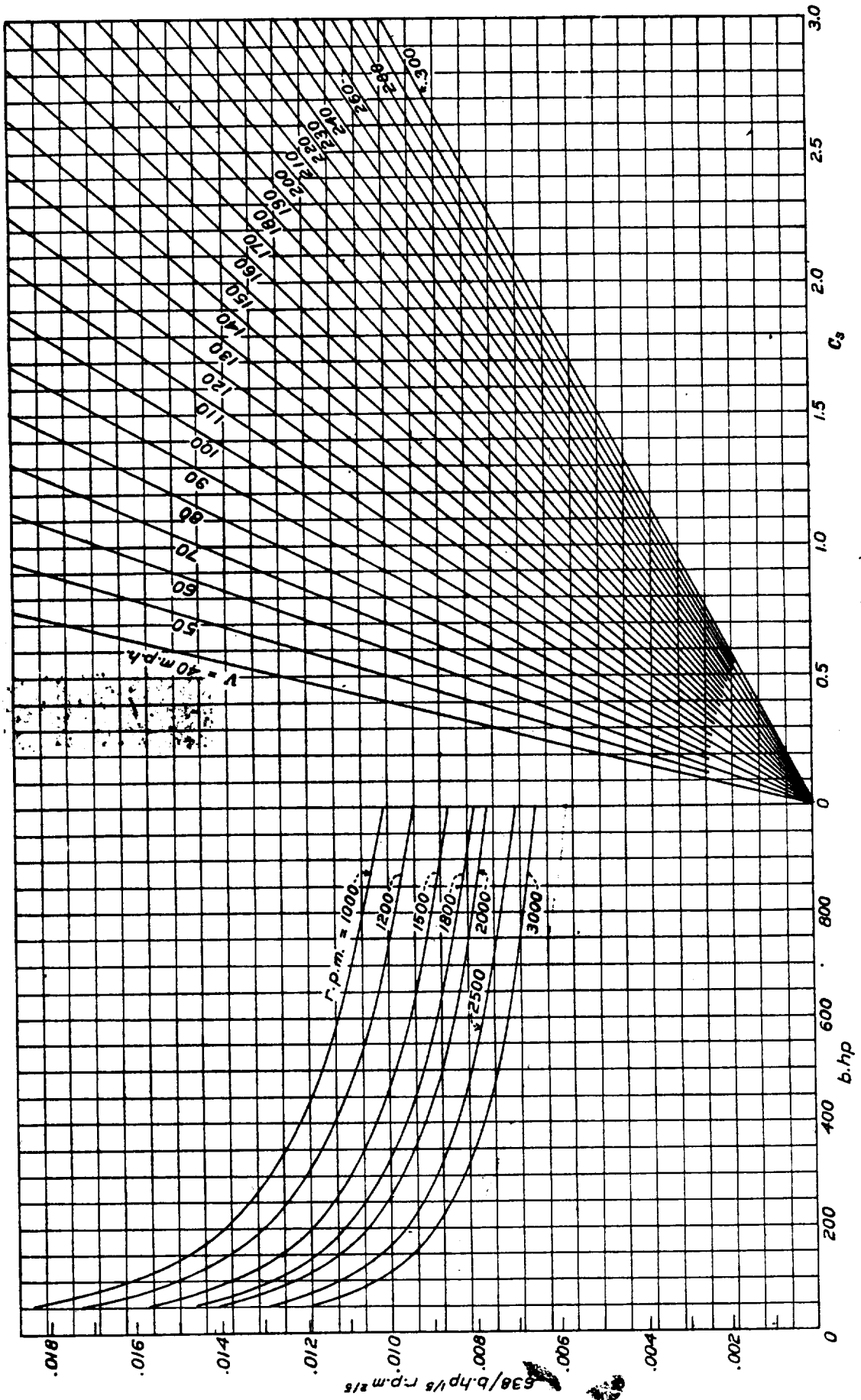


FIGURE 26.—Chart for graphical solution of $C_s = 0.638 m. p. h. / b. hp^{1/3}$ r. p. m. at sea level

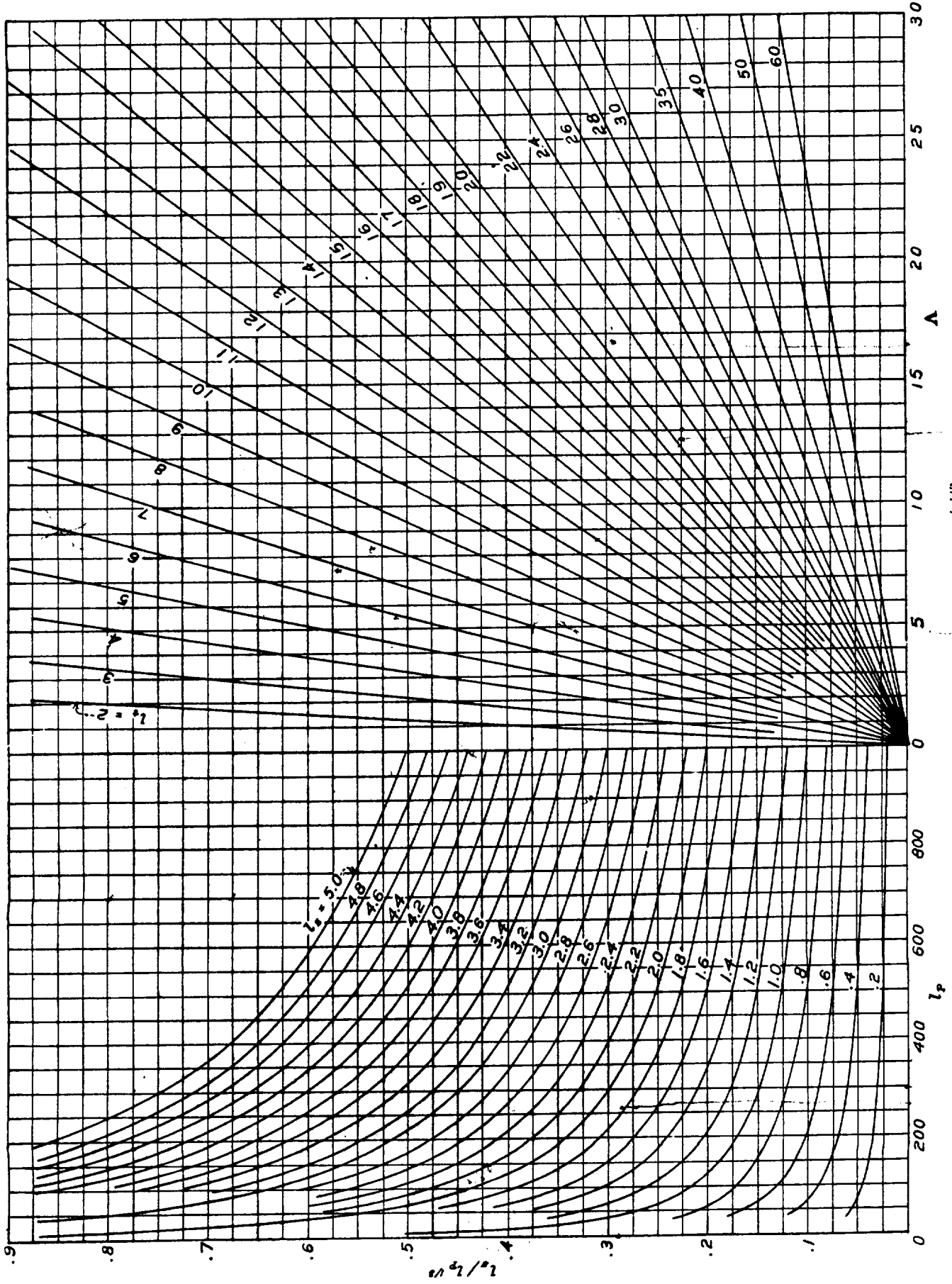


FIGURE 28.—Chart for the graphical solution of $C_p = l_p A^2$

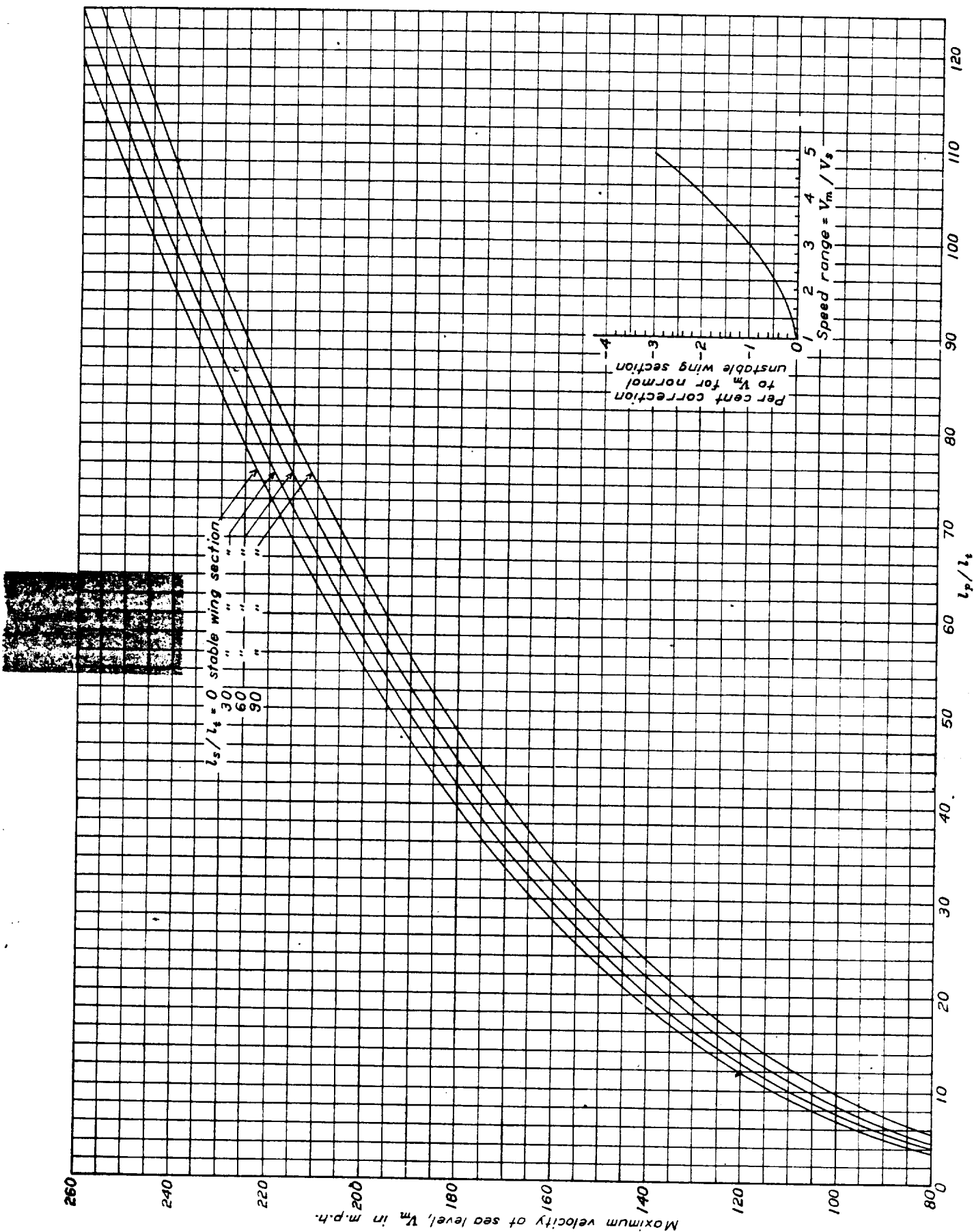


FIGURE 20.—Maximum velocity at sea level as a function of l_p/l_t

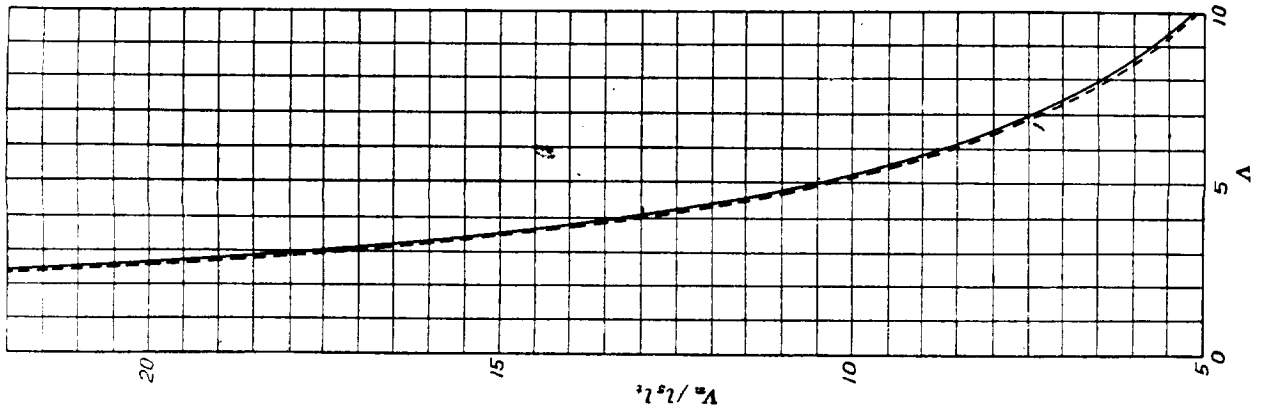
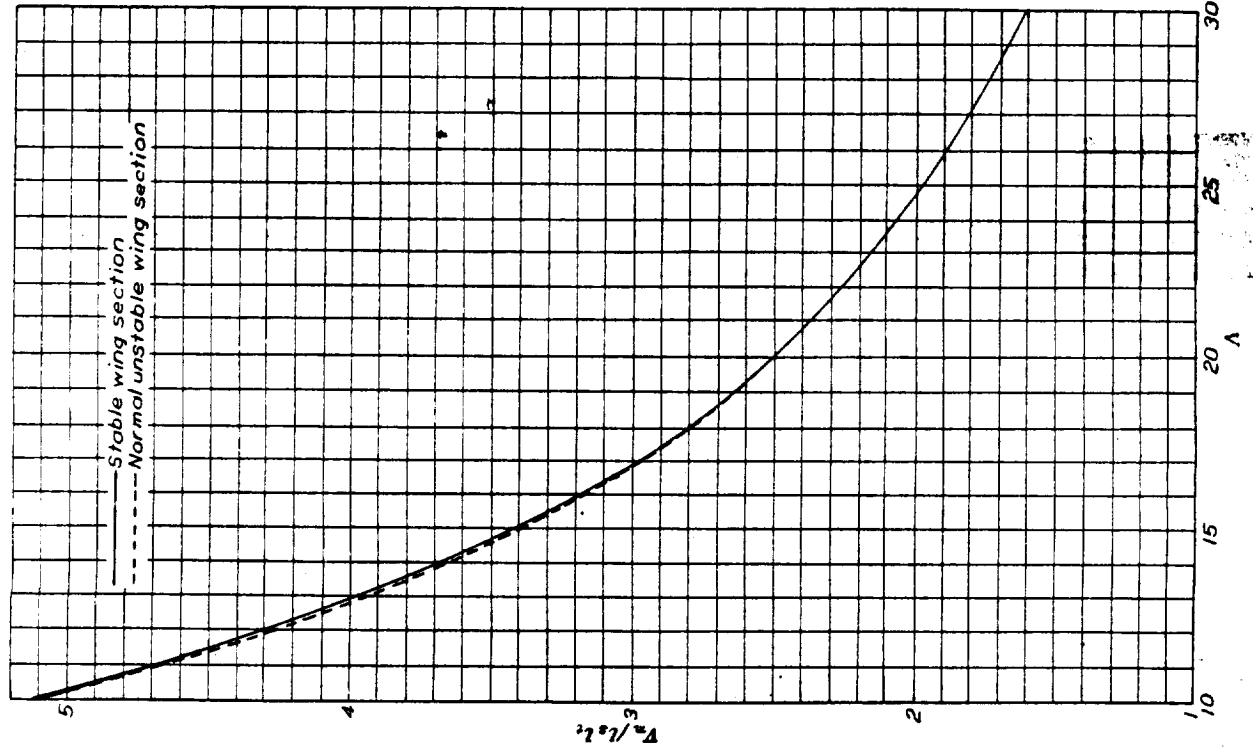
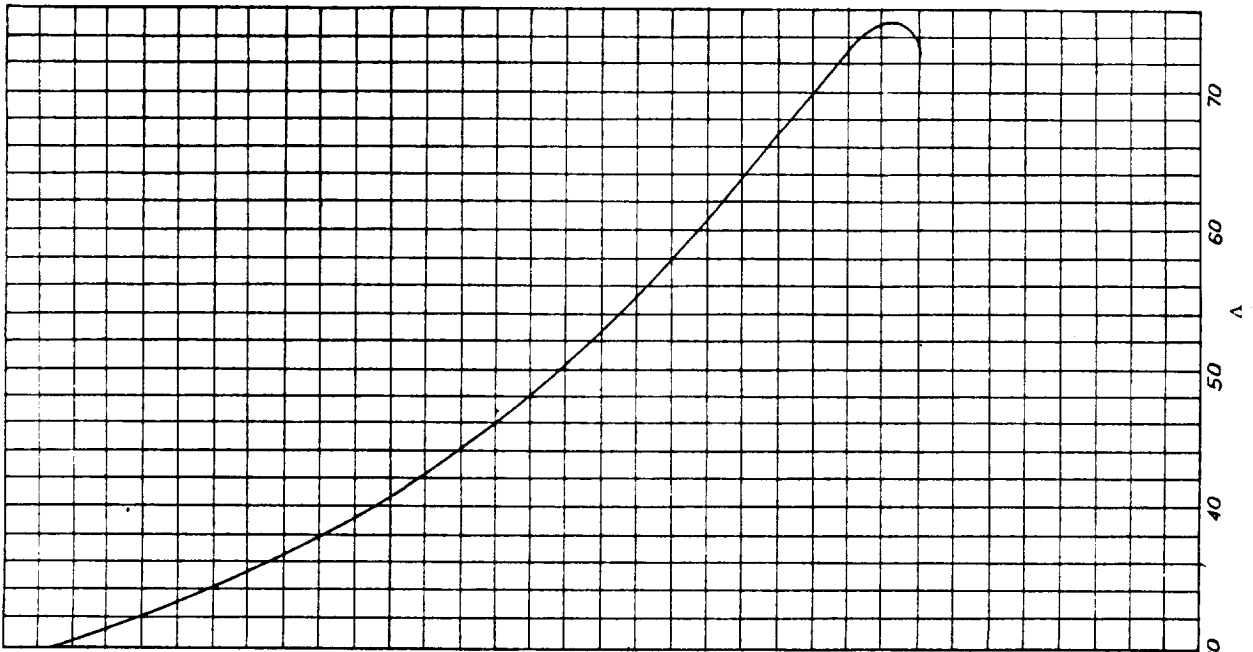


FIGURE 30. V_m as a function of λ . V_m - maximum velocity at sea level in m. p. h.

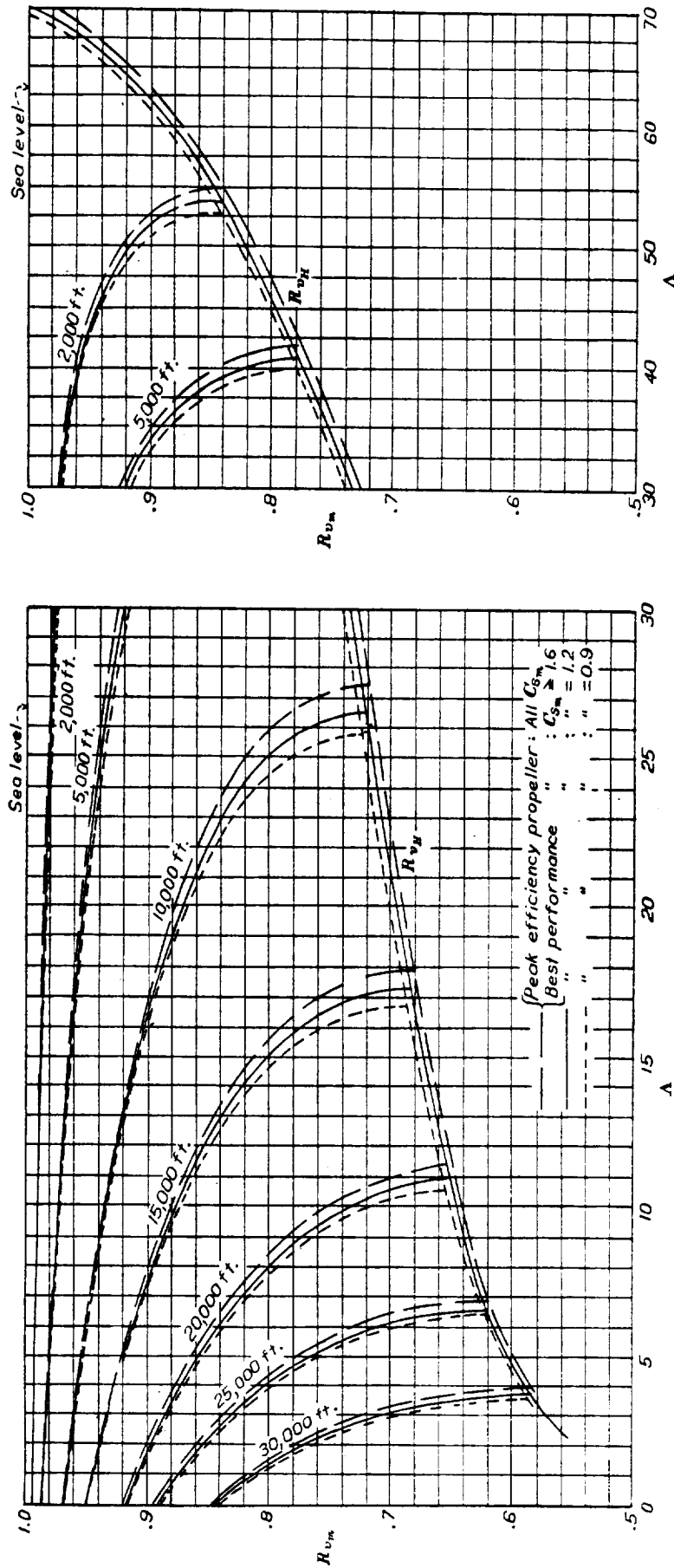


FIGURE 31.— R_{vm} max. velocity at altitude as a function of A , at various altitudes. R_{vm} max. velocity at sea level as a function of A . R_{vH} max. velocity at sea level as a function of A .

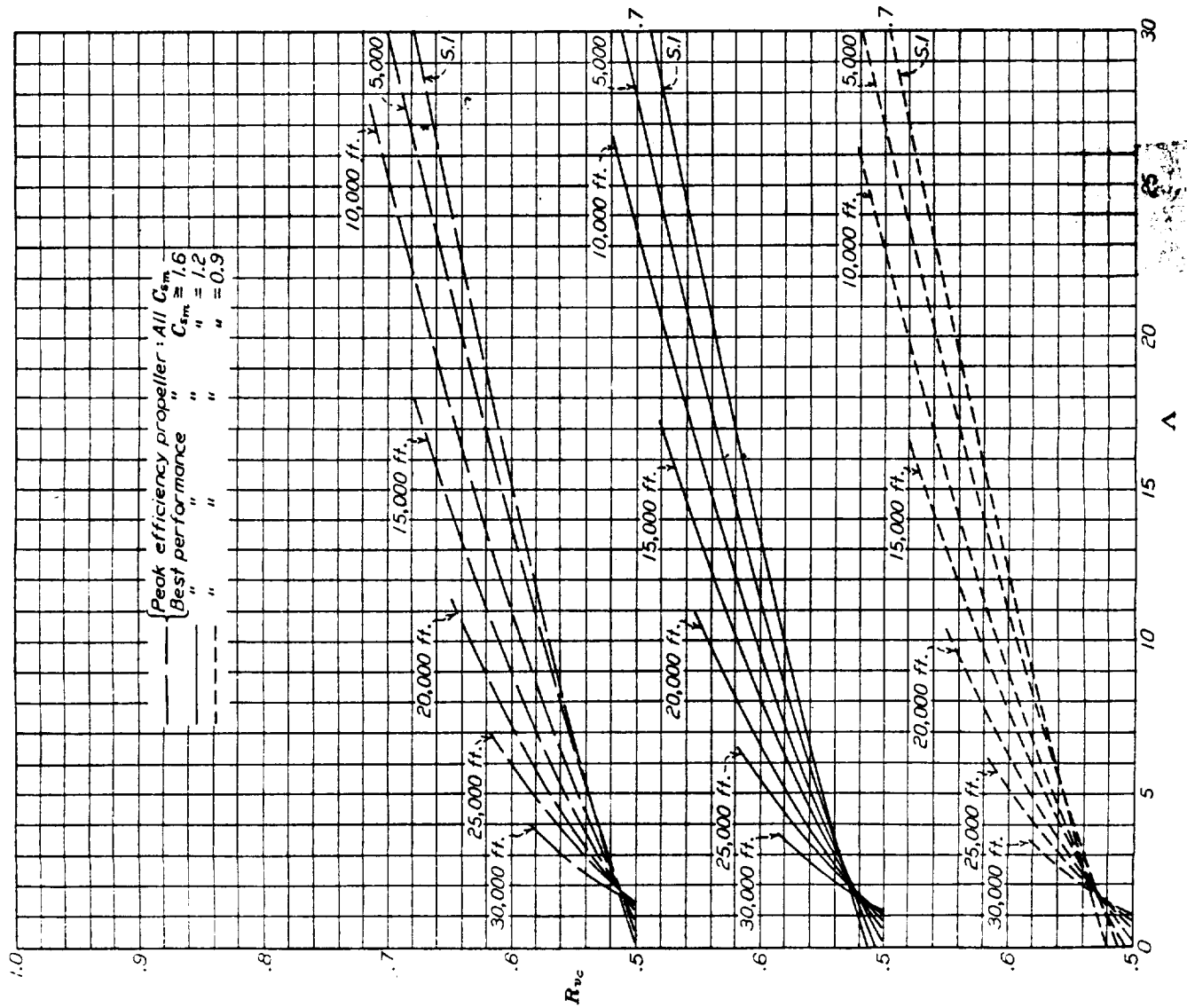
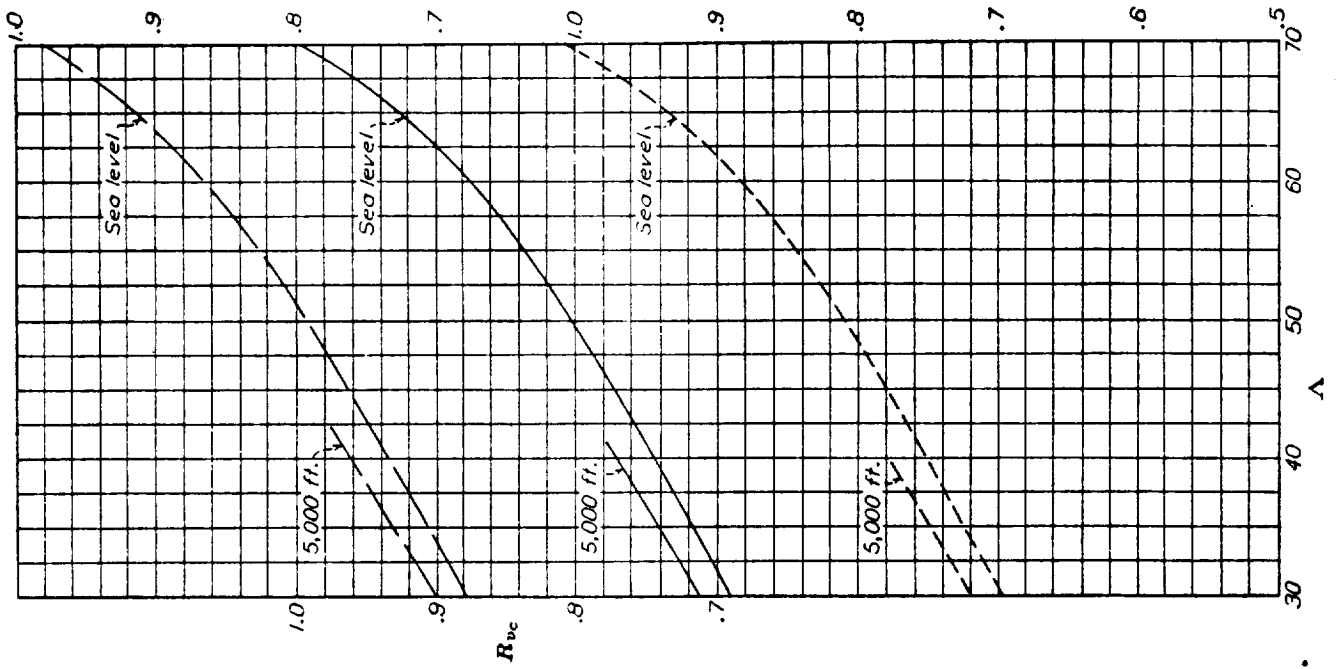


FIGURE 32. — R_{vc} — maximum velocity at sea level as a function of A , at various altitudes

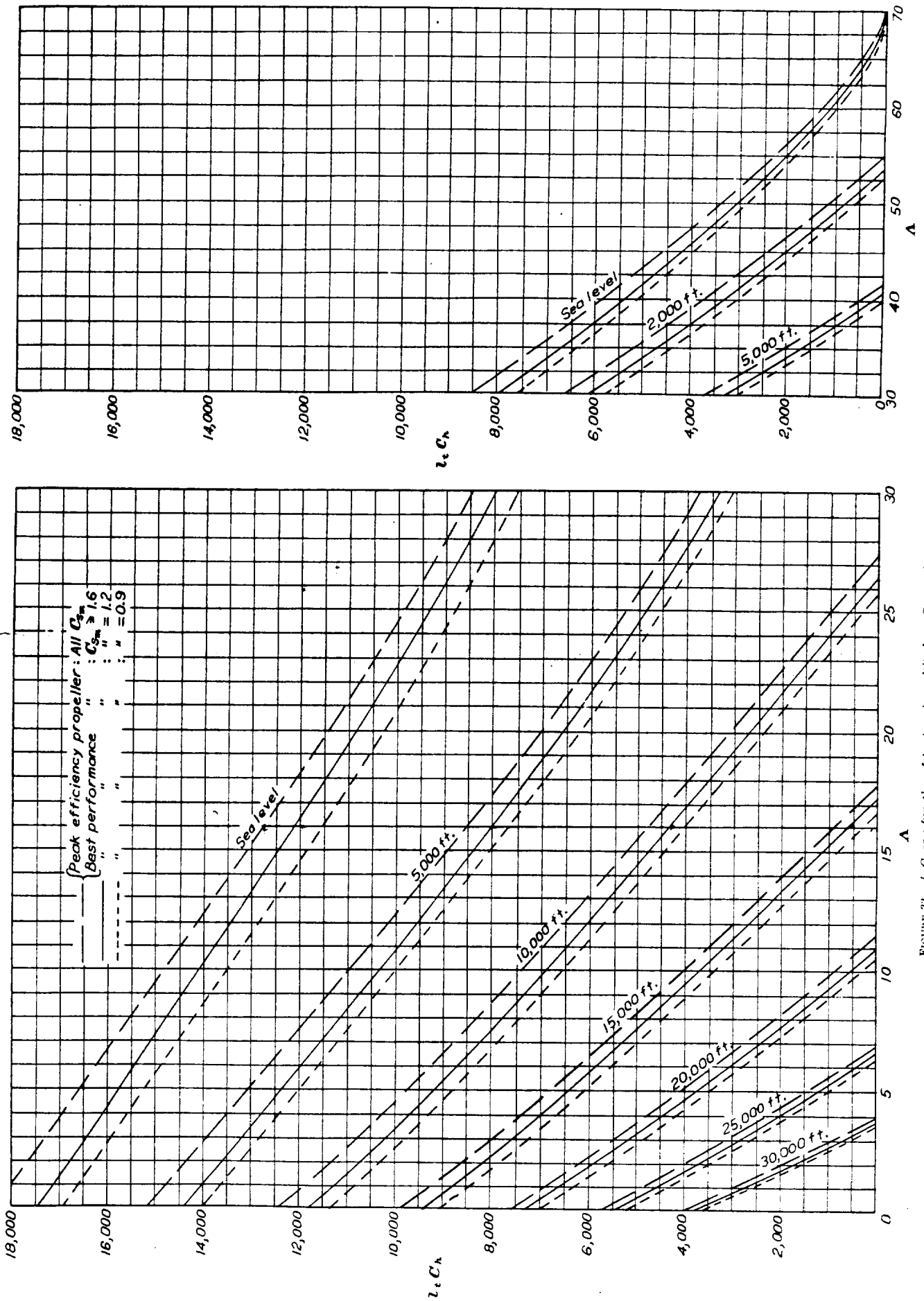


FIGURE 33.— $l_c C_v$ as a function of A , at various altitudes. C_v = maximum rate of climb in feet per minute

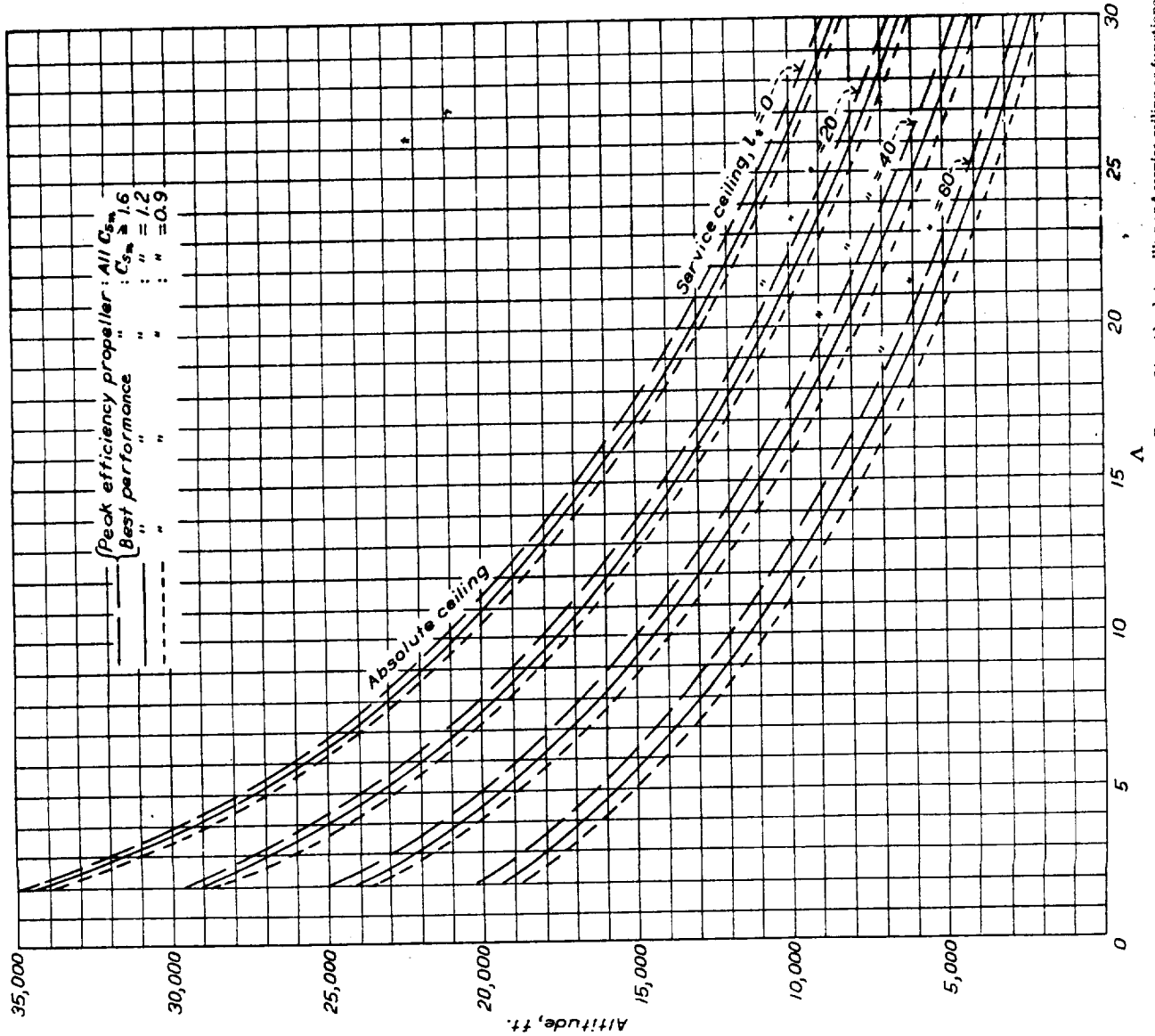
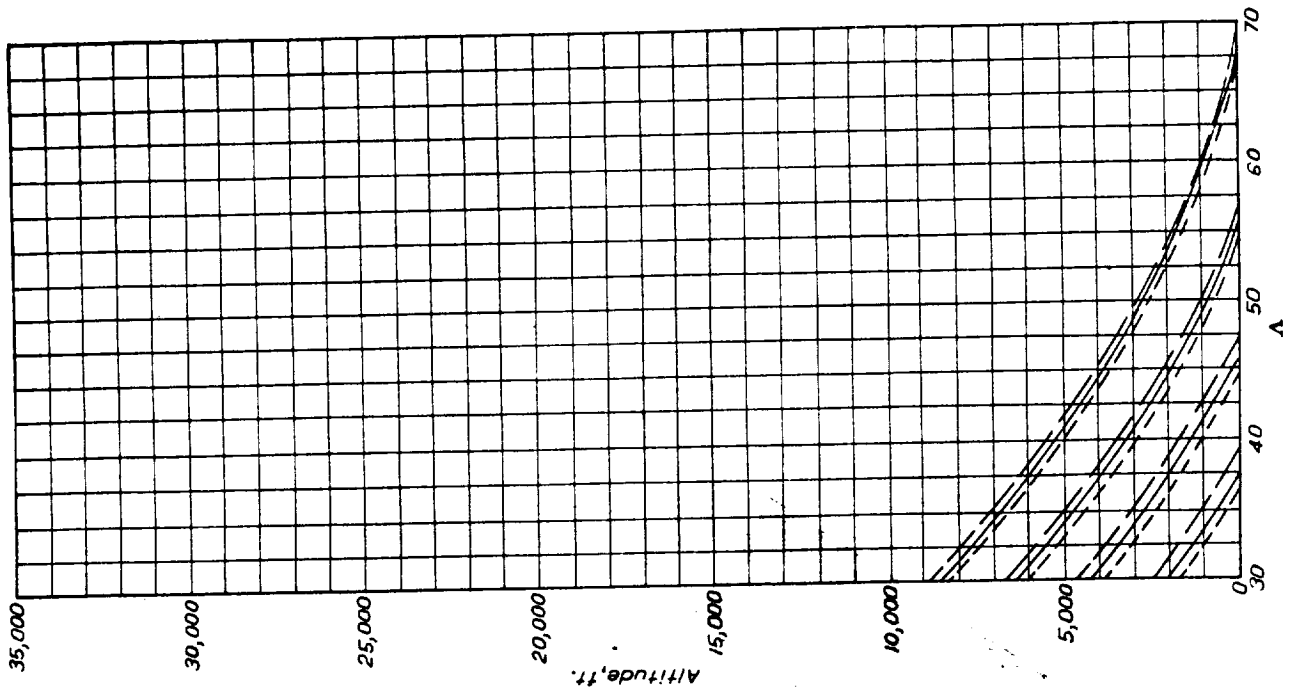


FIGURE 34.—Absolute ceiling and service ceiling as functions of A

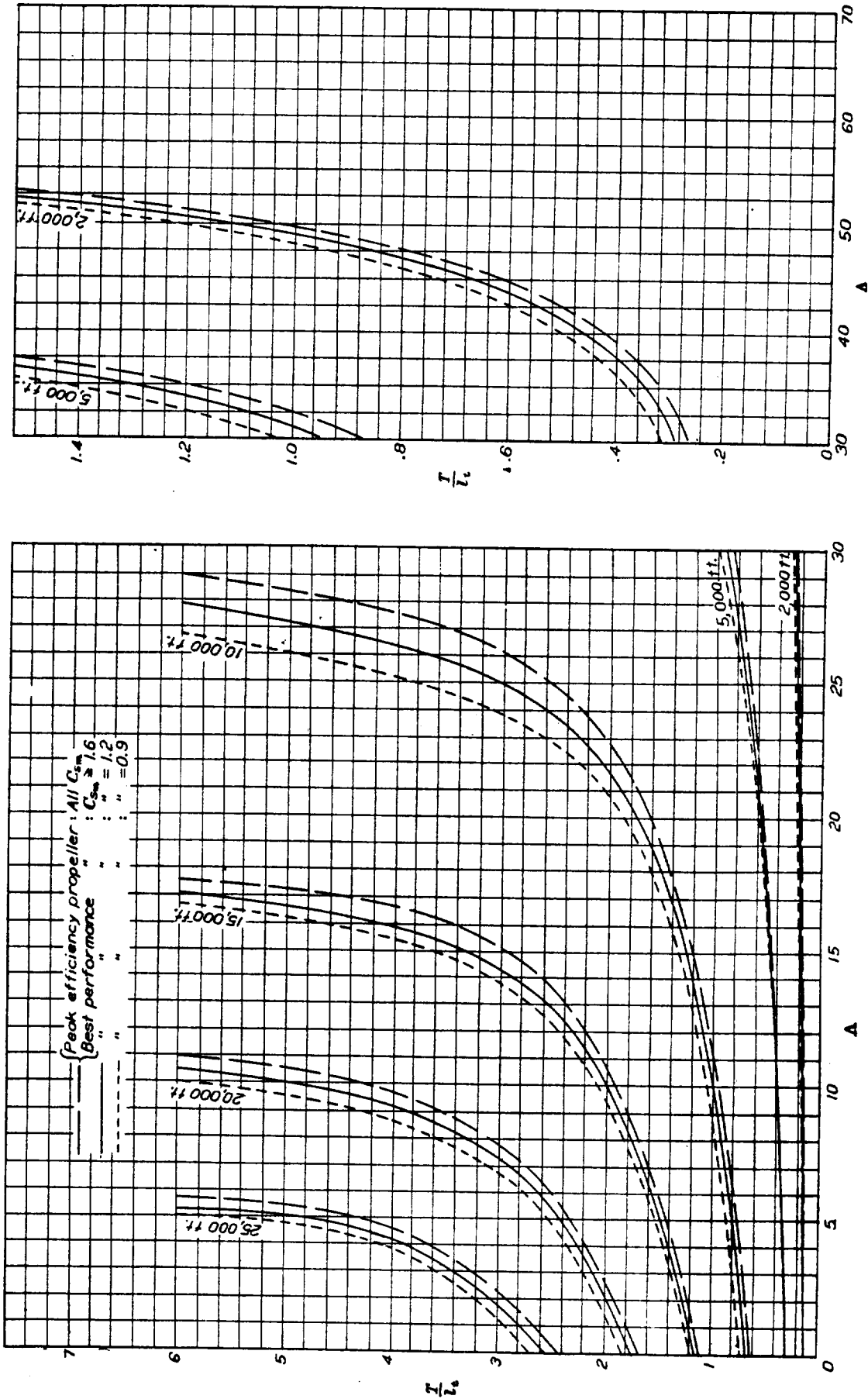


FIGURE 36.— T/T_0 as a function of A , at various altitudes. T = minimum time required to climb to altitude (minutes)

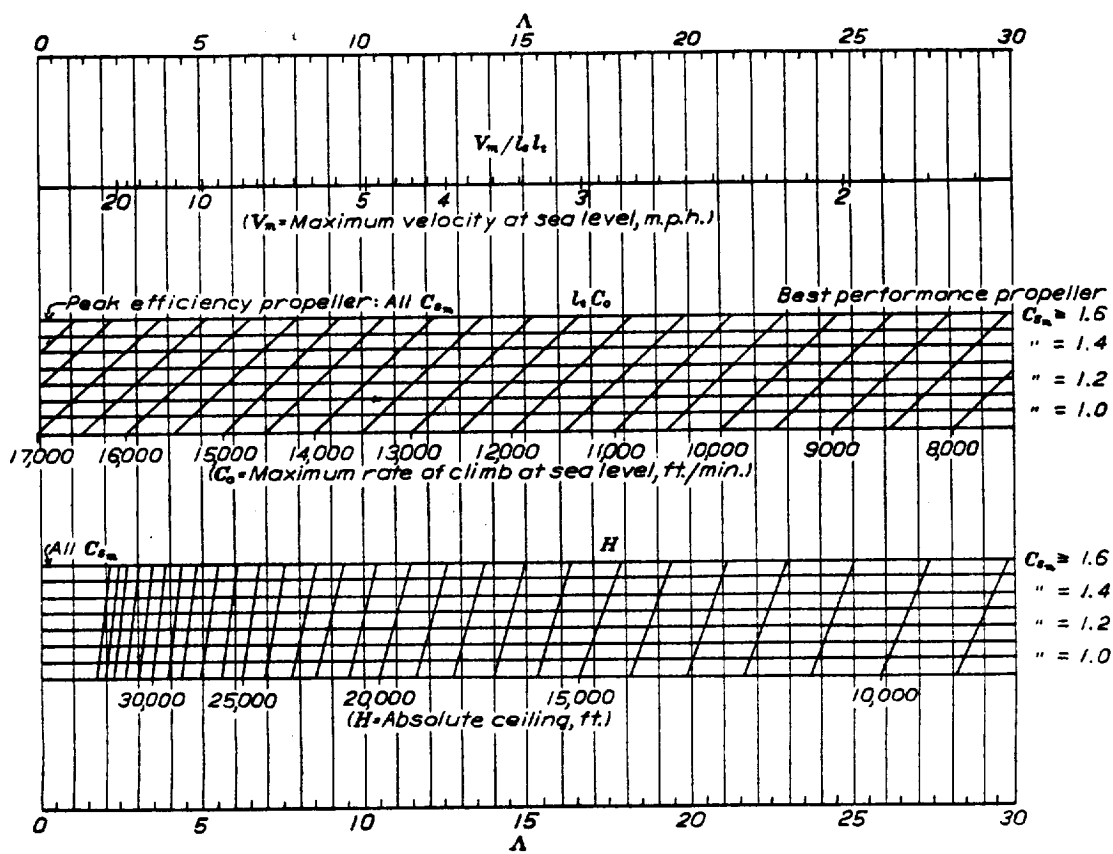


FIGURE 36.—Combination chart giving $\frac{V_m}{l_i}$, l_i , C_p , and H as functions of Λ

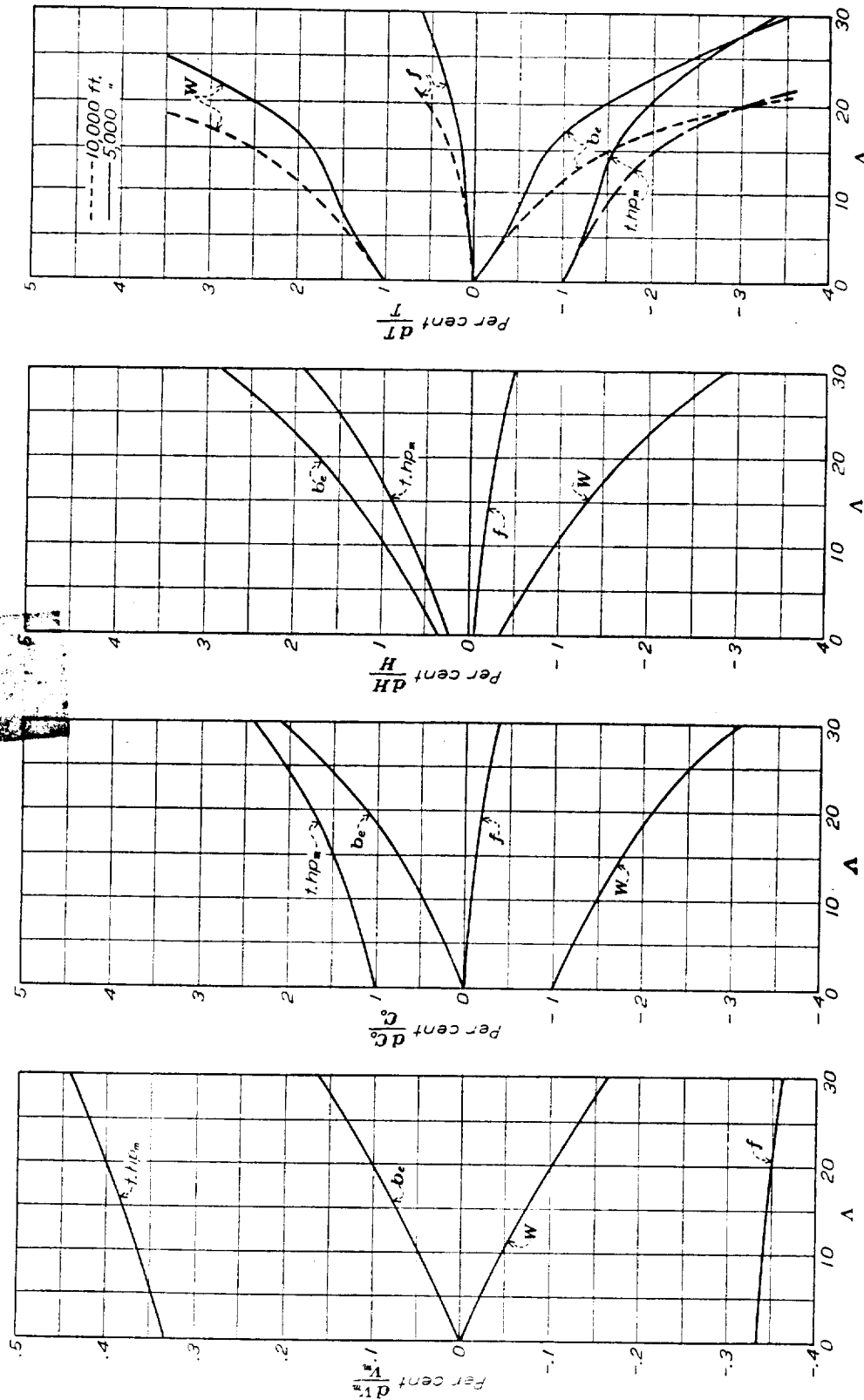


FIGURE 37.—Variation of performance with change of parameters. Charts show per cent change in performance due to 1 per cent (+1 per cent) change in parameter

V_{max} = max. velocity
 C_{max} = max. rate of climb at sea level
 H = absolute ceiling
 T = time to climb

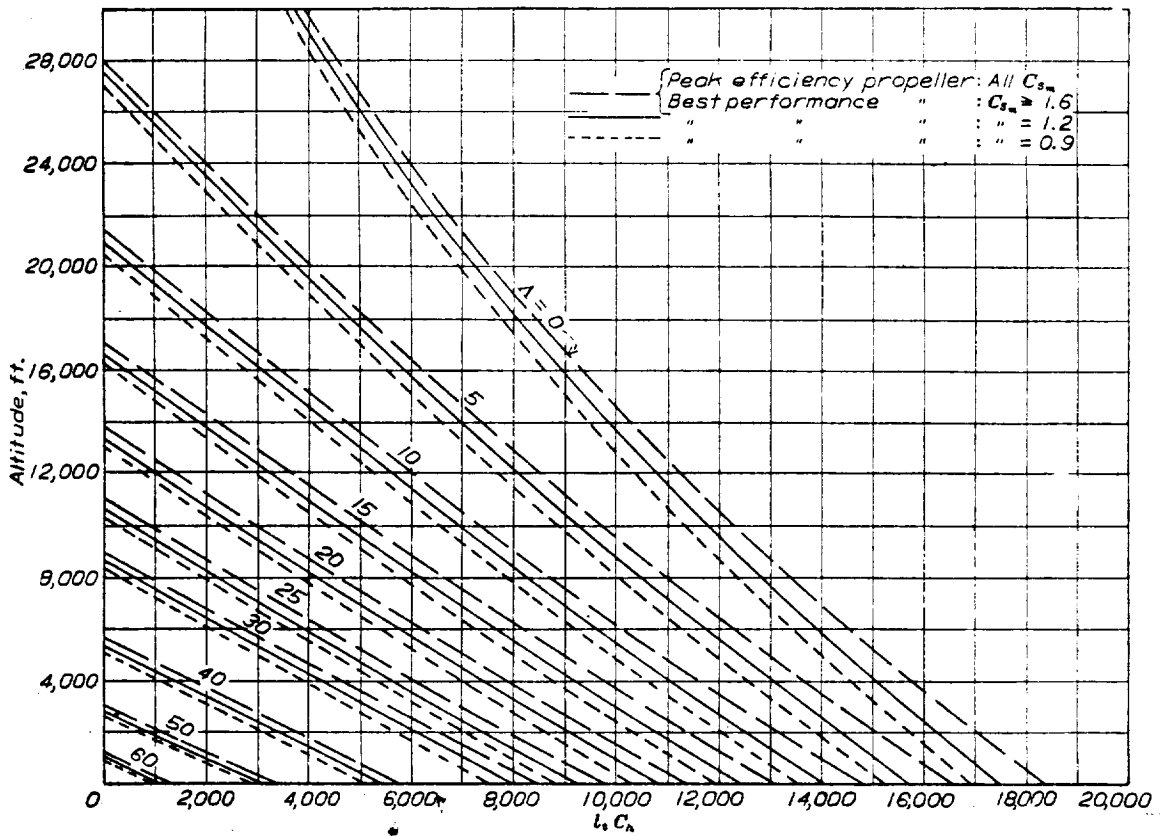


FIGURE 38.—Variation of l, C_a with altitude for various values of A

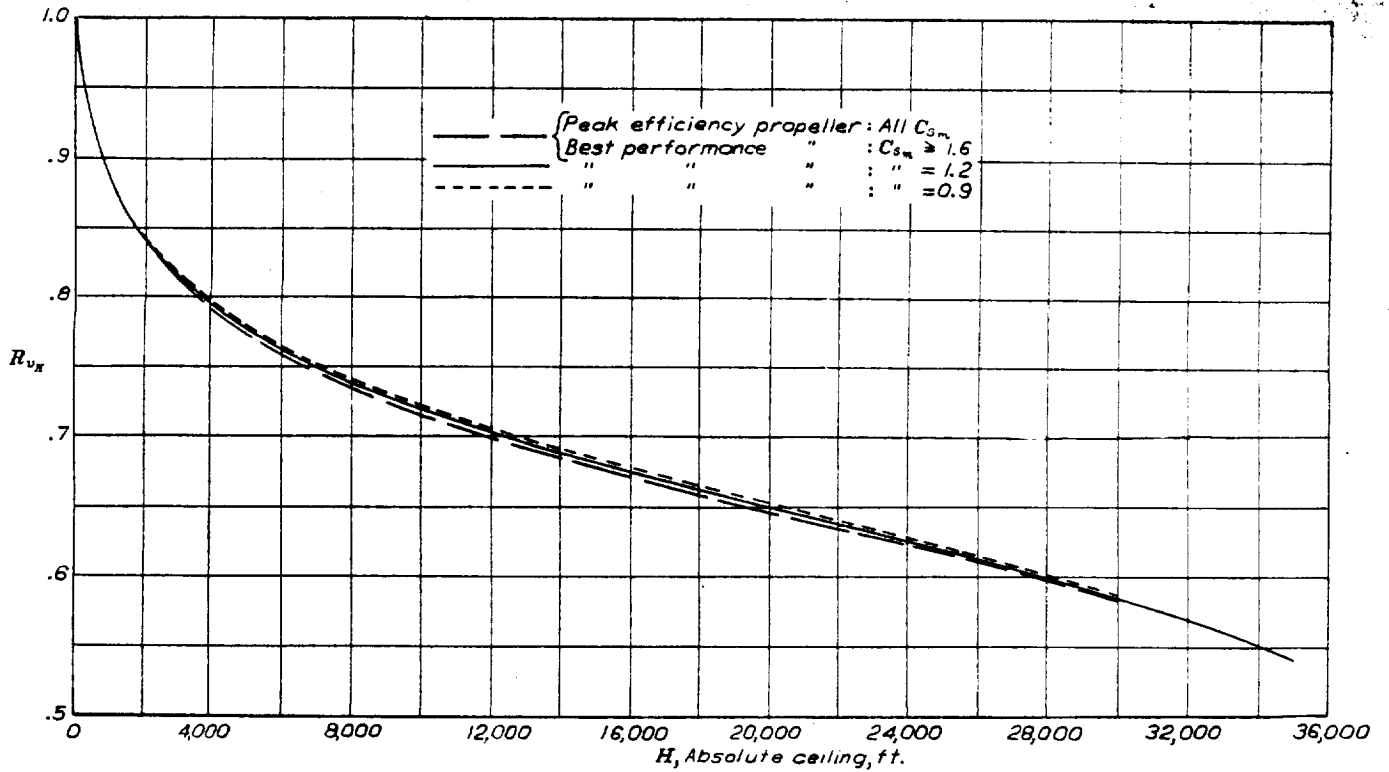


FIGURE 39.— R_{vH} as a function of absolute ceiling. R_{vH} = velocity at absolute ceiling / maximum velocity at sea level

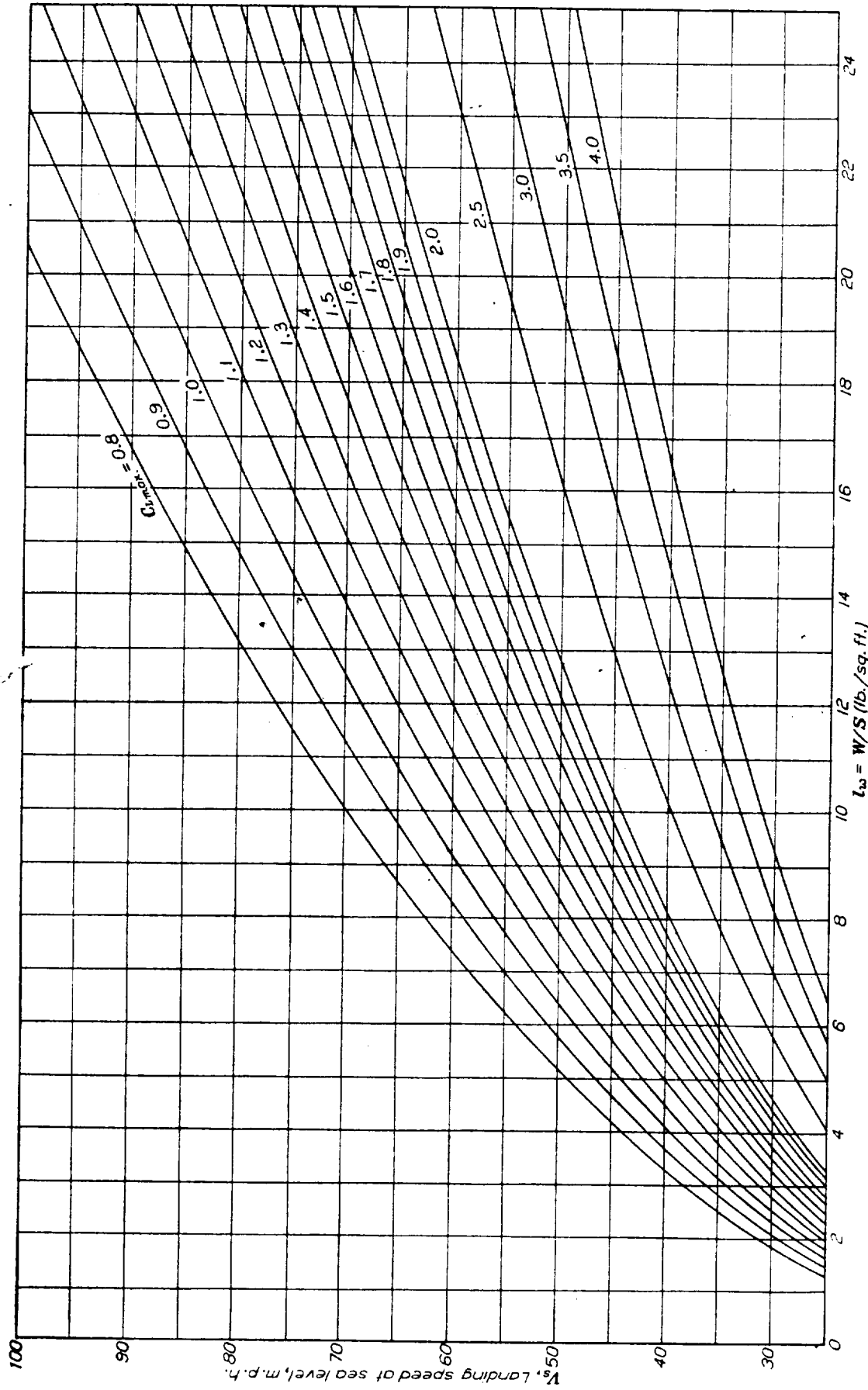


FIGURE 40.—Landing speed at sea level as a function of wing loading, W/S , and maximum lift coefficient, C_{Lmax} .

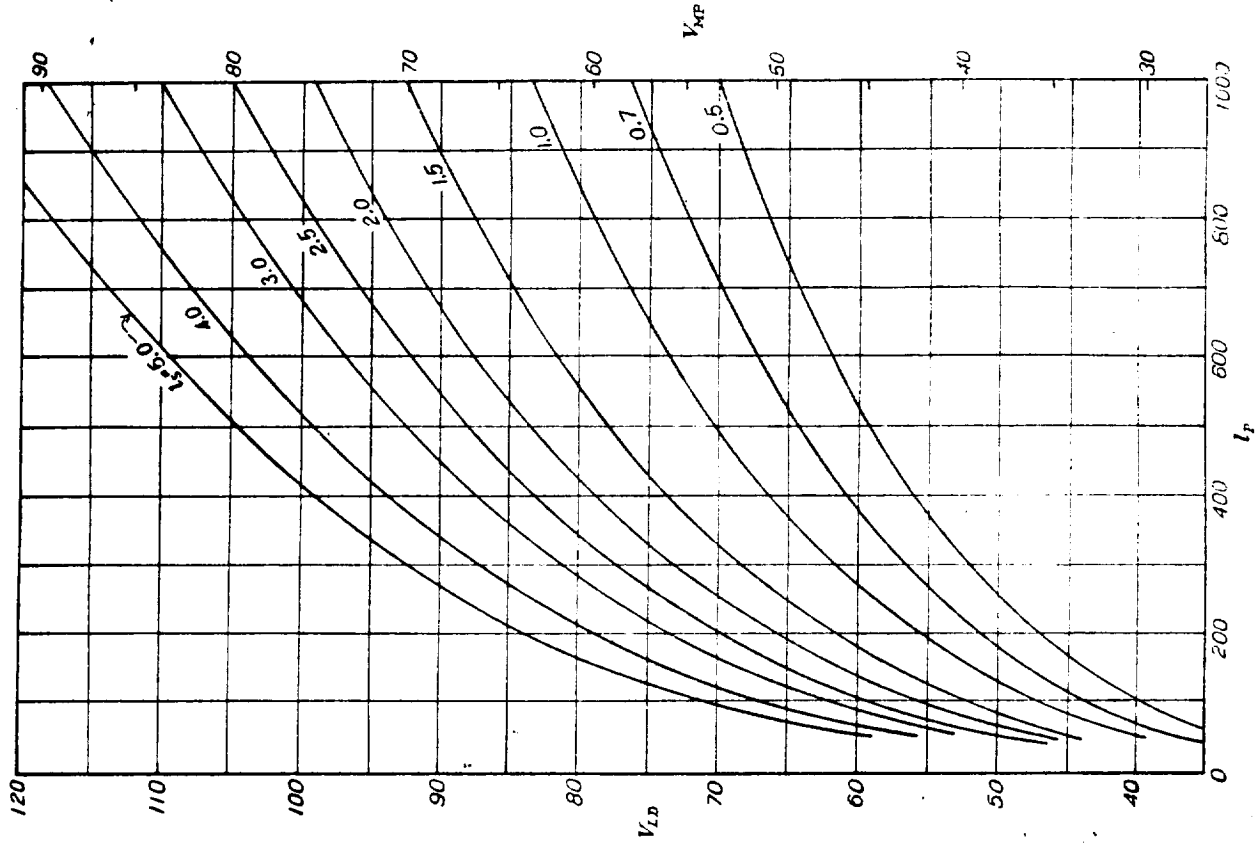


FIGURE 42.—Velocity for $(L/D)_{max}$, V_{L20} and velocity for minimum power, V_{AP} , as functions of L_p . Velocities in miles per hour

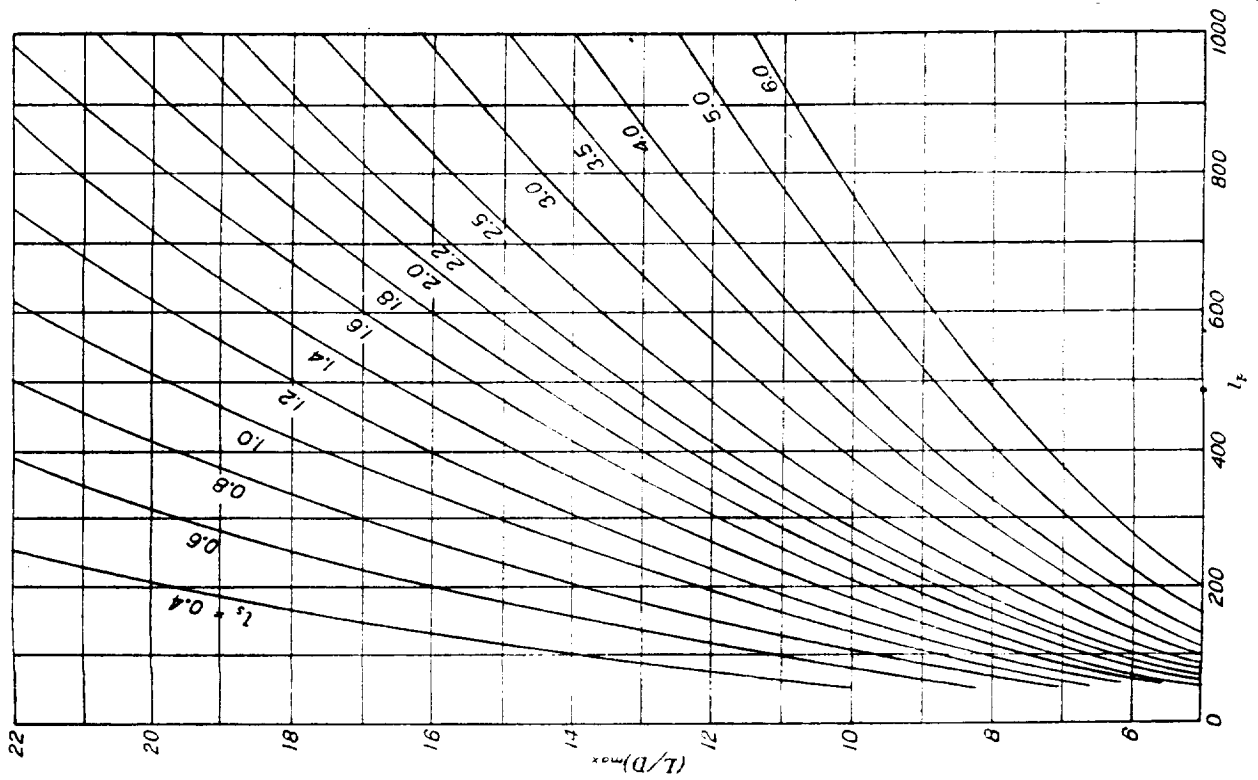


FIGURE 41.—Maximum lift/drag ratio as a function of L_p and L_c

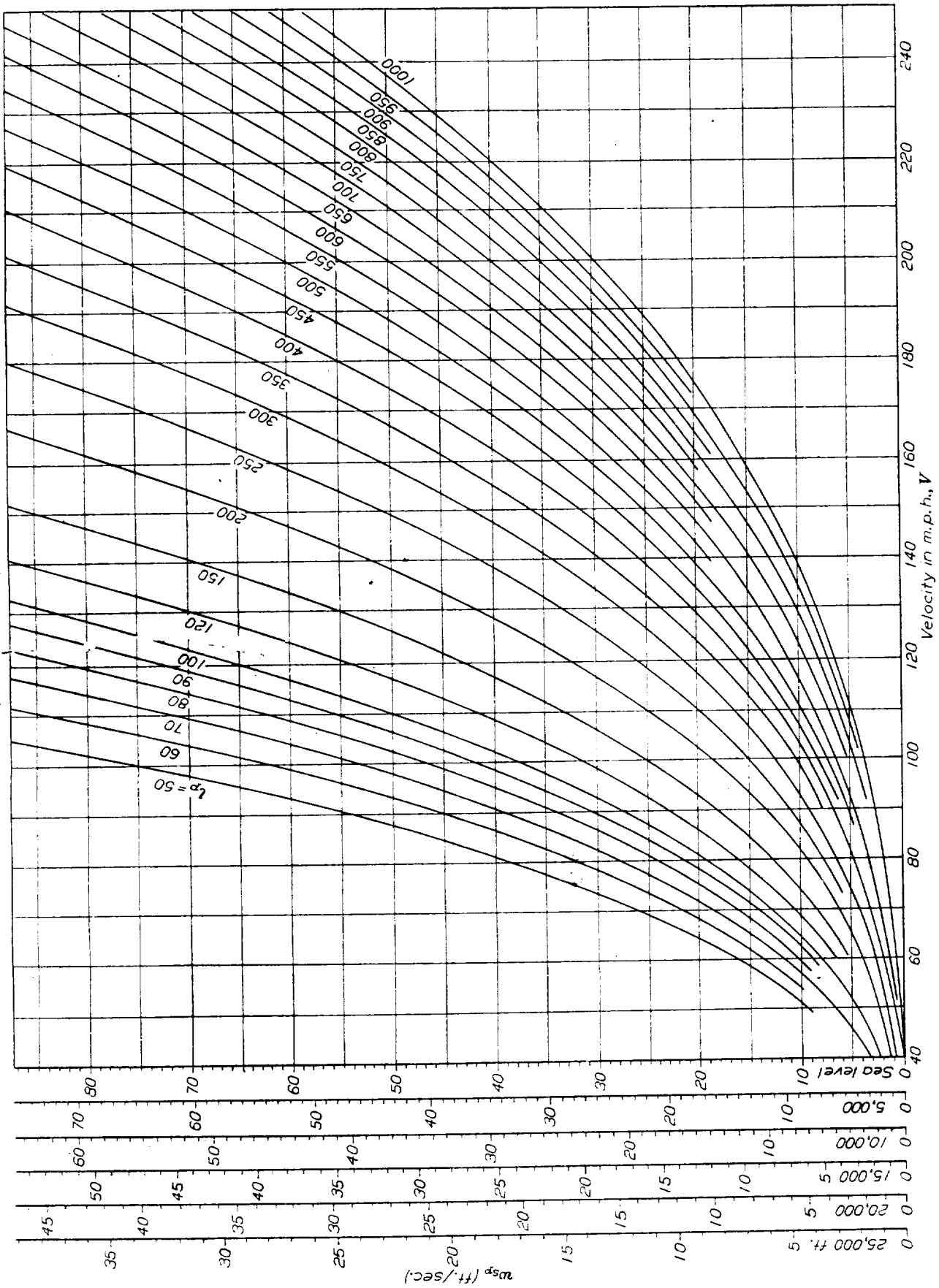


FIGURE 43.—The sinking speed w_{sp} , due to the parasite loading l_p , as a function of l_p and V , at various altitudes h . $W' = 550$ ($w_p + w_s$)

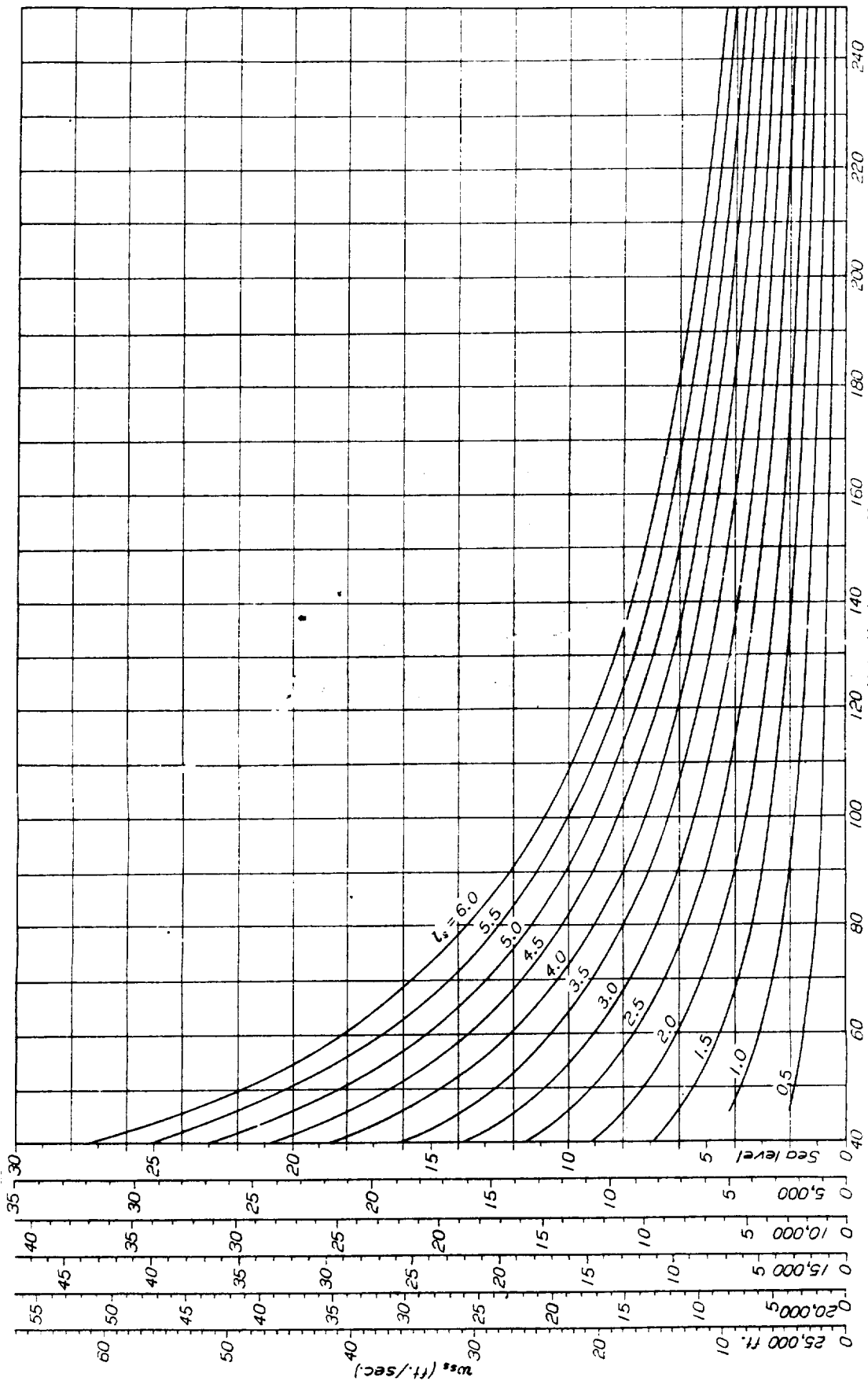


FIGURE 44.—The sinking speed w_s , due to the effective span loading L_s , as a function of L_s and V , at various altitudes
 $t.h.p. = 550 (w_s \cdot w_p)$

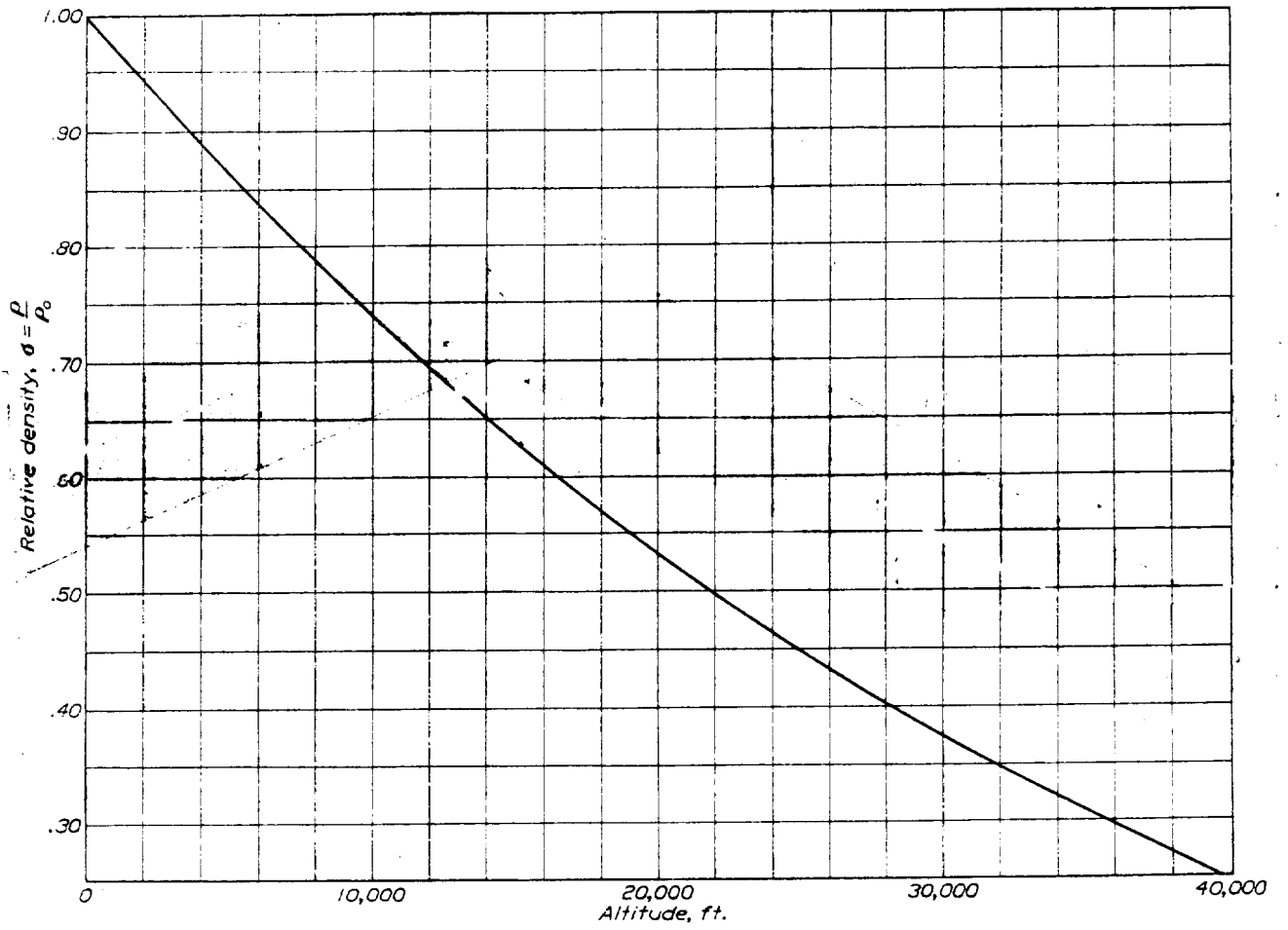


FIGURE 45.